universität wien

DISSERTATION

Titel der Dissertation

Comparative Studies of the Avian and the Mammalian LDLR

angestrebter akademischer Grad

Doktor/in der Naturwissenschaften (Dr. rer. nat.)

Verfasserin / Verfasser:	Mag. Melanie Schiff
Matrikel-Nummer:	9801745
Dissertationsgebiet (lt. Studienblatt):	Mikrobiologie und Genetik
Betreuerin / Betreuer:	O. Univ. Prof. DI. Dr. Wolfgang J. Schneider

Wien, im August 2009

Directory

Abbreviations

A

aa	amino acid
Aβ	amyloid β -peptide
ACAT	acyl-CoA:cholesterol acyltransferase
AD	Alzheimer's disease
α_2M	α_2-macroglobulin
α_2MR	α_2-macroglobulin receptor
Amn	Amnionless
AP	adaptor protein
apo	apolipoprotein
ApoER2	Apolipoprotein E receptor type 2
APP	amyloid precursor protein
ARH	Autosomal Recessive Hypercholesterolemia

B

bp	base pair
BMP	bone morphogenetic protein
BSA	bovine serum albumin

C

CCP	clathrin-coated pits
CCV	clathrin-coated vesicles
CLASP	clathrin-associated sorting proteins
CM	chylomicrons
CME	clathrin-mediated endocytosis
CR	chylomicron remnants
CRD	cysteine-rich domain
ct	cytoplasmic tail
Cubam	cubilin-amnionless complex

D

Dab	Disabled
DMEM	Dulbecco's modified minimum essential medium
DNA	deoxyribonucleic acid
DTT	dithiothreitol

E

EDTA	ethylenediaminetetraacetic acid
EGF	epidermal growth factor
ER	endoplasmic reticulum

F

FH	Familial Hypercholesterolemia

G

gg	*gallus gallus*
GST	glutathione S-transferase

H

h	hour
h	human
HDL	high-density lipoprotein
HMG-CoA	3-hydroxy-3-methylglutaryl-CoA
HRP	horseradish peroxidase
hs	*homo sapiens*

I

IgG	immunoglobulin G
IGS	Imerslund-Gräsbeck syndrome
IF	intrinsic factor
IF-B12	intrinsic factor-cobalamin
IPTG	isopropyl-beta-D-thiogalactopyranoside

K

kDa	kilo Dalton
kb	kilo bases

L

LA	LDLR type A repeat
LDL	low-density lipoprotein
LDLR	low-density lipoprotein receptor
LDLRAP1	LDLR adaptor protein 1
LH	laying hen
LR	LDLR relative
LRP	low-density lipoprotein receptor related protein

M

MBP	maltose-binding-protein
MEM	modified DMEM
µg	microgram
mg	milligram
min	minute
ml	milliliter
mm	*mus musculus*
mM	millimolar

N

NCBI	National Center for Biotechniology Information
ng	nanogram

P

PTB	phosphotyrosine-binding domain
PTBi	phosphotyrosine-binding domain insert
PRR	proline-rich region

PRRi	proline-rich region insert

R

RAP	receptor-associated protein
RNA	ribonucleic acid
R/O	restricted ovulator
RT-PCR	reverse transcription polymerase chain reaction

S

SDS	sodium dodecyl sulfate
SDS-PAGE	SDS polyacrylamide gel electrophoresis
sec	second

T

TBS	Tris buffered saline
TM	transmembrane domain

U

UTR	untranslated region

V

VE	visceral endoderm
VLDL	very low-density lipoprotein
VLDLR	very low-density lipoprotein receptor
VTG	vitellogenin

List of figures and tables

Abstract

Low-density lipoprotein-derived cholesterol and its intracellularly generated oxidated derivatives mediate control mechanisms that protect the cell from overaccumulation of cholesterol. The low-density lipoprotein receptor (LDLR) is the key component in the feed-back regulated maintenance of cholesterol homeostasis in the body. Members of the LDLR gene family are not only involved in lipoprotein transport, but also in diverse signal transduction pathways. Common features of these receptors are structurally and functionally defined modules, namely the ligand binding type A repeats, the epidermal growth factor (EGF) repeats, the so-called YWTD repeats, the O-linked sugar domain, the transmembrane domain, and a short cytoplasmic tail containing a consensus motif for internalization.

Endocytic members of the LDLR gene family employ adaptor proteins for efficient endocytosis. It is known that the soluble protein ARH interacts with the cytoplasmic tails of certain low-density lipoprotein receptor family members in humans. Numb, another adaptor protein originally shown to be involved in endocytosis in Drosophila, is closely related to ARH.

In this thesis, the chicken was used as model system, as it is a well characterized organism in terms of biology and molecular genetics for studies on receptor-mediated lipoprotein metabolism. For instance, the first avian LDLR has been identified in the chicken. Apolipoprotein E (apoE) is an important ligand for the mammalian LDLR, but is not expressed in birds and does not bind to the avian receptor. In order to shed further light on the requirements for recognition of apoE, one goal of the thesis was to mutate the chicken LDLR's ligand binding domain such that the receptor gains the ability to bind apoE. Accordingly, mutations were introduced, and the ligand binding behaviour of the altered LDLR was tested. The mutated ligand binding domains generated, retained binding of the common chaperone receptor-associated protein. However, in ligand blot studies, the mutated domains of the chicken LDLR failed to bind any of the human apoE isoforms. Thus, ligand binding properties are possibly determined by structural features other than, or in addition to, those investigated.

Recently, Numb was found in avian neuroepithelial cells. Through database search I localized the avian gene for Numb on chromosome 5, and I was able to identify 4 different isoforms containing various inserts and combinations thereof. I performed

interaction studies of the human and chicken LDLR's cytoplasmic tails with different Numb isoforms and could demonstrate that isoform 3 binds to both cytoplasmic tails despite lacking the phosphotyrosine-binding domain insert shown to be important for ARH's binding to the NPxY motif in the tails. These results indicate that, at least in the chicken, the phosphotyrosine-binding domain insert may not be crucial to the recognition of receptor-internalization motifs by the adaptor protein Numb.

Amnionless is a co-receptor for Cubilin, which is a protein, thought to complex only with LRP2, another member of the LDLR family. LRP2 contains three internalization motifs and binds ARH. Amnionless is not a bona-fide lipoprotein receptor, but contains two internalization signals for receptor-mediated endocytosis, which likely mediate the demonstrated binding of chicken ARH to the intracellular domain of avian Amnionless. I also investigated whether chicken Numb is also able to interact with this domain; however, the results indicate that such interaction does not take place, possibly related to the different physiology of avian species.

Zusammenfassung

LDL-Cholesterin und seine intrazellulär erzeugten oxidierten Derivate vermitteln eine Reihe von „Feedback“ Kontrollmechanismen, die die Zelle vor einer Überladung mit Cholesterin schützen. Der LDL Rezeptor (LDLR) ist die Hauptkomponente der regulierten Aufrechterhaltung der Cholesterinhomöostase im Körper. Mitglieder der LDLR Genfamilie sind nicht nur in den Lipoproteintransport involviert, sondern auch in verschiedene Signaltransduktionswege. Gemeinsame Merkmale dieser Rezeptoren sind strukturell und funktionell definierte Bausteine wie die Typ A Ligandenbindungsdomänen, die epidermalen Wachstumsfaktor-Domänen, die sogenannten YWTD Domänen, die O-glykosilierte Domäne, die Membranankerdomäne und eine kurze zytoplasmatische Domäne.

Endozytierende Mitglieder der LDLR Genfamilie setzen Adaptorproteine für effiziente Endozytose ein. Es ist bekannt, dass das lösliche Protein ARH mit dem zytoplasmatischen Teil von gewissen LDLR Familienmitgliedern im Menschen interagiert. Numb, ein weiteres Adaptorprotein welches ursprünglich in Drosophila entdeckt wurde, ist ebenfalls an Endozytose beteiligt und mit ARH nahe verwandt.

In meiner Arbeit wurde das Huhn als Modellorganismus benutzt, da es für Studien an rezeptor-vermitteltem Lipoproteinstoffwechsel und in Bezug auf Biologie und Molekulargenetik gut charakterisiert ist; so ist z.B. der erste Vogel-LDLR im Huhn identifiziert worden. In Säugetieren ist Apolipoprotein E (ApoE) ein wichtiger Bindungspartner für den LDLR. In Vögeln wird dieses Apolipoprotein allerdings nicht exprimiert und das humane ApoE bindet auch nicht an den Hühner-LDLR. Um tieferen Einblick in die Mechanismen der Ligandenbindung zu gewinnen, war es ein Ziel dieser Arbeit die LDLR Ligandenbindungsdomäne im Huhn so zu mutieren, dass der Rezeptor die Fähigkeit erlangt das ApoE zu binden. Dementsprechend wurden Mutationen eingebracht und das Bindungsverhalten des veränderten LDLRs getestet. Alle mutierten Ligandenbindungsdomänen waren in der Lage das bekannte Chaperon rezeptor-assoziiertes Protein zu binden, allerdings konnte die Bindung an keine der humanen ApoE-Isoformen, zumindest in Liganden Blot Studien, gezeigt werden. Die Resultate deuten darauf hin, dass die ApoE-Bindung wahrscheinlich durch andere, oder zusätzliche zu den untersuchten, Strukturelemente bestimmt wird.

Vor kurzem wurde Numb in neuroepithelialen Zellen im Huhn gefunden. Durch Datenbanksuche konnte ich das Numb-Gen auf Chromosom 5 lokalisieren und 4 verschiedene Isoformen, die 2 Arten von Inserts und Kombinationen davon enthalten, identifizieren. Durch Interaktionsstudien der zytoplasmatischen Teile des menschlichen und des Hühner-LDLR mit verschiedenen Numb Isoformen konnte ich zeigen, dass die Numb Isoform 3 in der Lage ist, beide zytoplasmatischen Domänen zu binden, selbst wenn das Insert in der Phosphotyrosin-Bindungsdomäne fehlt. Von diesem Insert weiß man, dass es für die Bindung von ARH an die NPxY Sequenz im zytoplasmatischen Teil des Rezeptors wichtig ist. Diese Ergebnisse weisen daraufhin, dass das Insert in der Phosphotyrosin-Bindungsdomäne von Numb, zumindest im Huhn, für die Erkennung von Rezeptor-Internalisierungssignalen durch das Adaptorprotein Numb nicht ausschlaggebend ist.

Amnionless wurde als Co-Rezeptor von Cubilin identifiziert. Cubilin war bisher nur als Interaktionspartner von LRP2, einem Protein aus der LDLR-Familie, bekannt. LRP2 besitzt drei Internalisierungssignale im zytoplasmatischen Teil und kann ARH binden. Obwohl Amnionless nicht zur LDLR-Familie gehört, weist es zwei Internalisierungssignale für Endozytose auf, und es wurde gezeigt, dass die intrazelluläre Domäne von Hühner-Amnionless an Hühner-ARH bindet.

Ich habe untersucht, ob Hühner-Numb auch mit der zytoplasmatischen Domäne von Hühner-Amnionless interagieren kann. Die Daten weisen daraufhin, dass eine solche Interaktion nicht stattfindet, was mit der unterschiedlichen Physiologie des Huhnes im Zusammenhang stehen könnte.

Introduction

Amnionless

Amnionless was initially identified as a yolk sac protein in the mouse, essential for amnion and primitive streak formation (Kalantry, Manning et al. 2001).
The amnionless gene*, amn,* located on mouse chromosome 12, encodes a type I transmembrane protein of approximately 50kDa (Kalantry, Manning et al. 2001). The Amnionless protein (Fig. 1) has one transmembrane domain (TM) separating a larger, N-terminal extracellular region and a smaller, C-terminal cytoplasmic region (Tanner, Aminoff et al. 2003). The extracellular region contains a cysteine-rich domain (CRD) consisting of 70 amino acids, and is the most conserved region of vertebrate Amnionless proteins.

Figure 1. Scheme of Amnionless structure.

A detailed description is given in the text. CRD, cysteine-rich domain; TM, transmembrane domain; NPxY, internalization sequence;

The CRD is also present in a small group of proteins known to function as bone morphogenetic protein (BMP) inhibitors, for example the *Xenopus laevis* protein Chordin (Kalantry, Manning et al. 2001). Two motifs for receptor internalization (NPxY), reminiscent of those in low-density lipoprotein receptor family members, are located in the C-terminal part of the protein. The Amnionless protein comprises two potential glycosylation sites on amino acid positions 27 and 355 (Uniprot/Swiss-Prot). Amnionless is exclusively expressed on the apical surface of the visceral endoderm (VE) facing the maternal environment during gastrulation (Kalantry, Manning et al. 2001). It is also expressed in kidney proximal tubules and intestinal epithelium, which, like the VE, are polarized epithelia specialized for resorption and secretion (Strope, Rivi et al. 2004). Homozygous inactivation of *amn* causes embryonic lethality in mice, whereas mice carrying the *amn* mutation, a transgene-induced

insertional mutation (Wang, Bornslaeger et al. 1996), are unable to develop an amnion (Tanner, Aminoff et al. 2003). In humans the amnionless gene lies on chromosome 14q32 (Kalantry, Manning et al. 2001), and there is no apparent need for Amnionless until after birth.

Amnionless in human disease

Imerslund-Gräsbeck syndrome (IGS or megaloblastic anemia 1) is an autosomal recessive disorder. It is characterized by selective cobalamin (vitamin B_{12}) malabsorption, despite normal function and production of intrinsic factor (IF) (Grasbeck, Gordin et al. 1960; Imerslund 1960), with proteinuria. Additionally, the disease includes failure to thrive and grow, infections and neurological damage (Grasbeck 2006).

Cobalamin is a coenzyme for methylmalonyl-CoA mutase and methionine synthase, enzymes of intermediate metabolism. Gastrointestinal malabsorption of this nutrient leads to megaloblastic anemia, neutropenia, degeneration of spinal cord nerve tracts, and dementia (Rosenblatt and Fenton 1999). In children, cobalamin deficiency may also lead to growth retardation and loss of developmental progress (He, Madsen et al. 2005).

IF is a glycoprotein, which binds to cobalamin and ensures its absorption from the intestine. The IF-cobalamin complex is recognized by Cubilin, which participates in the endocytosis of this complex (Moestrup and Verroust 2001; Christensen and Birn 2002). Data from an earlier study (Aminoff, Carter et al. 1999) provide evidence that mutations in Cubilin lead to IGS.

Recently, the group around Tanner SM (Tanner, Aminoff et al. 2003) showed that mutations in the amnionless gene also cause IGS. Canine IGS displays highly significant linkage to the same locus (He, Fyfe et al. 2003). Canine IGS was observed originally in purebred giant schnauzers and is a naturally occurring animal model of the human disorder.

The interaction of Amnionless and Cubilin

Cubilin, also known as intrinsic factor-cobalamin (IF-B12) receptor, is a multiligand receptor of about 460kDa. It is expressed in endocytic compartments of absorptive epithelia and at the apical plasma membrane, especially the kidney proximal tubule, the small intestine, and the visceral yolk sac (Coudroy, Gburek et al. 2005). Thus, its tissue distribution is very similar to that of Amnionless.

Cubilin binds and mediates the clearance of various specific nutrient-carrying proteins, such as IF-B12, vitamin-D-binding protein, albumin, transferrin, haemoglobin, apolipoprotein A-I, high-density lipoprotein, and Ig light chains (Christensen and Birn 2002). Cubilin (Fig. 2) contains no transmembrane domain and is composed of an amino-terminal stretch of 106 amino acids followed by eight EGF-type (epidermal growth factor) repeats, and 27 CUB domains (in all species).

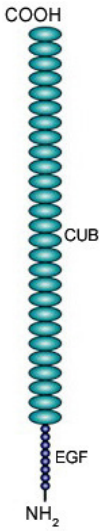

Figure 2. Schematic drawing of Cubilin.

For detailed description refer to the text.
CUB, 27 CUB domains; EGF, 8 EGF-type repeats;

It was shown that Amnionless and Cubilin colocalize early in the biosynthetic pathway that is essential for apical membrane localization. Amnionless associates with the EGF region of Cubilin to assist each other towards exiting the endoplasmic reticulum (Fyfe, Madsen et al. 2004; Coudroy, Gburek et al. 2005). Cubilin is highly glycosylated, which could be the major determinant for apical sorting.

The present data suggest a model in which Amnionless and Cubilin form a functional complex (Fig. 3), also designated as cubam complex, which is essential for intestinal

cobalamin uptake, renal protein reabsorption and early rodent embryogenesis (Grasbeck 2006).

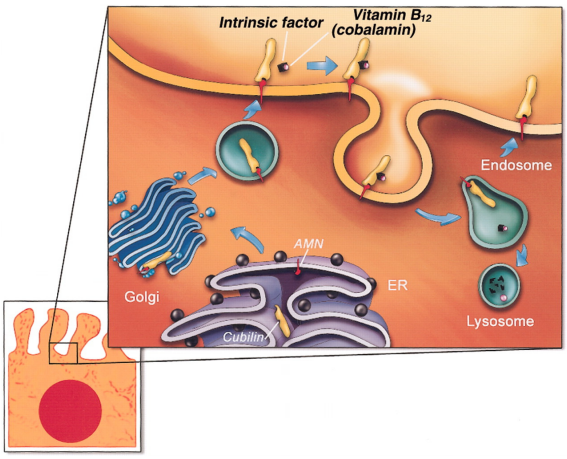

Figure 3. A model of Amnionless and Cubilin assembly in the biosynthetic pathway and recycling in the endocytic apparatus of polarized epithelial cells.

A detailed description is provided in the text. AMN, Amnionless; ER, endoplasmic reticulum (Fyfe, Madsen et al. 2004);

In this complex, Cubilin provides the ligand binding regions, whereas Amnionless is responsible for membrane anchorage, biosynthetic processing, and trafficking to the plasma membrane. Amnionless also provides two putative sequence motifs for endocytosis and receptor recycling.

Interestingly, Cubilin is coexpressed and colocalizes with LRP2 (formerly known as megalin) (Fig. 4), a type I transmembrane protein of around 600kDa. Since Cubilin has no transmembrane domain, LRP2 seems to mediate the co-internalization and possibly the recycling of Cubilin (Moestrup, Kozyraki et al. 1998). But whether the two proteins act mechanistically together is unknown. Recently published data show that the cubam complex alone is sufficient to internalize IF-B12 (Coudroy, Gburek et al. 2005), but it could not be excluded that LRP2 may accelerate the endocytic activity of this complex.

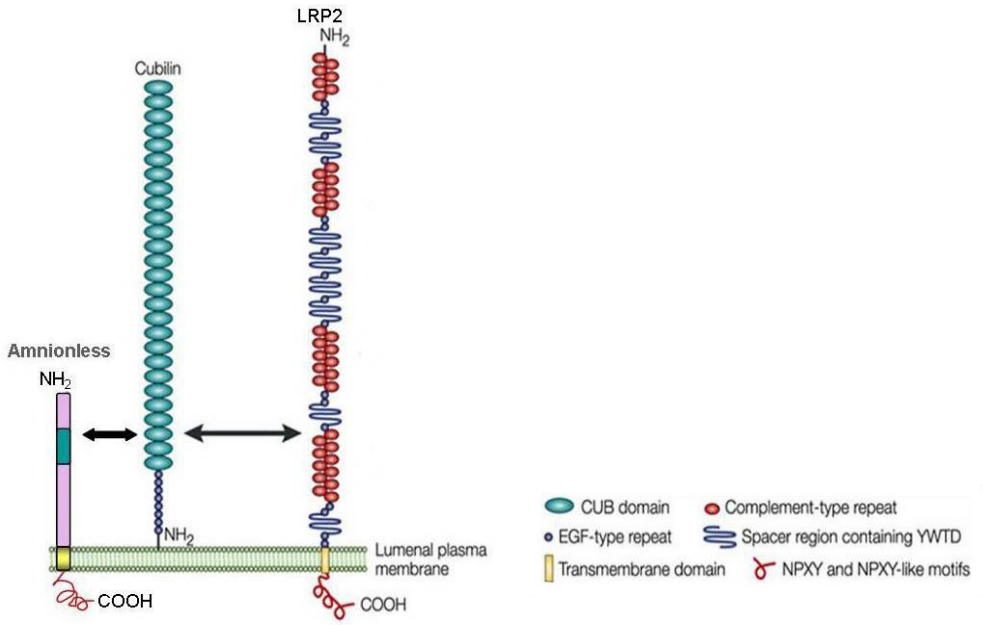

Figure 4. Model of Amnionless/Cubilin and Cubilin/LRP2 interactions.

Amnionless and LRP2 bind Cubilin. LRP2 might assist trafficking of Cubilin. Amnionless and LRP2 are involved in the endocytosis of Cubilin.

The role of cubam and LPR2 during embryonic development and nutrition

The Amnionless-Cubilin-LRP2 complex (Fig. 4) seems to be essential for normal embryonic development. Altered function of these three proteins during gestation, either by using specific antibodies or by knocking out the genes, leads to congenital defects and/or embryo-lethality. In LRP2 $^{-/-}$ mice, defective anterior central nervous system development was observed. In mice, Cubilin inactivation leads to developmental retardation, mesodermal defects, and embryonic lethality around midgestation. The absence of Amnionless leads to embryonic lethality at around embryonic day 7.5 (E 7.5), triggered by impaired primitive streak assembly (Kozyraki and Gofflot 2007).

The nutrition of the embryo depends on maternal-fetal transport of nutrients through the yolk sac VE. The VE has a very high endocytic capacity and expresses Amnionless, Cubilin, and LRP2. LRP2 mediates the uptake of cholesterol and does not appear to be essential for early embryogenesis.

Amnionless and Cubilin seem to be required for endocytosis and/or transcytosis of high-density lipoproteins and possibly other factors necessary for proper growth of the embryo (Strope, Rivi et al. 2004; Smith, Mussell et al. 2006).
The knock-out of *amn* and application of antibodies against Cubilin leads to severe defects in mice, but do not have such effects on embryonic development in humans and dogs (Aminoff, Carter et al. 1999; Tanner, Aminoff et al. 2003; He, Madsen et al. 2005). Null-mutations in humans and in the canine model result in the Imerslund-Gräsbeck syndrome due to malabsorption of IF-B12 complex. These findings suggest species-specific differences in visceral endoderm and yolk sac functions.
The murine visceral yolk sac completely surrounds the developing fetus and serves as a maternal-fetal interface required for the exchange of nutrients, oxygen, and waste products. In contrast, the human yolk sac becomes a vestigial appendage, and trophoblast derivatives act as the major maternal-fetal interface (Strope, Rivi et al. 2004). These differences possibly explain why cubam is not essential in human development.

The LDL receptor gene family

The low-density lipoprotein (LDL) receptor (LDLR) gene family comprises a large number of structurally closely related members. These proteins are engaged in various functions ranging from receptor-mediated endocytosis of a broad variety of ligands, especially lipoproteins, to signal transduction pathways as recent studies indicate (Li, Cam et al. 2001; Schneider and Nimpf 2003). The first characterized and most prominent member of the LDLR gene family is the LDLR (Brown and Goldstein 1974; Goldstein and Brown 1974). It is the most important component in the tightly controlled maintenance of cholesterol homeostasis in the body (Brown and Goldstein 1986).

The LDL receptor

The schematic structure of the LDLR is depicted in Fig. 5. Common features of the members of the LDLR gene family are structurally and functionally defined modules, which are frequently specified by distinct exons in the corresponding genes.

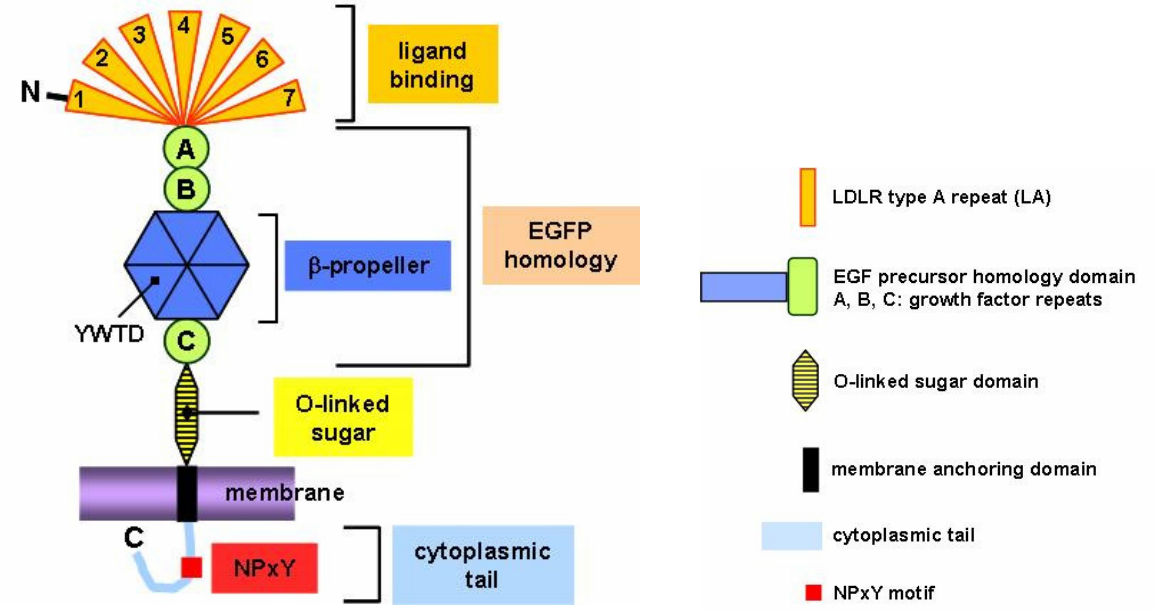

Figure 5. Schematic model of the LDL receptor.
A detailed description is given in the text.

These domains are head-to-tail-arranged and described as follows:

i. **Ligand binding domain:** This domain mediates the interaction between the receptor and lipoproteins containing apolipoproteinB-100 (apoB100) and/or apolipoproteinE (apoE) (Esser, Limbird et al. 1988). The domain, located at the amino terminus, consists of seven LDLR type A (LA1-7) repeats of approximately 40 residues each. Every repeat has six cysteines, which presumably mediate the folding of the domain in a compact structure with clusters of negatively charged residues on its surface (with the signature tripeptide SDE, Ser-Asp-Glu). These negatively charged clusters are thought to mediate binding of lipoproteins through the positively charged residues on apoB100 and apoE (Nimpf and Schneider 2000;

Schneider and Nimpf 2003). The linkers between the individual repeats are thought to provide flexibility to the ligand binding domain in order to allow the binding of lipoprotein ligands of different sizes.

ii. **EGF (epidermal growth factor) precursor homology domain:** The EGFP homology domain is located next to the ligand binding domain. Its remarkable characteristic is the sequence similarity to parts of the EGF precursor, i.e. three regions termed “growth factor repeats” (A, B, and C in Fig. 5: also called type-B repeats). Whereas repeats A and B are located aminoterminally, repeat C is located at the carboxyterminus. The residual part consists of 6 modules of about 40 residues with a consensus tetrapeptide YWTD (Tyr-Trp-Thr-Asp) forming the so-called six-bladed β-propeller. The β-propeller together with the 3 type-B repeats forms the EGF precursor homology domain (Jeon, Meng et al. 2001) of approximately 400 residues. The acidic conditions in the endosome lead to lipoprotein release from the LDLR ligand binding domain. This triggers a conformational change in the receptor, which in turn leads to a closing of the structure between the β-propeller and the binding repeats LA4 and LA5 (Beglova, Jeon et al. 2004; Beglova and Blacklow 2005).

iii. **O-linked sugar domain:** The O-linked sugar domain, located just outside the plasma membrane, is 58 amino acids long and enriched in serine and threonine residues. Most of the 18 hydroxylated amino acid side chains are glycosylated. The O-linked oligosaccharides undergo posttranslational elongation in the course of receptor maturation. Although the structure of this region is very well known, its function remains unclear (Davis, Elhammer et al. 1986).

iv. **Membrane anchoring domain:** This domain consists of about 20 hydrophobic amino acids and lies carboxyterminally to the O-linked carbohydrate cluster. The sequence of this domain is the least conserved of all receptor domains in seven mammalian species. This finding speaks against a specific function other than anchoring. Deletion of this domain, in naturally occurring mutations or by site-directed-mutagenesis, leads to secretion of truncated receptors from the cells.

v. **Cytoplasmic tail:** The cytoplasmic tail constitutes a short stretch of 50 amino acid residues, which are involved in the targeting of the LDLR to

clathrin-coated pits. Site-specific mutagenesis and naturally occurring mutations have identified an “internalization signal” NPxY (Asn-Pro-Xxx-Tyr, where x denotes any amino acid). Recently, the cytoplasmic domains of the LDLR and its relatives have come into focus due to their involvement in transduction of extracellular signaling processes (Willnow, Nykjaer et al. 1999).

Functions of the LDLR: The LDLR pathway

In the early 1970’s M.S. Brown and J.L. Goldstein started their work to investigate and hence to understand the human genetic disease, familial hypercholesterolemia (FH). In patients with this disease, the concentration of blood cholesterol is elevated many times above normal, and this leads to premature coronary heart diseases. These studies resulted in the discovery of the LDLR and to the elucidation of the mechanism by which this receptor mediates feedback control of cholesterol synthesis.

FH is caused by inherited defects in the gene encoding the LDLR. These defects disrupt the normal control of cholesterol metabolism.

Normal LDLR function plays a critical role in reducing the risk of atherosclerosis by binding to and internalizing lipoproteins that contain apoB100 or apoE.

In humans, apoB100 is synthesized by the liver and associates with LDL and VLDL. ApoE is expressed in liver, brain, kidney, and spleen and associates with VLDL, β-VLDL, chylomicrons, and less frequently with HDL. Both apolipoproteins, apoB100 and apoE, function as ligands and interact with the LDLR ligand binding domain.

The LDLR (Fig. 6) is synthesized by ribosomes and folded, with the help of the common chaperone receptor-associated protein (RAP), which is a specialized molecular chaperone for the members of the LDLR family, in the endoplasmic reticulum (ER). Upon transport to the Golgi network, the LDLR undergoes extensive O-linked glycosylation and is transported to the cell surface. At the plasma membrane, receptors bind lipoprotein ligands, and internalization occurs by endocytosis via clathrin-coated pits. After receptor-ligand complexes are taken up into clathrin-coated pits, they are delivered to endosomes. In the endosomes the low pH-environment triggers release of the bound lipoprotein particles (see below).

Subsequently, the receptors return to the cell surface in a process called receptor recycling (Brown and Goldstein 1986; Maxfield and McGraw 2004; Beglova and Blacklow 2005).

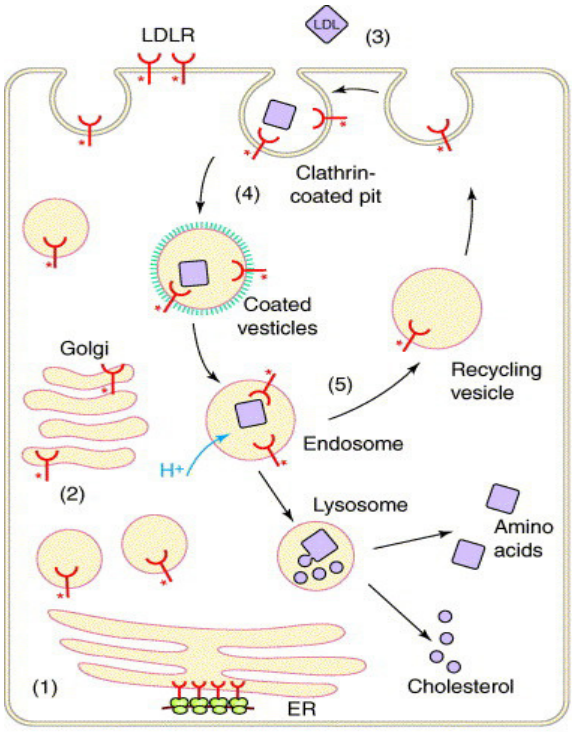

Figure 6. Cellular itinerary of the LDLR.

(1) Synthesis of the receptors occurs at the ribosomes and they are folded in the ER. (2) Receptors are glycosylated in the Golgi network and transported to the cell surface. (3) LDLRs bind ligands at the plasma membrane. (4) Internalization takes place via clathrin-coated pits, which deliver receptor-ligand complexes to endosomes. (5) The lipoproteins are released and the LDLRs are recycled back to the cell surface [figure 2 from (Beglova and Blacklow 2005)]

The LDLR is the key component in the feedback-regulated maintenance of cholesterol homeostasis in the body (Goldstein, Brown et al. 1985). Cholesterol derived from LDL and its intracellularly generated oxidated derivatives mediate a complex series of feedback control mechanisms that on the one hand provide the cells with cholesterol and on the other hand protect the cell from overaccumulation of cholesterol.

First, sterols suppress the activities of two key enzymes in cellular cholesterol biosynthesis, 3-hydroxy-3-methylglutaryl-CoA (HMG-CoA) synthase and HMG-CoA reductase. The second step is that cholesterol activates the cytoplasmic enzyme acyl-CoA:cholesterol acyltransferase (ACAT), which allows the cell to store spare

cholesterol in re-esterified form. Third, the synthesis of new LDLRs is suppressed to prevent cholesterol overloading (Fig. 7).

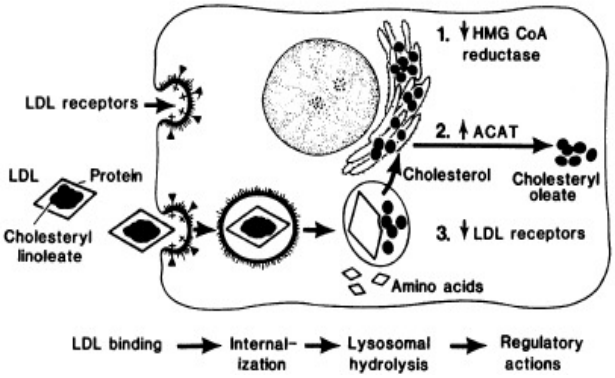

Figure 7. Sequential steps in the LDLR pathway in mammalian cells.

Details are described in the text. HMG CoA reductase, 3-hydroxy-3-methylglutaryl-CoA reductase; ACAT, acyl-CoA:cholesterol acyltransferase. LDL, low-density lipoprotein; Vertical arrows indicate the direction of the regulatory effects (Brown and Goldstein 1979).

Mammalian cells are able to survive without exogenously derived cholesterol, because they can synthesize cholesterol from acetyl-CoA. When LDL is available, most cells primarily use the LDLR to import LDL cholesterol and keep their own synthetic activity suppressed in order to maintain cholesterol homeostasis. Thereby, a constant level of cholesterol in the cells is sustained, while the external cholesterol supply can undergo large fluctuation (Schneider and Nimpf 2003).

Other members of the LDL receptor gene family

The most important members of the growing LDLR superfamily are listed below (table 1) in order of their discovery, and the structural organization of these receptors is shown in Fig. 8. The avian counterpart of each receptor is indicated in the table, because the chicken is the working model and the chicken receptors also demonstrate the high conservation of the key players in lipid metabolism.

Human	Chicken
LDLR Low-density lipoprotein receptor (Goldstein and Brown 1974)	**LDLR** Low-density lipoprotein receptor (Hummel, Lynn et al. 2003)
LRP2/megalin/gp330 Low-density lipoprotein receptor-related protein 2 (Kerjaschki and Farquhar 1982)	**LRP2/megalin** Low-density lipoprotein receptor-related protein 2 (currently characterized in our laboratory)
LRP1/ α_2-macroglobulin receptor Low-density lipoprotein receptor-related protein (Herz, Hamann et al. 1988)	**LRP1** Low-density lipoprotein receptor-related protein 1 (Stifani, Barber et al. 1991; Nimpf, Stifani et al. 1994)
VLDLR Very-low-density lipoprotein receptor (Takahashi, Kawarabayasi et al. 1992)	**LR8** LDLR relative with eight ligand binding repeats (Bujo, Hermann et al. 1994)
LR11/sorLA LDLR relative with 11 binding repeats/ sorting protein-related receptor (Yamazaki, Bujo et al. 1996; Morwald, Yamazaki et al. 1997)	**LR11** LDLR relative with 11 binding repeats (Morwald, Yamazaki et al. 1997)
ApoER2/LRP8 Apolipoprotein E receptor type 2 (Kim, Iijima et al. 1996)	**LR7/8B** Chicken homologue of ApoER2 (Novak, Hiesberger et al. 1996; Brandes, Novak et al. 1997)
LRP3, 4, 5, and 6 LDLR related protein -3, -4, -5, and -6 (Herz and Bock 2002; Strickland, Gonias et al. 2002)	**LRP4** (3, 5, 6 not characterized yet) LDLR related protein-4 (MEGF7) (Tomita, Kim et al. 1998)
LRP1B/LRP-DIT Low-density lipoprotein receptor-related protein 1 Lipoprotein receptor-related protein-deleted in tumors (Liu, Musco et al. 2000)	**LRP-DIT** Lipoprotein receptor-related protein-deleted in tumors (found in the chicken cell lines DT40 and DKO-R cells, unpublished)

Table 1. Members of the human LDLR gene family and their homologues in the chicken.

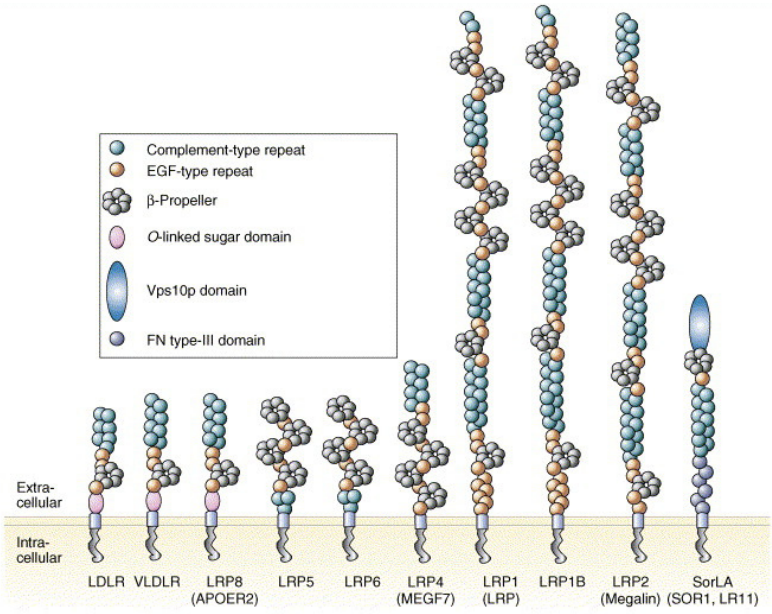

Figure 8. Domain structures of the members of the LDL receptor family.
For a detailed description refer to the text (Andersen and Willnow 2006).

VLDL receptor (VLDLR)

The VLDLR was discovered in 1992 by Takahashi et al (Takahashi, Kawarabayasi et al. 1992). A striking feature of the VLDLR is its structural similarity to the LDLR, except that the VLDLR ligand binding domain contains an additional LA repeat, which apparently preceeds the 7 present in the LDLR. This view is supported when the two genes are aligned. The VLDLR shows an amazing degree of conservation among different species. The mammalian VLDLR exists in variant forms, containing an O-linked sugar domain or not, arising from differential splicing (Magrane, Reina et al. 1998). The predominant expression sites are heart, skeletal muscle, and adipose tissue. Unlike the LDLR, which is expressed in most cells and notably in the liver, the expression of the VLDLR in the liver is virtually absent (Takahashi, Kawarabayasi et al. 1992). Despite the structural similarity between the LDLR and VLDLR, their ligand binding properties differ considerably. The LDLR binds apoE- and apoB-containing lipoproteins, whereas the VLDLR binds to apoE-containing lipoproteins, but does not bind to LDL. This might be because of the fact that it does not recognize apoB100 (Mikhailenko, Considine et al. 1999). Another difference to the LDLR is that the

VLDLR level is not regulated by cellular sterols, but seems to be influenced by hormones such as estrogen and thyroid hormone.
The tissue distribution of the VLDLR is highly suggestive of a role in triacylglycerol transport into metabolically active tissues, although uptake of high amounts of VLDL by this receptor has not been shown.
It now has been convincingly demonstrated that the VLDLR plays a role in a signal transduction cascade that controls neuronal migration and positioning. VLDLR binds the extracellular matrix-associated protein Reelin, and this interaction is needed for the downstream induction of tyrosine-phosphorylation of Disabled-1 (Dab1). Thus, a Reelin-VLDLR-Dab1 pathway is proposed that regulates neuronal positioning in cortex, hippocampus, and cerebellum during development (Hiesberger, Trommsdorff et al. 1999; Trommsdorff, Gotthardt et al. 1999).

LR8, the avian VLDLR homologue

Oviparous (egg-laying) species express LR8 (Fig. 9), which is highly homologous to the mammalian VLDLR (Bujo, Hermann et al. 1994). In contrast to mammals, the major function of LR8 in avian species is well established. Large amounts of yolk precursors, mainly VLDL and vitellogenin (VTG), are synthesized by the liver, transported via the circulation and subsequently deposited into the growing oocyte. This process, commonly known as vitellogenesis, is pivotal for reproduction in these species, because the developing embryo depends on the yolk components stored in the oocyte. The massive uptake into growing oocytes in the ovary of VLDL and VTG (approximately 12g during vitellogenesis) from the plasma is achieved by receptor-mediated endocytosis (Schneider 1995). LR8 binds to VLDL, VTG, α_2-macroglobulin, and lactoferrin (Bujo, Lindstedt et al. 1995). The receptor is specific for the apoB moiety of the VLDL particle, whereas apolipoprotein VLDL-II, a powerful lipoprotein lipase inhibitor (the only other major apolipoprotein present on VLDL from laying hens), is not involved in receptor binding (Nimpf, George et al. 1988).
The receptor gene is located on the chicken sex chromosome Z, and the protein is expressed almost exclusively in oocytes and at much lower levels in heart and skeletal muscle. Similar to the situation for the mammalian VLDLR, the chicken expresses two forms of LR8: in somatic cells LR8 is expressed as the larger isoform,

LR8+, which contains the O-linked sugar domain, whereas the oocyte expresses the LR8- isoform lacking the O-linked sugar domain (Bujo, Lindstedt et al. 1995).

The mutant restricted ovulator (R/O) chicken strain

The key role of LR8 in oocyte development in egg-laying species is also shown by a genetic model in which the receptor function is disrupted. The functional absence of the receptor, caused by a point mutation, which changes residue 682 in the *lr8* locus from cysteine into a serine (Fig. 9), leads to an inability of oocytes to take up yolk, and therefore to enter the rapid growth phase. The consequence is the absence of egg laying and the failure to produce offspring. The deficiency to deposit VLDL and VTG, which are produced at normal levels in the liver, into their oocytes leads to severe hyperlipidemia and features of atherosclerosis in the mutant females, thus being an ideal model for studies of atherogenesis (Nimpf, Radosavljevic et al. 1989; Bujo, Yamamoto et al. 1995).

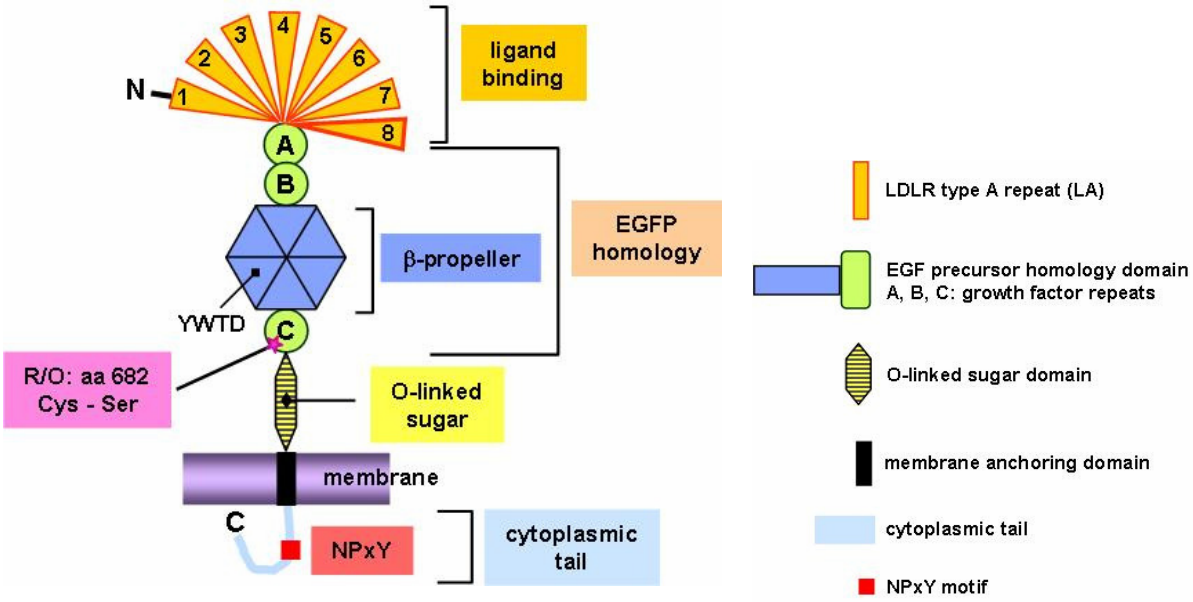

Figure 9. Schematic structure of the chicken VLDLR homologue LR8.

The domains of LR8 are: ligand binding domain with eight LA-repeats; an EGFP homology domain consisting of two EGF repeats (A, B) followed by a six-bladed beta-propeller and an adjacent C-terminal EGF repeat (C); an O-linked sugar domain that is either present (in the isoform LR8+) or absent (in the isoform LR8-); a short transmembrane domain; and finally, a short cytoplasmic tail containing an internalization motif (NPxY) required for endocytosis. The point mutation responsible for the R/O phenotype located in the EGF repeat C is indicated with an asterisk.

Apolipoprotein E receptor 2 (apoER2)

Apolipoprotein E receptor 2 (apoER2) is a member of the LDLR gene family, found mainly in brain, placenta, and testis, which acts in endocytosis and in signal transduction (Kim, Iijima et al. 1996). In particular, apoER2 functions as a cellular receptor for Reelin, a signaling factor that regulates neuronal migration processes in the embryonic brain. ApoER2-deficient mice display abnormal layering of neurons in the cortex, hippocampus, and cerebellum, and these mice also suffer from male infertility (Hiesberger, Trommsdorff et al. 1999; Trommsdorff, Gotthardt et al. 1999). In a recent study apoER2 has been identified to have a crucial role in sperm maturation, in particular in the acquisition and development of sperm motility (Andersen, Yeung et al. 2003).

LR7/8B, the chicken homologue of apoER2

The human apoER2 and LR7/8B in chicken are not two distinct new members of the LDLR gene family, but rather are variants derived from the same gene (Novak, Hiesberger et al. 1996; Brandes, Novak et al. 1997). LR7/8B in chicken is apparently only expressed in brain, which is in sharp contrast to other members of the LDLR gene family. The expression can be allocated to two different types of cells: first, to large neurons and second, to cells constituting brain barriers such as endothelial cells of blood vessels. LR7/8B was shown to be a receptor for activated α_2-macroglobulin (Stockinger, Hengstschlager-Ottnad et al. 1998).

Mammalian and chicken LRP1/ α_2-macroglobulin receptor

LRP1 is a multiligand receptor involved in a variety of independent processes such as lipoprotein metabolism (binding mainly apoE-enriched lipoproteins) and extracellular proteinase homeostasis (Herz, Hamann et al. 1988; Strickland, Kounnas et al. 1995). The latter function is mediated by α_2-macroglobulin (α_2M), a multifunctional proteinase inhibitor. α_2M forms complexes with a variety of

proteinases that are rapidly removed from the circulation by specifically binding to hepatic LRP1. The cytoplasmic tail harbours, additionally to the two NPxY motifs, a YxxL motif, which appears to be the dominant determinant for internalization (Li, Marzolo et al. 2000).

Recently, it has been shown that LRP1 inhibits complement protease expression by suppressing cell signaling through the IκB kinase (IKK)/nuclear factor-κB (NF-κB) pathway. NF-κB is a ubiquitous regulator of inflammation and cell survival in diverse cell types. This ability of LRP1 to regulate cell signaling represents a novel mechanism by which LRP1 controls cell physiology (Gaultier, Arandjelovic et al. 2008).

The avian LRP1/ α_2-macroglobulin receptor (α_2MR) shows an overall identity of 83% with human LRP1/α_2MR (Stifani, Barber et al. 1991; Nimpf, Stifani et al. 1994). It is expressed in somatic cells, and it was shown that LRP1 does not metabolize chylomicron remnants. LRP1 binds Ca^{2+}, α_2M, and VTG. These results indicate that avian LRP1 plays a crucial role in the reproduction of oviparous species, i.e. in vitellogenesis.

LR11/SorLA and its chicken counterpart

LR11 is a complex seven-domain mosaic protein containing a cluster of 11 ligand binding repeats and a domain with homology to VPS10, a yeast receptor for vacuolar protein sorting. It has been first identified in rabbit and was subsequently found in chicken. The mammalian receptor is highly expressed in brain and is present at significant levels in liver, adrenal glands, and testis (Yamazaki, Bujo et al. 1996; Morwald, Yamazaki et al. 1997).

LR11 is sterol insensitive; this fact suggests functions other than in lipoprotein metabolism, but the expression of LR11 in tissues with active cholesterol metabolism should not be overlooked.

Thus, the chicken, human, rabbit LR11 and LR7/8B in chicken and mouse (Novak, Hiesberger et al. 1996) are proposed to be members of a hitherto unknown branch of the LDLR gene family, which may participate in brain-specific physiological processes.

A few years ago, it was reported that LR11 acts as neuronal sorting receptor that binds amyloid precursor protein (APP) and regulates its trafficking and proteolytic processing into amyloid β-peptide (Aβ), the process causative to Alzheimer's disease (Andersen, Reiche et al. 2005; Dodson, Andersen et al. 2008).

LRP2, previously named gp330 and megalin

LRP2, originally identified as a pathogenic antigen of Heymann nephritis, is a member of the LDLR gene family. LRP2 is a 600kDa type I transmembrane protein (Kerjaschki and Farquhar 1982) with a large, amino-terminal extracellular domain, a single transmembrane domain, and a short carboxy-terminal cytoplasmic tail containing 3 NPxY motifs, which mediate clustering in clathrin-coated pits (Christensen and Birn 2002). LRP2 is a multiligand, endocytic receptor, which is localized to the plasma membrane and the endocytic apparatus of epithelial cells including the small intestine, renal proximal tubule, and the visceral yolk sac (Kozyraki and Gofflot 2007). Ligands for LRP2 are vitamin-binding proteins like vitamin-D-binding protein, apolipoproteins like apoB, apoE, apoJ (clusterin), steroid hormones, enzymes like lipoprotein lipase, immune- and stress-response-related proteins like Ig light chain, drugs and toxins, and other carrier proteins such as albumin, lactoferrin, and haemoglobin. LRP2 also binds receptor-associated protein (RAP), which is involved in folding of the receptor (Christensen and Birn 2002). Besides this, LRP2 is a calcium-sensing protein (Christensen, Gliemann et al. 1992) that interacts with Cubilin (Fig. 4). Essential functions are associated with this receptor-complex, like ileal absorption of vitamin B_{12}, renal reabsorption and handling of proteins, vitamins, lipids, and iron, embryonic nutrition and development (Moestrup and Verroust 2001; Kozyraki and Gofflot 2007). In the chicken, LRP2 has not been extensively characterized, but there are unpublished data showing that LRP2 is present in the chicken yolk sac and in the embryonic and adult kidney (Plieschnig 2008).

LRP1B/LRP-DIT

LRP1B has been initially discovered as a putative tumor suppressor, involved in non-small cell lung carcinoma (Liu, Musco et al. 2000), and was therefore also designated LRP-DIT (LRP deleted in tumor). LRP1B shows the highest homology to LRP1, containing one additional ligand binding repeat and an insertion of 33 amino acids in the cytoplasmic domain compared to LRP1. Although the biological functions of LRP1B have not been clearly defined, LRP1B has been shown to bind several LRP1 ligands, and therefore may also play roles in a wide variety of cellular processes. Despite the similarities between LRP1 and LRP1B, the endocytosis rate of LRP1B is markedly slower (Liu, Li et al. 2001; Knisely, Li et al. 2007). This difference in endocytic rate could have important implications for the biological and tumor suppressor functions of LRP1B.
A predicted sequence (XM_422146.2) in the NCBI database likely encodes a putative chicken LRP1B.

Interaction of the LDLR with apolipoproteins

Apolipoprotein B (apoB)

Apolipoprotein B (apoB) is a large amphipathic protein that serves an essential role in the assembly and secretion of lipids, including triglycerides and cholesterol of both dietary and endogenous source, and also in the intravascular transport and receptor-mediated uptake and delivery of distinct classes of lipoproteins. The importance of apoB ranges from the absorption and processing of dietary lipids to the regulation of circulating lipoprotein levels (Davidson and Shelness 2000; Olofsson and Boren 2005).
In mammals, apoB circulates in two distinct forms, apoB100 and apoB48. Both forms are encoded by a single *apoB* gene. The molecular mechanism responsible for the production of the two isoforms involves a site-specific mRNA modification by deamination, referred to as C-to-U editing (see Fig. 10).

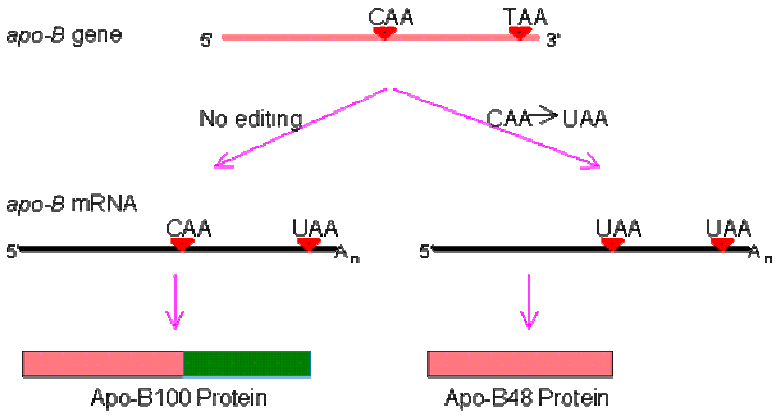

Figure 10. mRNA editing of the *apoB* gene.

In mammals, the *apoB* gene is expressed in hepatocytes and intestinal epithelial cells. However, in liver cells, its product is a 500 kDa protein called apoB100, whereas in intestinal cells, its product is a smaller protein called apoB48. The apoB100 is translated from unedited RNA, but the apoB48 is synthesized from mRNA, whose sequence has been altered by a specific enzyme. This enzyme changes codon 2153, CAA, in the middle of the original mRNA to the stop codon UAA, thereby causing early termination of the protein synthesis.

ApoB100 (Fig. 11) representing the full-length protein of about 500kDa, is exclusively expressed in the liver and is required for the synthesis and secretion of very-low-density lipoprotein (VLDL). ApoB100 is the major protein component of low-density lipoprotein (LDL), a catabolic product of VLDL, and contains the domain required for the interaction with the LDLR (Young 1990; Davidson and Shelness 2000).

ApoB100 also plays a central role in the development of atherosclerosis. Two proteoglycan-binding sequences in apoB100 have been identified, which are important for retaining the lipoprotein in the intima of the artery. Retention is essential for the development of atherosclerotic lesions (Glass and Witztum 2001; Skalen, Gustafsson et al. 2002; Olofsson and Boren 2005).

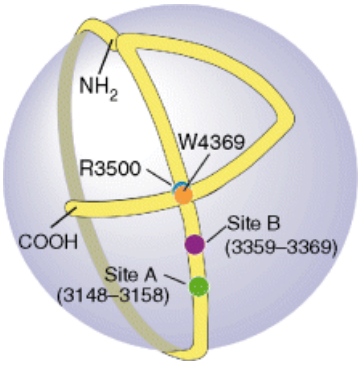

Figure 11. Organization of apoB100 on the LDL particle.

ApoB100 (yellow band) spans the entire circumference of the LDL particle and there is an interaction between the C-terminal part and the N-terminal part. The C-terminal end folds back over the preceding portion of the molecule, a folding that is dependent on the interaction between amino acid 3500 and 4369, which prevents the C-terminal part from sliding over the LDLR-binding site (site B amino acids 3359-3369). The proteoglycan-binding sites A and B (B is also the LDLR-binding site) are indicated (Olofsson and Boren 2005).

ApoB48 corresponds exactly to the N-terminal 48% of apoB100, has a size of about 240kDa and is synthesized by the intestinal epithelial cells. In humans, apoB48 circulates in association with chylomicrons (CM) and chylomicron remnants (CR). Under normal circumstances, plasma residence time of chylomicrons in humans is very short (minutes to hours) compared with that of LDL (~two days). Thus apoB48 can be viewed as a crucial adaptation by which dietary lipids are delivered from small intestine to liver. In contrast, apoB100 can be regarded as participating in the transport and delivery of endogenous plasma cholesterol (Young 1990; Davidson and Shelness 2000).

Apolipoprotein E (apoE)

Apolipoprotein E (apoE) is a 34kDa protein consisting of 299 amino acids. Its complete amino acid sequence has been published in 1982 (Rall, Weisgraber et al. 1982), and is associated with VLDL, β-VLDL, chylomicrons, and less frequently with HDL (Mahley 1988). ApoE, which stabilizes lipoprotein particles, plays an important role in regulating cholesterol homeostasis as well as in regulating plasma triglyceride clearance through its interaction with members of the LDLR gene family (Mahley 1988).

ApoE-containing lipoproteins are the principal lipid transport vehicles in cerebrospinal fluid. Another feature of apoE is that its expression is induced at high concentration in peripheral nerve injury and appears to play a key role in repair by redistributing lipids to regenerating axons (Pitas, Boyles et al. 1987; Mahley and Huang 1999).

ApoE is also involved in immunoregulation and host defense. ApoE improves resistance to *Klebsiella pneumoniae* and *Listeria monocytogenes* infection and inhibits malaria sporozoite invasion of hepatocytes. The mechanisms of immune modulation by apoE are diverse and complex, and the impact of apoE on human immunity is poorly understood (Mahley and Rall 2000; Li, Thompson et al. 2008).

ApoE is a ligand for LDLR, VLDLR, apoER2, LRP1, and LRP2. Unlike other apolipoproteins, apoE is not only synthesized in the liver, but also in brain, spleen, lung, kidney, smooth muscle cells, ovaries, and in macrophages (Lin, Xu et al. 1986; Li, Thompson et al. 2008). ApoE (Fig. 12) is composed of two structurally and functionally independent domains, a 22kDa N-terminal domain (residues 1-191) that

is recognized by receptors and a 10kDa C-terminal domain (residues 218-299) with high affinity for lipid, responsible for the association of apoE with lipoproteins (Aggerbeck, Wetterau et al. 1988; Wetterau, Aggerbeck et al. 1988; Morrow, Segall et al. 2000). This amphipathic α-helical lipid-binding domain allows apoE to switch between a lipoprotein-bound and a lipid-free state. The LDLR-binding region (in the vicinity of residues 136-150) of apoE, located in helix 4 (Fig. 12), is enriched in basic amino acids (lysyl- and arginyl-residues) that are thought to interact with acidic residues in the ligand binding domains of members of the LDLR gene family (Weisgraber 1994).

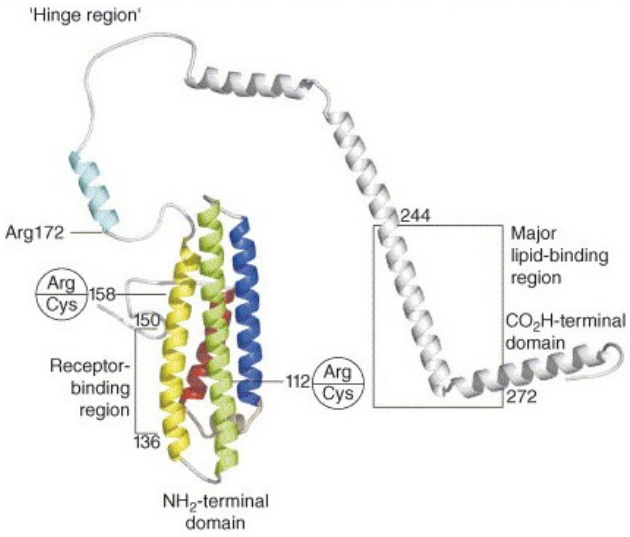

Figure 12. Model of the structure of lipid-free apoE.

The N-terminal domain consists of a four helix-bundle (1, red; 2, blue; 3, green; 4, yellow). The LDLR-binding region resides on helix 4. The hinge region, connecting N- and C-terminus, contains Arg172 for high-affinity binding to the LDLR. The N-terminus also contains the polymorphic positions 112 and 158 that distinguish the three common isoforms. The C-terminal domain (gray) contains the main lipoprotein-binding elements [modified from (Hatters, Peters-Libeu et al. 2006)].

Full receptor-binding activity also requires an arginine at position 172, which is located in the hinge region (see Fig. 12) (Morrow, Arnold et al. 2000). Lipid-free apoE does not bind with high affinity to the LDLRs, and therefore apoE must be associated with lipids. Although the N-terminal domain binds lipid, the principal lipoprotein-binding elements lie in the C-terminus at residues 244-272 (Hatters, Peters-Libeu et al. 2006).

ApoE is polymorphic, which influences its functional and structural properties. The three common allelic isoforms, apoE2, apoE3, and apoE4, differ at positions 112 and

158. ApoE3, the most common isoform, contains cysteine and arginine, whereas apoE2 has two cysteines, and apoE4 has two arginines at these positions (see Fig. 13).

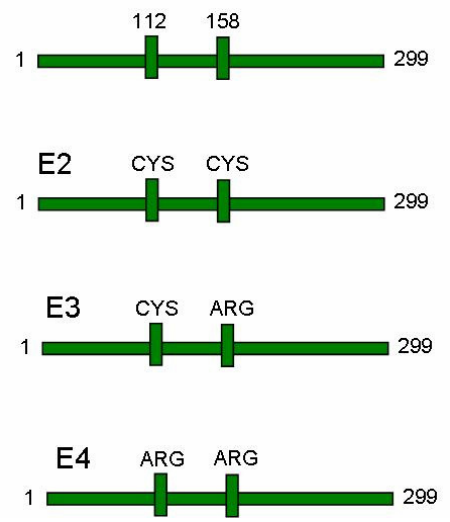

Figure 13. Scheme of the 3 common allelic isoforms of apoE.

ApoE2 contains 2 cysteines on positions 112 and 158, apoE3 comprises cysteine and arginine, and apoE4 has two arginines.

			Functional differences		
Isoform	**Average allelic frequency (%)**	**Amino acid variation (residue) 112 158**	**LDLR affinity**	**Lipoprotein-binding preference**	**Associated disorders**
ApoE2	7	Cys Cys	low	HDL	Type III hyperlipoproteinemia
ApoE3	78	Cys Arg	high	HDL	none known
ApoE4	15	Arg Arg	high	VLDL, LDL	Alzheimer's disease; atherosclerosis

Table 2. Prevalence of the human apoE isoforms and their key differences.

The table is modified from (Hatters, Peters-Libeu et al. 2006).

ApoE3 and apoE4 bind the LDLRs with similar affinity, but the binding of apoE2 is 50- to 100-times weaker (see table 2). This binding defect results in delayed receptor-mediated clearance of lipoproteins from the circulation and in combination with genetic, hormonal or environmental influences results in familial type III hyperlipoproteinemia. Type III hyperlipoproteinemia is a genetic disorder characterized by elevated plasma cholesterol and triglyceride levels and accelerated coronary artery disease. The cysteine at position 158 leads to a new salt bridge between Arg150 and Asp154. This salt bridge alters the conformation of Arg 150 with

respect to the other basic residues in the receptor-binding region (amino acids 136-150), reducing the ability of apoE2 to interact effectively with the LDL receptor (Dong, Parkin et al. 1996; Hatters, Peters-Libeu et al. 2006).

The most pronounced pathological effect attributable to the apoE polymorphism is the association of apoE4 with common late-onset familial and sporadic forms of Alzheimer's disease (AD). ApoE4 is a major risk factor for AD, accounting for 40-60% of the genetic variability observed in the disease. Its presence not only increases the risk but also lowers the age of onset, of AD (Corder, Saunders et al. 1993; Saunders, Strittmatter et al. 1993). The biochemical mechanism by which apoE4 increases the risk of AD is unknown, but AD patients who are homozygous for the apoE4 allele exhibit more highly developed senile plaques at autopsy than other AD patients. Thus, because neuronal pathology is a characteristic of AD (Nathan, Bellosta et al. 1994), apoE4 may contribute to the pathogenesis of AD.

Binding of apoE to the LDL receptor

The ligand binding domain of the LDLR contains seven imperfect repeats of a 40-amino acid cysteine-rich sequence (see Fig. 5). The LDLR has been shown to bind two different proteins, apoB100 and apoE. LDL contains a single copy of apoB100, and β-migrating VLDL (β-VLDL) contains apoB100 or apoB48 and multiple molecules of apoE.

Each repeat comprises clustered negative charges that have been postulated as ligand binding sites. An early study has gained insights in the ligand binding domain of the LDLR via mutational analysis (Esser, Limbird et al. 1988). It was shown that the seven repeats in the ligand binding domain of the LDLR are functionally not equivalent. Deletion of repeat 1 (ΔR1) does not change the binding of LDL or β-VLDL (see Fig. 14). Repeat 2 plus 3 (ΔR1-3) and repeat 6 plus 7 (ΔR6, 7) are required for maximal binding of LDL, but not of β-VLDL. Repeat 5 of the ligand binding domain seems crucial for binding of both ligands, as shown with deletion of repeats 1-5 (Fig. 14).

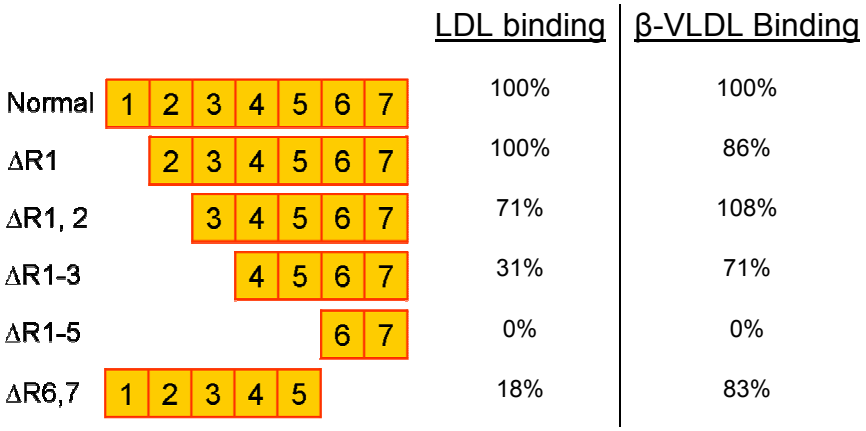

Figure 14. Deletion mutations in the ligand binding domain of the LDL receptor.

Normal: all 7 repeats of the ligand binding domain are present; the repeats remaining in five deletion mutations are depicted below the normal ligand binding domain, and the individual mutations are named on the left. The results are presented as a percentage of the LDL/β-VLDL binding values observed in cells transfected with the normal cDNA [modified from (Esser, Limbird et al. 1988)].

The most definitive evidence for a functional difference between repeats arises if tyrosine is substituted for aspartate in the negatively charged cluster of serine-aspartate-glutamate (SDE). This substitution in repeat 5 (Asp^{206}) nearly abolishes the binding of β-VLDL as well as of LDL (see Fig. 15). The same mutation in repeat 6 (Asp^{245}) had no effect on β-VLDL binding, and LDL binding is only reduced. In repeat 1 (Asp^{36}) this substitution has no effect. These data suggest that repeat 5 plays a much more critical role in binding than do repeats 1 or 6.

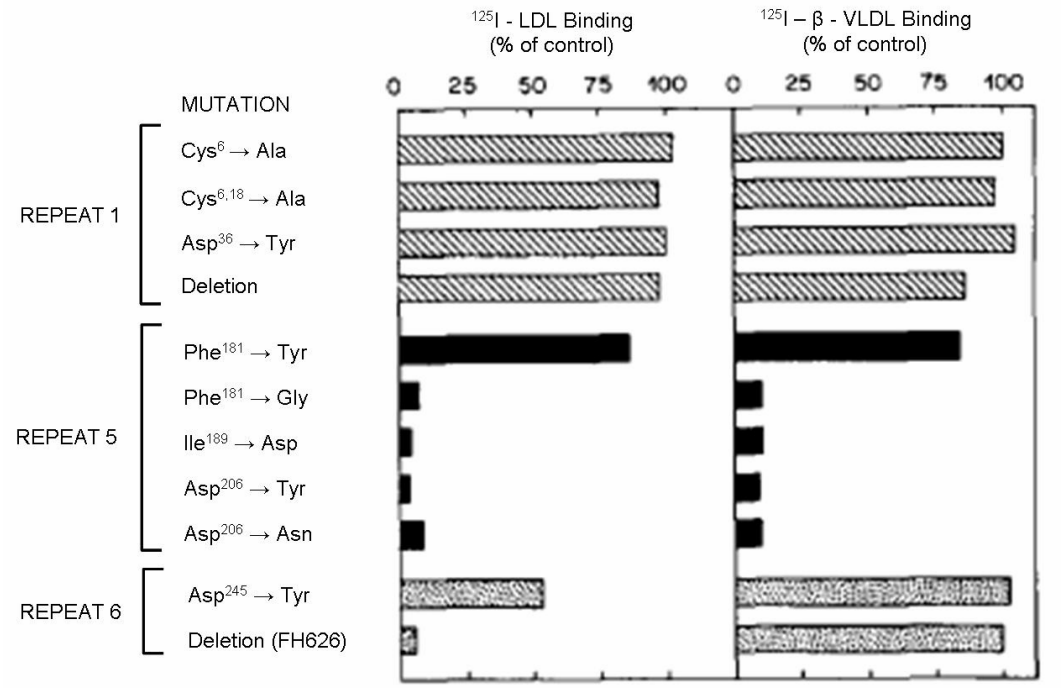

Figure 15. Effects of mutations in residues 1-292 of the LDLR on ligand binding activity.
The mean values obtained at saturating concentrations of ^{125}I-LDL or ^{125}I-β-VLDL for a given mutant LDLR are plotted in histogram form and expressed as percent of control. The repeats in which the mutations occur are indicated on the left (Esser, Limbird et al. 1988).

A recent investigation revealed that the LA4-5 two-repeat pair is sufficient for binding of apoE-containing ligands, and that LA5 alone is not sufficient to recognize these ligands. It has been observed that more than one receptor-binding site in its lipid-activated conformation is required to bind to the LDLR with high affinity (Fisher, Abdul-Aziz et al. 2004).

In another study, swapping and replacing specific LA repeats within the ligand binding module of the LDLR has been performed. They show that LA5 must not only be present, but must exist in the correct context with respect to other LA repeats within the ligand binding domain. The data indicate that the sequential order of LA repeats plays a key role in the binding properties of the LDLR (Yamamoto and Ryan 2009).

The LA5 repeat is particularly important for LDL binding and release. LA5 contains 40 residues, including six cysteines that form three disulfide bridges, and four acidic residues, involved in binding of a structural calcium ion. The calcium ion is structurally and functionally important. In its absence the recombinant LA5 repeat cannot form native disulfide bonds, and LDL binding is impaired at low Ca^{2+} concentrations (Blacklow and Kim 1996).

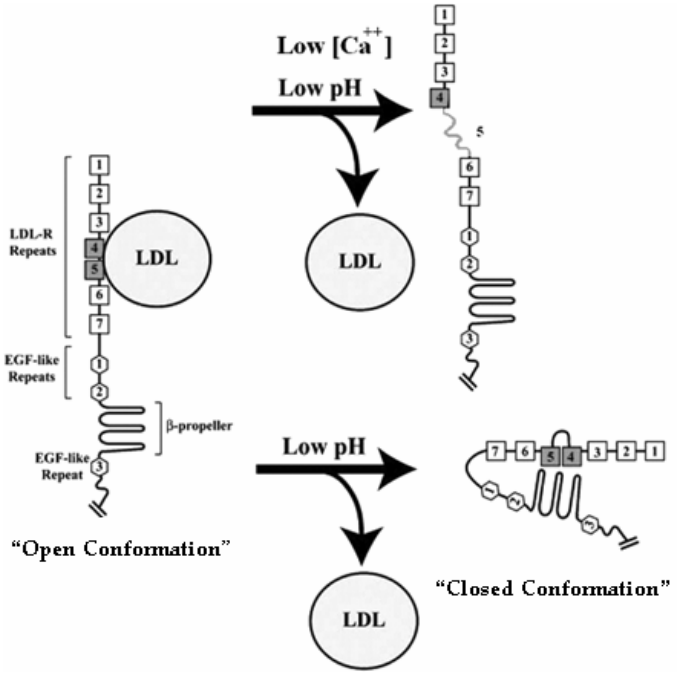

Figure 16. Proposal of a new mechanism for the release of LDL particles in the endosome based on the instability at endosomal low pH and low Ca^{2+} concentrations.

Lower pathway: The conventional model for low pH-induced release of LDL from the LDLR. *Upper pathway:* A new proposal, which shows that under low pH and low Ca^{2+} concentration, LA5 is unable to bind Ca^{2+} and appears in an unfolded conformation not expected to bind LDL particles (Arias-Moreno, Velazquez-Campoy et al. 2008).

Low pH and low Ca^{2+} concentration decrease the stability of LA5, which triggers its unfolding in the endosome, thus providing a mechanism for LDL release from the receptor (see Fig. 16, upper pathway) (Arias-Moreno, Velazquez-Campoy et al. 2008).

In Fig. 16, the lower pathway represents the currently accepted view of pH-induced release of LDL from the LDLR. The LDLR forms an "open conformation" at neutral pH, exposing LA repeats for LDL binding. The acidic environment of endosomes triggers the LDLR to adopt the "closed conformation". At endosomal pH, the β–propeller, rather than LDL, associates with LDL binding repeats, resulting in displacement of LDL (Rudenko, Henry et al. 2002; Debose-Boyd 2004).

Adaptor proteins in endocytosis

Endocytosis, a highly coordinated process, plays a key role in cell homeostasis and signaling (Evans and Owen 2002). Through endocytosis, cells internalize plasma membrane components and nutrients in response to environmental cues or intracellular signals, control the composition of the plasma membrane, downregulate signaling receptors, and recycle transmembrane proteins (Sorkin 2004; Szymkiewicz, Shupliakov et al. 2004). Among the different forms of endocytosis, the most extensively studied and best characterized at the molecular level is the clathrin-mediated endocytosis (CME) pathway (Fig. 17) (Mousavi, Malerod et al. 2004), in which clathrin-coated vesicles (CCV) are formed at the plasma membrane. This pathway requires the action of endocytic adaptor proteins, which select receptors for internalization. These adaptor proteins recruit their cargo into clathrin-coated pits (CCPs) by binding to clathrin and to internalization signals within the cytoplasmic regions of the receptor, which in the case of LDLR family members is the FxNPxY motif.

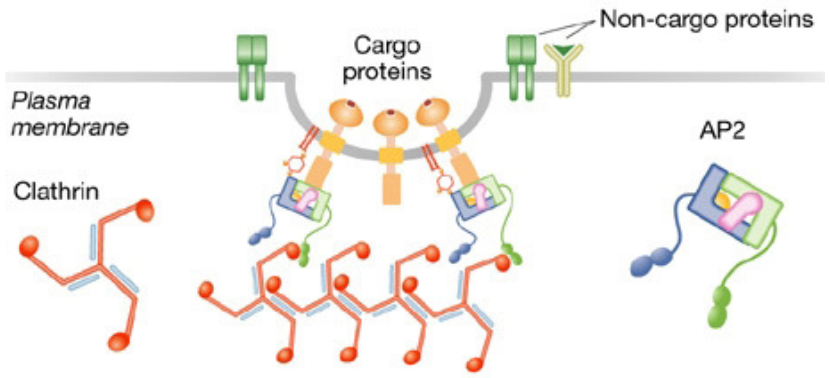

Figure 17. Clathrin-mediated endocytosis.

Transmembrane proteins destined to endosomes are selectively accumulated in clathrin-coated pits at the plasma membrane and rapidly internalized in clathrin-coated vesicles. The recognition of specific sequence motifs in transmembrane cargo by coated-pit proteins confers specificity on the endocytic process. Interaction of membrane cargo with the clathrin adaptor protein complex AP2 is the major mechanism of cargo sorting into coated pits (Puertollano 2004).

The designation “endocytic” adaptors is generally reserved for proteins that bind to the lipid phosphatidylinositol-4,5-bisphosphate (PtdIns(4,5)P_2) and also to clathrin and to internalization motifs. There are two major classes of endocytic adaptors: the classical (multimeric) adaptors like adaptor protein 2 (AP2) (Fig. 18), adaptor protein

3 (AP3), and the alternative (monomeric) adaptors, also known as clathrin-associated sorting proteins (CLASP) like epsins, Dab2, ARH, and Numb (Traub 2003).

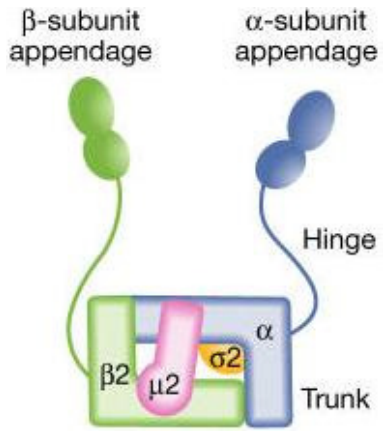

Figure 18. Schematic representation of AP2.

AP2 is a tetramer, which contains large (α and β2 adaptins), medium (μ2), and small (σ2) subunits. The large subunits can be subdivided into an N-terminal (trunk) domain and a globular C-terminal (appendage) region, which are connected via a hinge. AP2 binds clathrin through the β2-hinge and the appendage domains. Alternative adaptors and regulatory proteins are bound via the α- and β2-appendage domains. The μ2 domain functions in the recognition of sorting motifs that are present in the cytosolic tail of different cargo proteins. PtdIns(4,5)P_2 binding sites are present in both α- and μ2-subunits (Puertollano 2004).

Recently, the identification of the molecular defect responsible for a recessive form of hypercholesterolemia that clinically resembles FH provided new insights into LDLR physiology. This disorder, called Autosomal Recessive Hypercholesterolemia (ARH), is caused by mutations in the adaptor protein ARH, also termed LDLR adaptor protein 1 (LDLRAP1) (Garcia, Wilund et al. 2001). ARH is a newly discovered adaptor protein required for the efficient activity of LDLR in selected tissues and for the efficient internalization of the LDL-LDLR complex (Eden, Patel et al. 2002). It has been shown that ARH binds to the LDLR cytoplasmic tail as well as to two components of the clathrin-coated pit, the heavy chain of clathrin (Fig. 19), and the β2-subunit of the adaptor protein AP2 (He, Gupta et al. 2002).

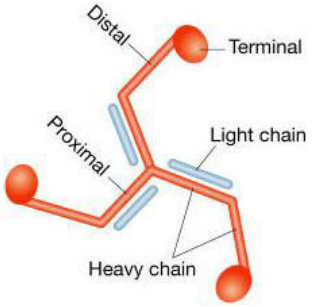

Figure 19. Schematic drawing of clathrin.

The assembly unit of clathrin, commonly referred to as the “triskelion”, consists of three heavy chains and three light chains that oligomerize to form three-dimensional polygonal lattices, or cage-like structures (Puertollano 2004).

ARH binds the FxNPxY motif in the cytoplasmic tails of the LDLR family members and PtdIns(4,5)P_2 via the N-terminal phosphotyrosine binding (PTB) domain. ARH

also binds to clathrin and to AP2 via a C-terminal clathrin-box (aa 212-216: LLDLE) and an AP2 binding region (aa 249-276: WELDDGLDEAFSRLAQSRTNPQVLDTGL) (Fig. 20) (Mishra, Watkins et al. 2002).

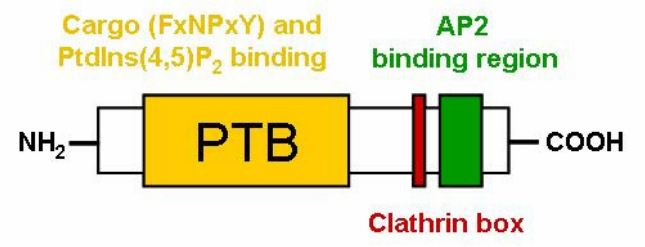

Figure 20. Scheme of the human adaptor protein ARH.

For details see the text. PTB, phosphotyrosine binding domain; AP2, adaptor protein 2
AP2 binding region, WELDDGLDEAFSRLAQSRTNPQVLDTGL;
Clathrin box, LLDLE;

The adaptor protein Numb

Numb is an evolutionarily conserved protein identified two decades ago as a cell fate determinant in the nervous system of *Drosophila*. Numb was reported to regulate cell fate by its asymmetrical segregation in daughter cells during cell division (Uemura, Shepherd et al. 1989; Rhyu, Jan et al. 1994). In contrast, a Numb homologue, identified in chickens, localizes basally rather than apically in dividing avian neuroepithelial cells. Thus, chicken Numb would be segregated to the basal daughter rather than the apical daughter, when a neuroepithelial cell divides with a vertical spindle (Wakamatsu, Maynard et al. 1999).

Numb contains two protein-protein interaction domains, a phosphotyrosine-binding (PTB) domain and a proline-rich region (PRR) that function as a Src-homology-3 (SH3)-binding domain. In *Drosophila* only one form of Numb has been identified. In contrast, in mammals, four different isoforms are known. Mammals produce these four isoforms (Fig. 21) through alternative splicing. The variants differ in the length of their PTB (lacking or containing an insert) and PRR (lacking or containing an insert) domains (Verdi, Schmandt et al. 1996; Dho, French et al. 1999).

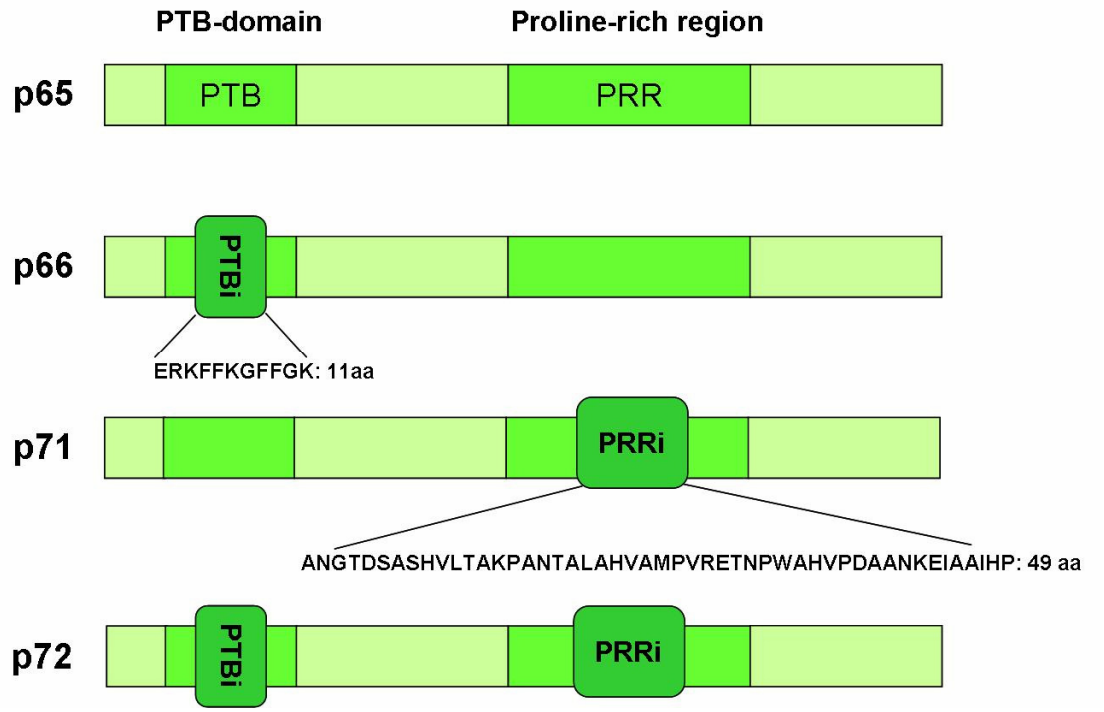

Figure 21. Four different isoforms of mouse Numb.

PTB, phosphotyrosine-binding domain; PTBi, PTB with insert; PRR, proline-rich region; PRRi, PRR with insert;
The insert in the PTB domain is 100% conserved in mammals.

The PTB domain of Numb is evolutionarily and most closely related to that of ARH. The Numb PTB domain is 31% identical (46% similar) to the human ARH PTB domain (Mishra, Watkins et al. 2002). All Numb proteins contain the NPF and DPF motifs critical for interaction with proteins containing the Eps15 homology (EH) domain and with the clathrin protein AP2. It has been shown that the in vivo binding of Eps15 to Numb is most likely mediated by an EH-NPF interaction, and that an intact NPF is necessary but not sufficient for binding (Salcini, Confalonieri et al. 1997). The interaction of Numb with the AP2 complex is dynamically regulated by phosphorylation of Numb. It was suggested that phosphorylation-dependent binding of 14-3-3 protein may regulate AP2 binding to Numb (Tokumitsu, Hatano et al. 2006). Numb can associate with CCPs, vesicles, and endosomes, suggesting that it functions as an endocytic adaptor protein (Santolini, Puri et al. 2000; Berdnik, Torok et al. 2002).

A recent study has found that phosphorylation by adaptor-associated kinase 1 (AAK1), which is an endocytic kinase homologue to the *Drosophila* Numb-associated kinase, may regulate Numb interaction with the coat protein machinery and that

AAK1-dependent phosphorylation may increase Numb affinity for AP2 (Sorensen and Conner 2008).

The PTB domain of Numb seems to be required for the interaction with Sanopodo, which is a four-pass transmembrane protein that regulates Notch signaling in the central nervous system, in vivo. The results in this study establish Numb- and α-Adaptin-dependent endocytosis of Sanopodo as the mechanism by which Notch is regulated during external sensory organ development (Hutterer and Knoblich 2005).

Numb plays a role in the internalization of receptors that are involved in cell fate decisions during central nervous system development, in neuronal maturation, differentiation, and survival. The different human Numb isoforms are suggested to play distinct roles in APP metabolism. They also may provide a novel potential link between altered Numb isoform expression and increased Aβ generation, the principal component of amyloid plaques (Kyriazis, Wei et al. 2008).

Numb negatively regulates Notch, which is an important player in cellular differentiation, proliferation, and apoptotic events, and binds Notch via the PTB-domain (Guo, Jan et al. 1996). A few years ago it was demonstrated that mammalian Numb expression promotes the ubiquitination of membrane-tethered Notch and the degradation of the intracellular domain following receptor activation (Guo, Jan et al. 1996; McGill and McGlade 2003).

The facts that Numb is closely related to ARH and is involved in endocytosis provides two important reasons for considering chicken Numb in the context of studies on chicken LDLR family members.

Aims of the thesis

One aim was to further characterize the protein-protein interaction properties of extracellular and intracellular domains of the avian LDLR. The identification of binding sites in the ligand binding domain necessary to facilitate binding of human apoE to the chicken LDLR was sought. Another aim was to molecularly identify chicken Numb and its isoforms and to investigate their binding to cytoplasmic tails of receptors of the LDLR family. I analyzed possible differences between the interaction of chicken Numb with the human and chicken LDLR. Another aim was to elucidate the relationship of chicken LR8 and LR8B in terms of interaction with chicken Numb, as the internalization motifs of the cytoplasmic tails of these receptors are identical to that of the human LDLR. Finally, since the co-receptor Amnionless contains two internalization signals for receptor-mediated endocytosis and its cytoplasmic tail interacts with chicken ARH, the aim was to study the binding of the chicken Numb to the cytoplasmic domain of chicken Amnionless.

Materials and Methods

Animals

Derco-brown laying hens (purchased from Heindl Co. Vienna, Austria), White Leghorn laying hens, and the R/O breeding colony, derived from a White Leghorn Carrier, were maintained on layer's mash with free access to water and feed under a daily light period of 16 hours. The genotype of the R/O chickens was determined as described before (Bujo, Elkin et al. 1996). Animals were sacrified by decapitation. Polyclonal antibodies were raised in adult New Zealand White rabbits according to standard procedures. All procedures were performed according to the protocols approved by the Animal Care Committee of the Medical University of Vienna.

Preparation of membrane protein extracts

Freshly obtained tissues were placed in ice-cold buffer A (4ml/g tissue) containing 20mM Tris/HCl pH 8.0, 1mM $CaCl_2$, 150mM NaCl, and proteinase inhibitor cocktail tablets (complete Mini, EDTA free, Roche) and were then homogenized with an Ultra Turrax T25 homogenizer 5 times for 30 seconds each. Total homogenates were spun for 10min at 3000 x g. The supernatant was filtered through 4 layers of cheesecloth (gauze) and was ultracentrifuged at 100000 x g for 1h at 4°C. The resulting supernatant was discarded and the centrifugation tube was wiped out to remove remaining lipid. The pellet was washed with 3ml buffer A and subsequent ultracentrifugation for 1h at 4°C. Then the supernatant was discarded and the pellet was solubilized in 1ml buffer B containing 250mM Tris/maleate pH 6.0, 2mM $CaCl_2$ and proteinase inhibitor cocktail tablets (complete Mini, EDTA free, Roche). 4% of the total volume of 4M NaCl was added and the samples were sonicated for 30 sec. After adding 10% Triton X-100 to a final concentration of 2%, and ddH_2O to a total volume of 2ml, the extract was ultracentrifuged for 1h at 100000 x g at 4°C. The resulting supernatant was stored at -80°C until use. Protein concentrations were determined according to Bradford (Bio-Rad Protein Assay).

SDS-PAGE and Western blot analysis

One-dimensional SDS-PAGE (7,5% - 15%) was performed using a minigel system (Bio-Rad). Samples were prepared in the presence (reducing conditions) or in the absence (non-reducing conditions) of 25mM DTT or beta-Mercaptoethanol. Molecular weights were estimated by use of molecular weight markers (Kaleidoscope Prestained Standards, Bio-Rad; PageRuler Plus Prestained Protein Ladder, Fermentas). The gels were either stained with Coomassie Blue (10% glacial acetic acid, 25% isopropanol, 0,278g/l Coomassie Blue R250; GelCode Blue Stain Reagent, Pierce) or subjected to Western blot analysis. Proteins were transferred to a nitrocellulose-membrane (Hybond-C, Amersham Pharmacia Biotech) by wet blotting at 100V. Nonspecific binding sites were blocked with TBS (25mM Tris/HCl pH 7.4, 140mM NaCl, and 2,5mM KCl) containing 0,1% Tween-20 and either 5% (w/v) non-fat dry milk or 2% BSA (bovine serum albumin) (blocking buffer) for 1h at room temperature (RT). Primary antibodies were detected with horseradish peroxidase (HRP)-conjugated goat anti-rabbit IgG (1:50000, Sigma) or HRP-conjugated goat anti-mouse IgG (1:1500, Promega) and enhanced chemiluminescence (Pierce).

Ligand blotting

For ligand blotting, nitrocellulose strips containing SDS-PAGE separated protein extracts were incubated for 1h at RT with TBS (25mM Tris/HCl pH 7.4, 140mM NaCl, and 2,5mM KCl) containing 0,1% Tween-20 and either 5% (w/v) nonfat dry milk or 2% BSA (bovine serum albumin), and 2mM $CaCl_2$ (blocking buffer). The strips were then incubated with the indicated ligand at 4°C overnight. Subsequently the strips were washed three times for 20min with TBS containing 2mM $CaCl_2$ and 0,1% Tween-20 and then incubated with the primary antibodies in blocking buffer for 1h at RT. After washing three times for 10min, the bound primary antibody was detected with either HRP-conjugated goat anti-rabbit IgG (1:50000, Sigma) or HRP-conjugated goat anti-mouse IgG (1:1500, Promega) and enhanced chemiluminescence (Pierce).

Site-directed mutagenesis of the ligand binding domain (LA7) of the chicken LDLR

Mutations were introduced by site-directed mutagenesis according to the protocol (QuikChange II XL Site-Directed Mutagenesis Kit, Stratagene).

The pMAL-vector containing the ligand binding domain of the LDLR (Hummel, Lynn et al. 2003) was used as template for the site-directed mutagenesis.

Mutagenesis was performed with the following mutagenic sense and antisense primer (table 3):

LA7m	sense	5'- GAC GGC AGC GAT GAG **TC**G CCC GAA ATG TGC CGC GG-3'
	antisense	5'- GCG GCA CAT TTC GGG C**GA** CTC ATC GCT GCC GTC GG-3'
LA7m5	sense	5'-GAT GGG TCC GAC GAG GA**A** GGA TGC GAC CCC CCC-3'
	antisense	5'-GGG GGG GTC GCA TCC **T**TC CTC GTC GGA CCC ATC-3'
LA7Δ	sense	5'-GAA CGG AGC CCG ACG TGC Δ GGG GTC GTC CCC CGG CCC-3'
	antisense	5'-GGG CCG GGG GAC GAC CCC Δ GCA CGT CGG GCT CCG TTC-3'
LA7dbl	sense	5'-GAT GGG TCC GAC GAG GA**A** GGA TGC GAC CCC CCC-3'
	antisense	5'-GGG GGG GTC GCA TCC **T**TC CTC GTC GGA CCC ATC-3'

Table 3. Primers used for the site-directed mutagenesis of ggLA7.
Letters or symbols in green indicate the site of mutations.

For the LA7 double mutant (LA7dbl) the LA7m plasmid DNA was applied as a template and the LA7m5 primers were used for introducing the second mutation. The constructs were verified by sequencing using pMAL-seq forward and reverse primer (table 4), primers specific for the pMAL-vector.

pMAL-seq forward	5'-AAC CTC GGG ATC GAG GG-3'
pMAL-seq reverse	5'-CCA GTG CCA AGC TTG GTA CC-3'

Table 4. Primers specific for pMAL sequencing.

Expression, purification, and refolding of ggLA7 wild type and ggLA7 mutants

The expression was carried out as previously described (Bajari, Strasser et al. 2005), besides that the induction was done at an OD_{600} of 0.6 and at 37°C. The recombinant His fusion proteins were purified by Ni-NTA affinity chromatography according to the manufacturer's instructions (Qiagen). For refolding of the recombinant proteins, purified HisRAPmyc was coupled to CNBr-activated Sepharose (Amersham-Pharmacia Biotech) according to the manufacturer's protocol. The proteins were refolded as described before (Bajari, Strasser et al. 2005).

Co-Immunoprecipitation

The receptor was incubated with the ligand for 2h at room temperature on an overhead shaker. After this incubation step the appropriate antibody was added and incubated at 4°C for 2h on an overhead shaker. After that 50µl of Protein A Sepharose were added and rotated over night at 4°C. The beads were washed four times with 1xTBST + 2mM $CaCl_2$ supplied with protease inhibitors with centrifugation steps at 370 x g for 2min at 4°C in-between. After the final centrifugation step 70µl reducing Laemmli buffer were added and the mixture was heated for 10min at 95°C. Then the samples were applied to SDS-PAGE and analyzed by Western blotting.

Antibodies

Murine monoclonal Penta-His antibody (Qiagen; used at 1:2000), mouse anti-glutathione S-transferase (GST) antibody (BD Pharming; used at 1:2000), mouse anti-maltose-binding-protein (MBP) antibody (New England Biolabs; used at 1:30000), mouse anti-HSV antibody (Novagen; used at 1:20000) and mouse anti-human ApoE (Sigma; used at 1:5000) were purchased from the indicated source. Mouse anti-c-myc was secreted of the hybridoma cell line clone 9E10 (ATCC; used 1:100). The hybridoma cell line was purchased from the indicated source. Rabbit

anti-ggLR8 IgG (used at 2µg/µl) was prepared as described previously (Bujo, Yamamoto et al. 1995). Polyclonal Antibody against the chicken LA domain (anti-LA1-7; used at 1:1000) was prepared as described before (Hummel, Lynn et al. 2003). The antiserum against chicken Numb (anti-Numb; used at 1:500), against a peptide representing the C-terminal 20 aa, was prepared as described previously (Dichlberger 2004). The human ARH antibody (#65; used at 1:500), against a peptide corresponding to the amino acids 89-117, was prepared as described elsewhere (Grünstäudl 2005). Anti-rabbit HRP (horseradish peroxidase)-conjugated antibodies (Sigma; used at 1:50000), and anti-mouse HRP-conjugated antibodies (Promega; used at 1:1500) were purchased from the indicated source.

Cell culture and ApoE preparation

Chinese hamster ovary (CHO) cells secreting human apoE2, apoE3, and apoE4 isoforms characterized in (Stannard, Riddell et al. 2001; Sacre, Stannard et al. 2003) were used as source of human apoE-containing lipoprotein particles. ApoE-secreting cells and control CHO cells were cultured in 100 mm dishes with Iscove's MEM supplemented with 5% FCS, 1% non essential amino acids, 1% glutamine, and 1% penicillin/streptomycin. Before harvesting the apoE isoforms, cells were cultured in 150 mm dishes. At a confluence of 80% the growth medium was switched to harvesting media (OptiMEM, Invitrogen). The isoform conditioned media were collected 3-4 times after 12 h conditioning period and concentrated using Amicon-Ultra concentration columns with a 30 MWCO (molecular weight cut off). ApoE isoform levels were quantified by ELISA (ApoE/Pan-ApoE ELISA kit, MBL).
DKO-R cells were maintained as described in Wettey et al (Wettey, Hawkins et al. 2002). The cells were harvested, if they were 80% confluent.

Cloning of chicken Numb isoforms

cDNA was generated by reverse-transcriptase PCR (Superscript II, Invitrogen) using total RNA (Nucleo Spin, Macherey&Nagel) of different tissues of laying hens.

Sequence-specific primers for RT-PCR were designed using the potential chicken *Numb* sequence from the NCBI (www.ncbi.nlm.nih.gov) and Ensembl (www.ensembl.org) databases. PCR of full-length chicken *Numb* was performed using the forward primer including an EcoRI restriction site (bold) 5'-AA**GAATTC**CATGAATAAATTACGGCAG-3' corresponding to nucleotides 1 to 18 of the NCBI sequence and the reverse primer including a XhoI restriction site (bold) 5'-GT**CTCGAG**AAGTTCAATCTCAAATGTC-3' corresponding to nucleotides 1728 to 1746. The PCR product was T/A cloned into the pCR2.1 vector (Invitrogen) and confirmed by DNA sequencing using the standard sequencing primer M13 forward and M13 reverse.

Prokaryotic expression of recombinant His-tagged chicken Numb isoforms

The insert of the clone with the right sequence (see above) was cut out and directly cloned in-frame into the pET-25b+-expression vector (Novagen) providing a C-terminal HSV- and His-tag. Recombinant ggNumb-His was expressed in *E. coli* BL21 Star chemically competent cells (Invitrogen). Expression was performed according to the protocol from Qiagen.

Cloning of the chicken Numb PRR insert and prokaryotic expression

The cloning procedure was carried out as for the chicken Numb isoforms and also the prokaryotic expression.
Unless for full-length PRRi RT-PCR the following primers were used, the forward primer including an EcoRI restriction site (bold) 5'-CA**GAATTC**CGTTAATGGCACTGCC-3' and the reverse primer containing a XhoI restriction site (bold) 5'-GT**CTCGAG**GCCAGAGACCATGGC-3'.

GST-tagged fusion proteins

For my studies, I used four different cytoplasmic tails (ct), these are: chicken LDLR ct, human LDLR ct, chicken LR8 ct, and chicken LR8B ct. The cloning, expression, and purification of GST-His-ggLDLRct and GST-humanLDLRct-myc were described in (Grünstäudl 2005). The design of GST-ggLR8ct-myc and GST-ggLR8Bct-myc were described in (Gschmeidler 2004).
The full-length ARH was cloned into pGEX-5X-1 vector (Amersham Biosciences) to generate a GST-tagged fusion protein. The cloning, expression, and purification of GST-ARH were described in (Grünstäudl 2005).

His-tagged fusion proteins

His-tagged chicken Amnionless cytoplasmic tail (ggAmnionless ct-His) was cloned, expressed, and purified as described in (Christian 2006).
The expression of His- and myc-tagged RAP was performed as depicted in (Bajari, Strasser et al. 2005).

Results

LDL receptor in human and chicken

The LDLR (Brown and Goldstein 1974; Goldstein and Brown 1974; Brown and Goldstein 1986) is an important component in the feed-back maintenance of cholesterol homeostasis, a well-understood mechanism in mammals. Following LDLR-mediated endocytosis, LDL-derived cholesterol and its intracellularly generated oxidated derivatives mediate a complex series of feedback mechanisms to protect the cell from overaccumulation of cholesterol.

The first avian LDLR was identified only in 2003 (Hummel, Lynn et al. 2003). Likely reasons for the long-term failure to identify and characterize LDLRs in egg-laying species are their low expression levels and modest sterol-mediated regulation compared to their mammalian relatives. The chicken LDLR cDNA (NCBI; AJ 515243) displays an open reading frame of 2676bp, and the gene's chromosomal location has not been established yet.

The structure of the novel protein entirely conforms to that of the mammalian LDLR (see Fig. 22). Besides containing all of the common structural elements of the lipoprotein receptor family, the hallmarks of the LDLR are *i)* a ligand binding domain consisting of seven LA repeats, where the first four are separated from repeats five through seven by a linker of variable length; *ii)* the EGF precursor homology domain; *iii)* an O-linked sugar domain; *iv)* a membrane anchoring domain and *v)* a short cytoplasmic tail containing an internalization signal, which is important for endocytic activity.

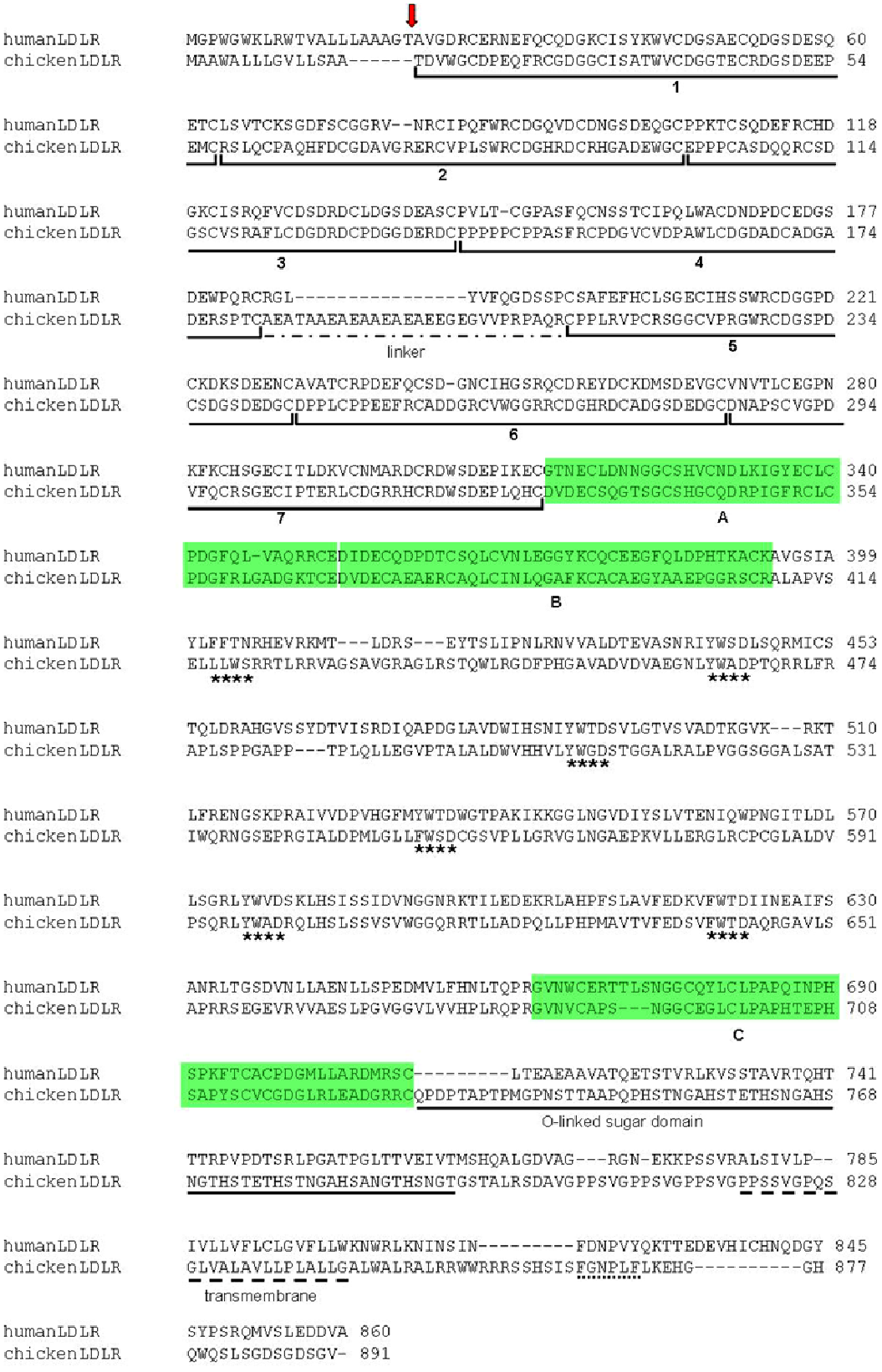

Figure 22. Sequence comparison of chicken LDLR and human LDLR.

Numbering of the amino acid sequences starts at the methionine residue corresponding to the initiation codon. Gaps (-) have been introduced to optimize the alignment.
1-7 are the seven ligand binding (LA) repeats; the EGF repeats A, B, and C are in green; the O-linked sugar domain is underlined; the transmembrane domain is indicated by a dashed line; the internalization signal is indicated by a dotted underline; the six “YWTD” tetrapeptides (Jeon, Meng et al. 2001) are marked with asterisks. The red arrow shows the signal peptide cleavage site.

The chicken LDLR appears to interact prefentially with chicken LDL, and less with chicken VLDL. This is significant, since avian LDL and VLDL particles differ in lipid composition. Furthermore, chicken LDL and VLDL contain only the apoB100 isoform of apoB and lack apoE, which is not expressed in birds.

Characterization of the chicken LDLR ligand binding domain

Site-directed mutagenesis of the ligand binding domain

The human LDLR and the chicken LR8 (Steyrer, Barber et al. 1990) both bind apoE, i.e. apoE3 and apoE4 with high affinity and apoE2 with much reduced affinity. Due to the fact that the human LDLR and the ggLR8 bind apoE (Fig. 24), but the ggLDLR does not, one aim of my thesis was to mutate the ggLDLR ligand binding domain at specific positions, which are known to be important for apoE binding in mammalian receptors. The objective was to determine the sites, which are crucial for binding of apoE to the LDLR and to exploit the avian system to better understand the interaction of apoE with the LDLR at the molecular level.

The specific mutations shown in Fig. 23 were introduced with site-directed mutagenesis as described in Materials and Methods, in an attempt to change the chicken receptor's ligand binding domain more like that of the human protein and thereby to gain insight into the overall structure of the ligand binding domain and the details of its interaction with apoE.

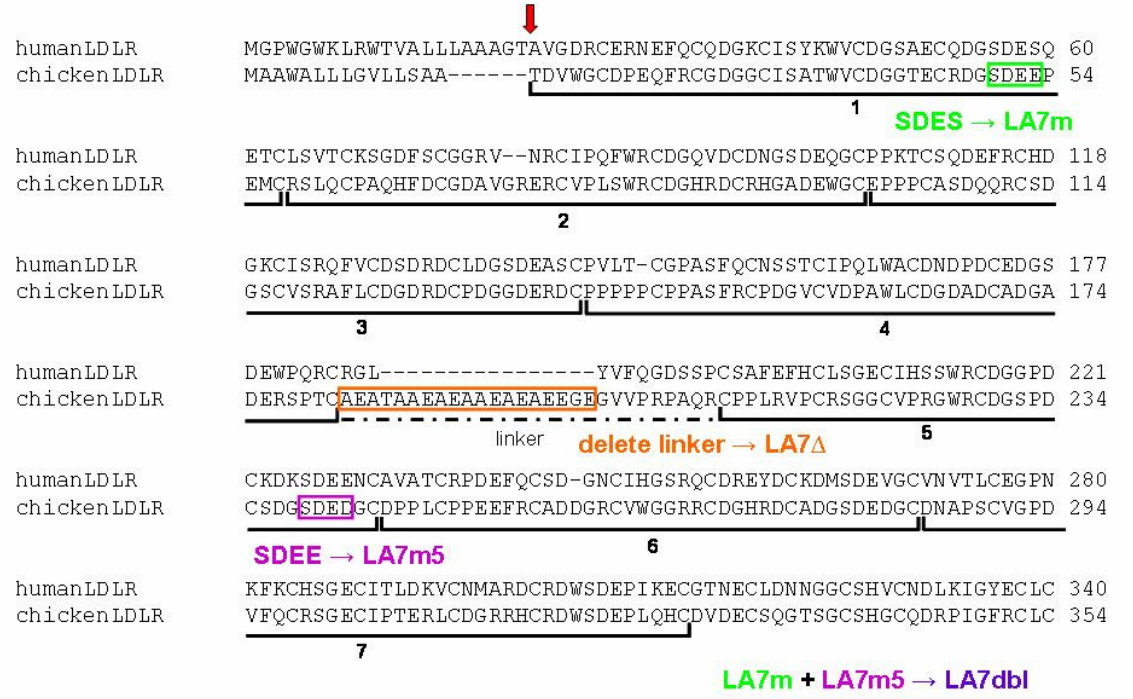

Figure 23. The specific mutations in the chicken LDLR ligand binding domain (LA 1-7).

In the LA7m mutant the sequence SDEE in the first LA repeat were mutated into SDES. In the LA7Δ, the long A/E-rich linker between repeats 4 and 5 was deleted. The LA7m5 mutant was generated by substitution of aa SDED with SDEE in the fifth repeat. In the LA7dbl double mutant the mutations LA7m and LA7m5 were introduced together.
The red arrow indicates the signal peptide cleavage site.

As a template for the site-directed mutagenesis the LA7wt (wild type, without mutations) plasmid as described in Hummel et al (Hummel, Lynn et al. 2003) was used.

In order to confirm that LR8 binds to apoE for control purposes, membrane proteins of chicken ovarian follicles, which are enriched in LR8, were electrophoretically separated under non-reducing conditions (Fig. 24, lanes 1-5), blotted onto nitrocellulose membrane and incubated with apoE2 (Fig. 24, lane 3), apoE3 (Fig. 24, lane 4), and apoE4 (Fig. 24, lane 5). The apoE isoforms were produced in and secreted from CHO cells (see Materials and Methods). Medium from control CHO cells, not secreting apoE isoforms, was used for incubations not containing the ligand (Fig. 24, lane 2).

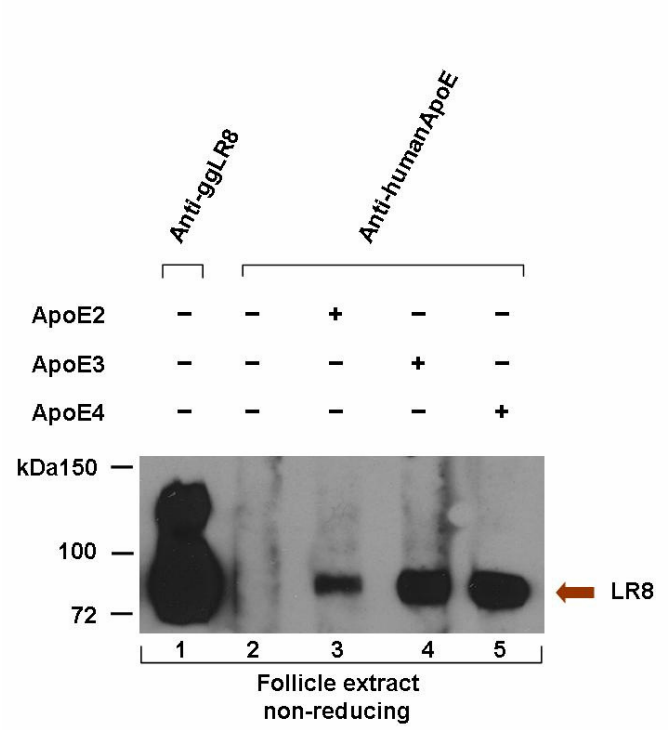

Figure 24. Human apoE binds to the chicken VLDLR homolog LR8.

Nitrocellulose strips containing proteins from ovarian follicle membrane extracts (25µg each), separated by 12% SDS-PAGE under non-reducing (lanes 1-5) conditions, were incubated with control medium of CHO cells (lane 2), apoE2 (1µg, lane 3), apoE3 (1µg, lane 4), and apoE4 (1µg, lane 5). The strips were washed and incubated with anti-human ApoE antibody (lanes 2-5). LR8, enriched in the ovarian follicle membrane protein extract, was visualized by Western blotting with anti-ggLR8 antiserum (lane 1). The primary antibodies were detected with HRP-conjugated goat anti-rabbit IgG (1:50000, lane 1) or HRP-conjugated goat anti-mouse IgG (1:1500, lanes 2-5) and enhanced chemiluminescence. The positions of migration (kDa) of marker proteins are indicated.

The position of the bound ligand was visualized by immunoblotting with anti-human ApoE antibody (Fig. 24, lanes 3-5). The apoE isoforms clearly bound to LR8, a 95 kDa protein in the ovarian follicle membrane extract, which was visualized with anti-ggLR8 antiserum (Fig. 24, lane 1). The binding of apoE2 (Fig. 24, lane 3) is weaker than that of apoE3 (Fig. 24, lane 4) and apoE4 (Fig. 24, lane 5) in agreement with a previous publication from our group (Steyrer, Barber et al. 1990). Incubation with control medium of the CHO cells, i.e. without apoE, gave no signal (Fig. 24, lane 2).

Expression, purification, and refolding of the LDLR ligand binding domains

The wt and mutated LA7 (Fig. 25) were expressed in BL21 *Escherichia coli* cells as fusion proteins with maltose-binding protein (MBP), purified, and refolded as described in Materials and Methods.

Figure 25. Scheme of the MBP•chicken LA7•6xHis recombinant fusion protein.

The wt and mutated LA7 domains, lacking the N-terminal signal peptide, were cloned into the pMAL vector, providing an N-terminal maltose-binding protein and a C-terminal His-tag.

After refolding, the different LA7 proteins were applied to SDS-PAGE under reducing (reverting to the unfolded form of the domains) and non-reducing conditions and subsequently analyzed with Coomassie Blue stain (Fig. 26) and Western blotting using an anti-His antibody (Fig. 27).

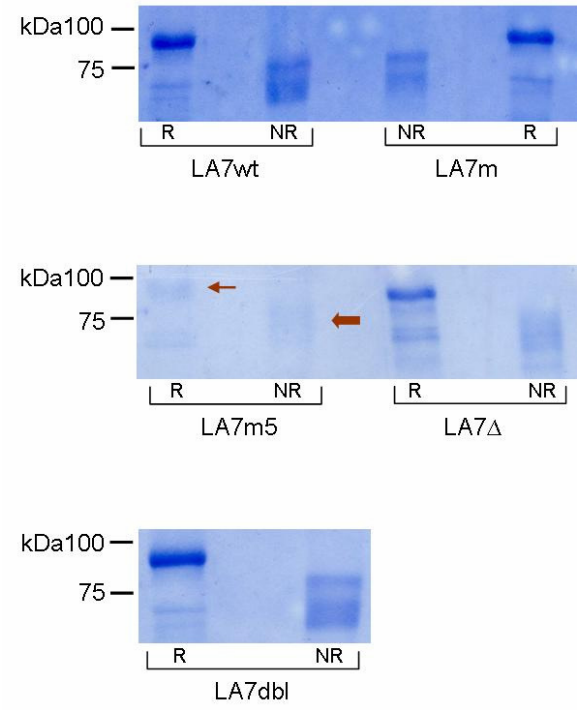

Figure 26. SDS-PAGE/ Coomassie Blue stain of the folded and unfolded MBP•LA7•His fusion proteins.

2µg each of the proteins were subjected to SDS-PAGE under reducing (R), by adding 25mM DTT, and under non-reducing (NR) conditions and analyzed by Coomassie Blue stain. The LA7m5 is marked with brown arrows, as it shows weak staining.
The positions of migration (kDa) of marker proteins are indicated.

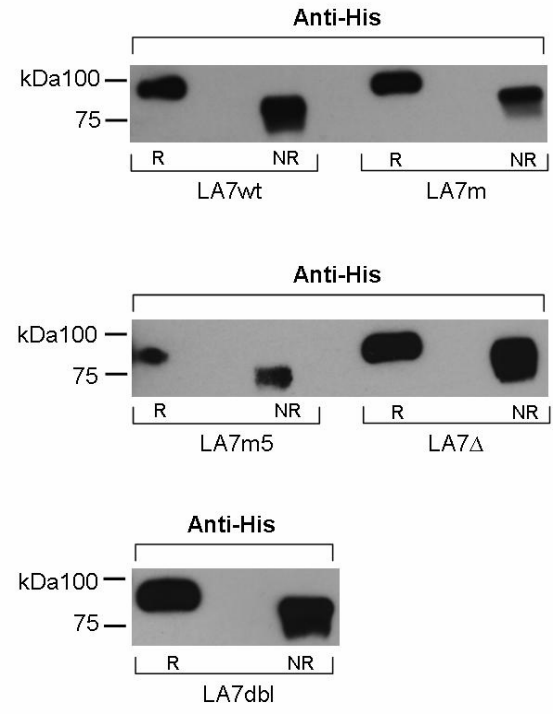

Figure 27. Western blot analysis of the folded and unfolded MBP•LA7•His fusion proteins.

2µg each of the proteins shown in Fig. 26 were subjected to SDS-PAGE under reducing (25mM DTT) and under non-reducing conditions, and analyzed by Western blotting using an anti-His antibody. The bound primary antibodies were detected with HRP-conjugated goat anti-mouse IgG (1:1500) and enhanced chemiluminescence.
The positions of migration (kDa) of marker proteins are indicated.

The reducing conditions unfold the receptor ligand binding domains, and therefore the proteins have reduced electrophoretic mobility.

Analysis of the ligand binding ability of the recombinant LA7 fusion proteins

RAP, receptor-associated protein, is an endoplasmic reticulum (ER) - resident chaperone that is required for maturation of members of the LDLR family. It is known that RAP binds to all LDLR family member proteins and can antagonize the binding of a wide variety of ligands (Herz, Goldstein et al. 1991; Willnow, Rohlmann et al. 1996). Therefore, RAP was used as a positive control to test the binding ability of the refolded receptor binding domains. The LA7 proteins were incubated with the recombinant RAP and co-immunoprecipitated with His-RAP-myc (Koch, Strasser et al. 2002) using the anti-myc antibody, and then analyzed on Western blots using anti-LA1-7 antibody as the primary antibody (see Fig. 28).

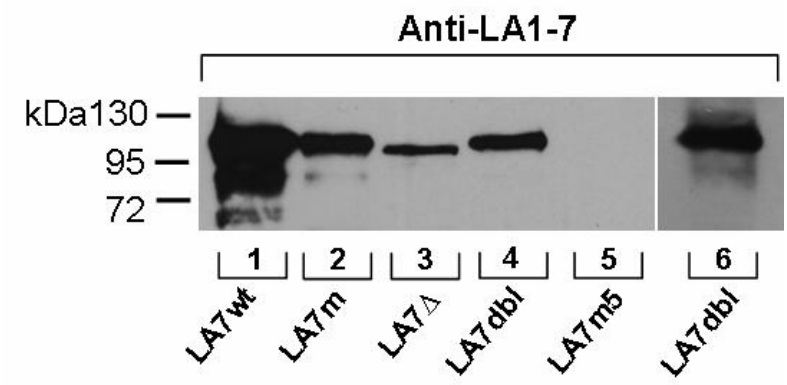

Figure 28. LA7 wt and mutants bind to the recombinant His•RAP•myc fusion protein.

20µg of LA7 proteins (lanes 1-5) were preincubated with 15µg of RAP and then mixed with anti-myc antibody. Subsequently, Protein A Sepharose was added. After the co-immunoprecipitation the samples were separated by 7,5% SDS-PAGE under reducing conditions. The nitrocellulose membrane was then incubated with anti-LA1-7 antiserum. In lane 6 the LA7 domain, in this case LA7dbl, was visualized. The primary antibody was detected with HRP-conjugated goat anti-rabbit IgG (1:50000, lanes 1-6) and enhanced chemiluminescence. The positions of migration (kDa) of marker proteins are indicated.

The LA7wt, LA7m, LA7Δ, LA7dbl, and LA7m5 were incubated with His-RAP-myc and precipitated with anti-myc antibody. The samples were subjected to SDS-PAGE and analyzed by Western blot using anti-LA1-7 antiserum (Fig. 28, lanes 1-5). The

position of the LA7 binding domain was visualized with anti-LA1-7 antiserum (Fig. 28, lane 6).

The co-immunoprecipitation (Fig. 28) demonstrated that the receptor ligand binding domain is able to bind the His-RAP-myc protein, except LA7m5. LA7m5 does not appear to bind RAP, which could be due to the fact that the expression of LA7m5 protein did not work well (cf. Fig. 26 and 27) and therefore less protein was available than in the other mutants.

If the immunoprecipitation was performed in the absence of His-RAP-myc, i.e. LA7 domains were incubated with anti-myc antibody and Protein A Sepharose alone, no signal could be obtained on the Western blot (data not shown).

Characterization of the protein interaction properties of the intracellular binding domain of LDLR family members

Interaction of adaptor proteins with the cytoplasmic tail of the LDLR

It is known that the adaptor protein ARH interacts with the FxNPxY motif in the cytoplasmic tails of the LDLR family members (Mishra, Watkins et al. 2002). ARH is required for the efficient internalization of the LDL-LDLR complex (Eden, Patel et al. 2002). It has been shown in our laboratory previously that the human ARH also binds to the chicken LDLR cytoplasmic tail (ggLDLRct), but to a lesser extent than to that of the human receptor. In turn, chicken ARH, cloned in our laboratory, binds to both the ggLDLRct and human LDLR cytoplasmic tail (hLDLRct), but the heterologous interaction displays much lower affinity (Grünstäudl 2005). Furthermore it has been observed that chicken ARH interacts with the chicken LR8B's cytoplasmic tail (ggLR8Bct), but not with the chicken LR8's cytoplasmic tail (ggLR8ct) although they possess the same internalization signal, FDNPVY (Gschmeidler 2004). Due to the fact that Numb is closely related to ARH (Mishra, Watkins et al. 2002) and is involved in endocytosis (Santolini, Puri et al. 2000; Berdnik, Torok et al. 2002), I considered investigating chicken Numb in the context of chicken LDLR family members.

Chicken Numb

Genomic organization of chicken Numb according to the Ensembl chicken database

Concerning the genomic organization of chicken Numb, searches in the Ensembl chicken database revealed its location on chicken chromosome 5. The *Numb* gene spans an 92,8 kb stretch on chromosome 5 from basepairs 28,378,441 to 28,471,234 (ENSGALT00000015137). The predicted chicken Numb transcript is 2,245bp long and contains 12 exons (Fig. 29). Exon 1, exon 2, exon 3, and the 5' part of exon 4 contain a 5' untranslated region (5' UTR). The actual protein is encoded by the region, which spans from the 3' part of exon 4 to exon 12 (Fig. 29).

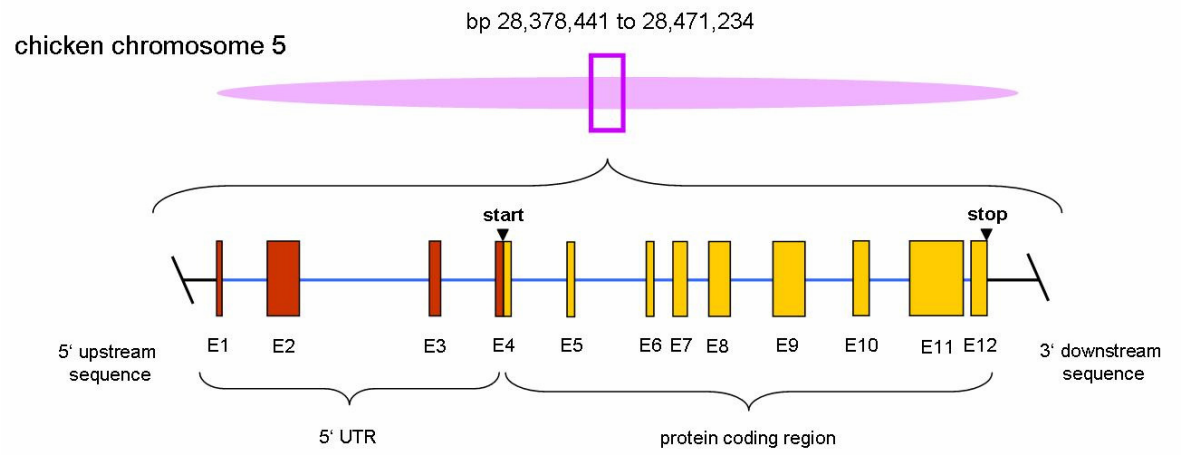

Figure 29. Genomic organization of chicken Numb.

The chicken Numb gene locus can be found on chicken chromosome 5 (lavender box in the upper panel). The gene contains 12 exons, which are depicted as boxes in the lower panel. The 5' untranslated region (5' UTR) is shown as brown boxes. The start and stop codon (yellow boxes) are marked with arrowheads. The 5 'upstream and 3' downstream sequences are shown in black. The introns are represented as blue lines.

Chicken Numb protein

The chicken Numb protein consists of 585 amino acids and has a calculated (PROTEIN CALCULATOR v3.3) molecular mass of approximately 64kDa. Chicken Numb displays about 83% sequence identity to human and murine Numb (Fig. 30),

whereas human and murine Numb share 94% sequence identity (Fig. 30). Hence, Numb appears to be an evolutionarily well conserved protein.

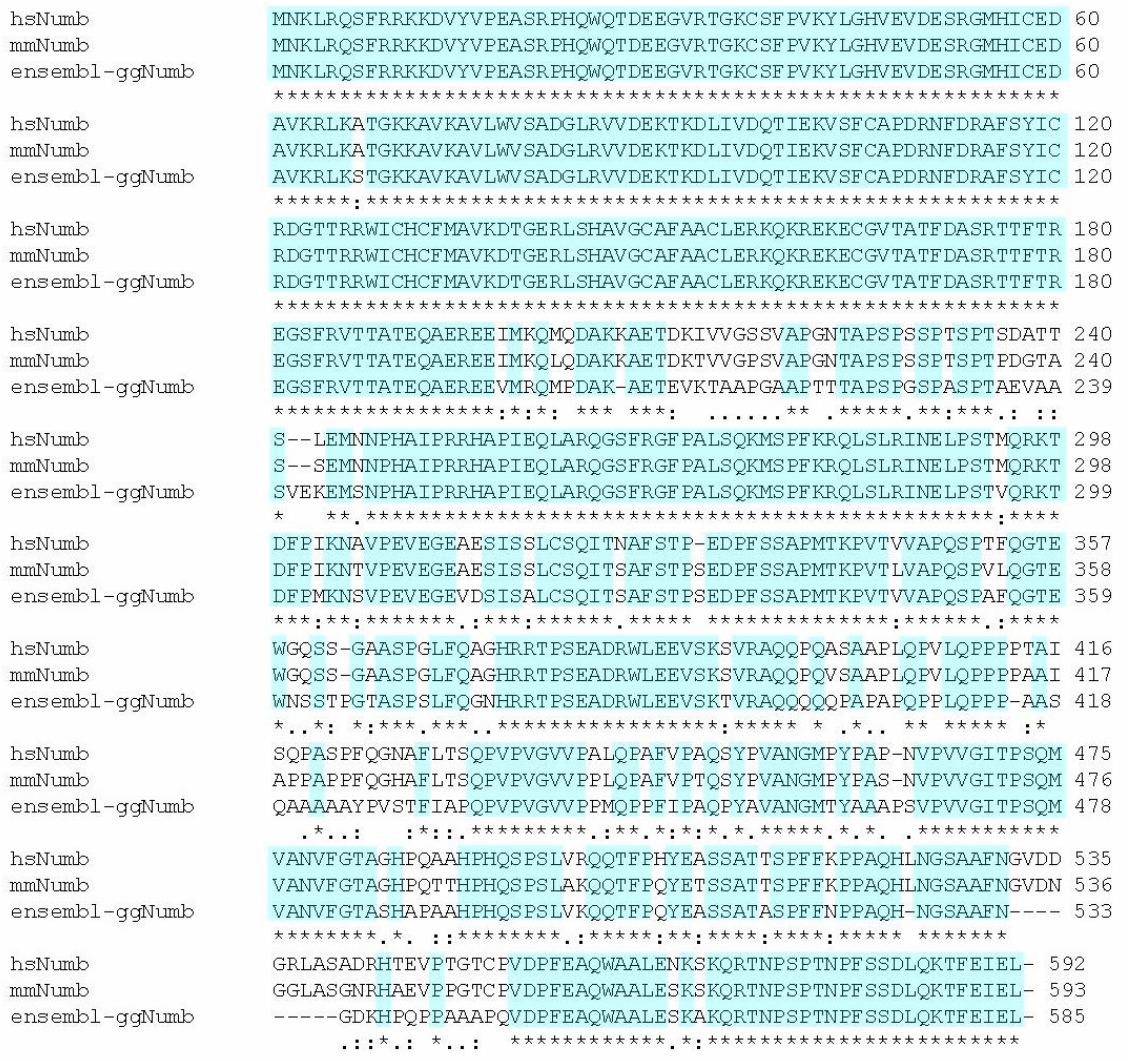

Figure 30. Protein sequence alignment of Numb from chicken, mouse, and man.
The chicken Numb sequence originates from the Ensembl database (NP_990166.1).

Wakamatsu et al (Wakamatsu, Maynard et al. 1999) have reported the detection of an approximately 80 kDa band in chicken E3 neuronal tube extract by immunoblotting (Wakamatsu, Maynard et al. 1999). They showed that ggNumb can modulate neurogenesis by binding directly to the cytoplasmic domain of the activated form of ggNotch-1.

The protein sequences from the Ensembl database and that published by Wakamatsu et al differ in a few positions, as can be seen in Fig. 31.

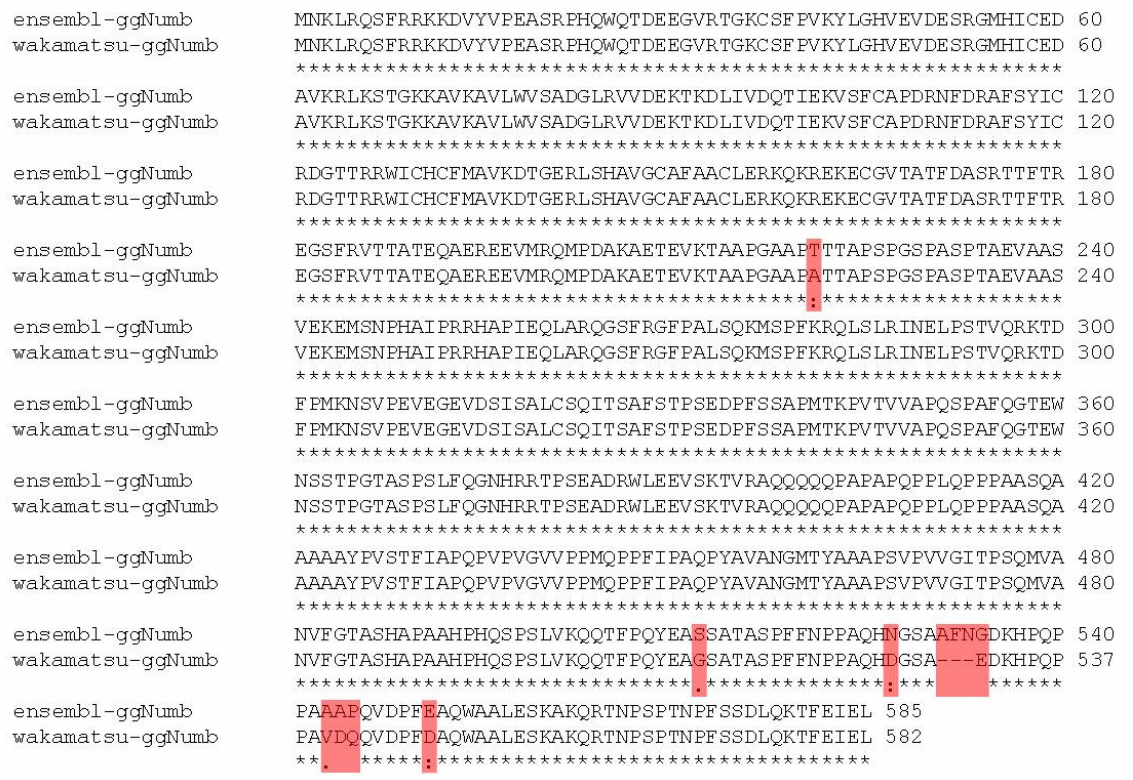

Figure 31. Alignment of the Ensembl ggNumb sequence (ensembl) and that published by Wakamatsu et al. (wakamatsu).

Differences in the sequences are enboxed in red.

According to computational sequence analysis the chicken Numb protein contains three potential N-glycosylation motifs (NxS/T) at aa positions 361, 527, and 566 (Fig. 32).

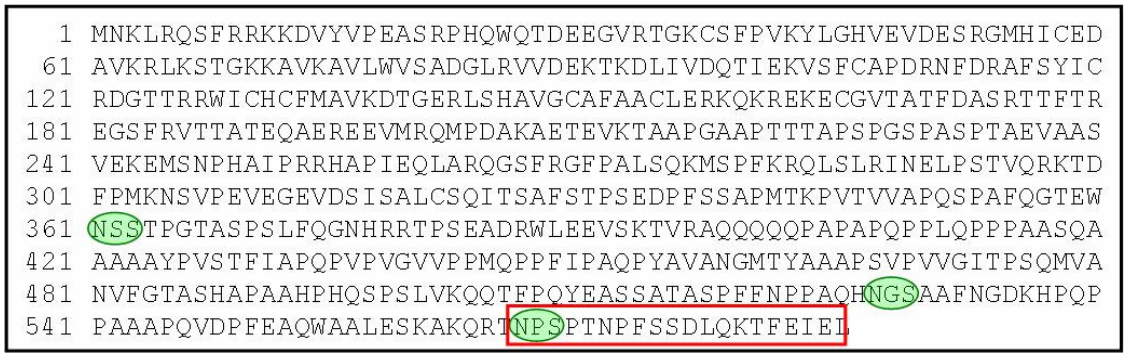

Figure 32. Chicken Numb protein sequence.

The predicted putative N-glycosylation sites are encircled in green. The 20 aa peptide synthesized for the generation of a peptide antibody is enboxed in red.

Recently, in our laboratory an antibody against chicken Numb was raised. The peptide antibody was generated against a peptide corresponding to the C-terminal 20 amino acids of the chicken Numb (shown in Fig. 32).

Chicken Numb isoforms

In mammals, four different isoforms of Numb are known. Sequence alignments of chicken Numb with human and murine Numb have shown a high homology and sequence conservation. Through nucleotide-nucleotide and protein-protein BLAST analysis of the specific phosphotyrosine-binding domain insert (PTBi) and proline-rich region insert (PRRi) of the human Numb against the chicken genome, different chicken Numb isoforms have been revealed (Dichlberger 2004). These potential chicken Numb sequences differ in the presence or absence of inserts in the phosphotyrosine-binding domain (PTB) and the proline-rich region (PRR), respectively (Fig. 33).

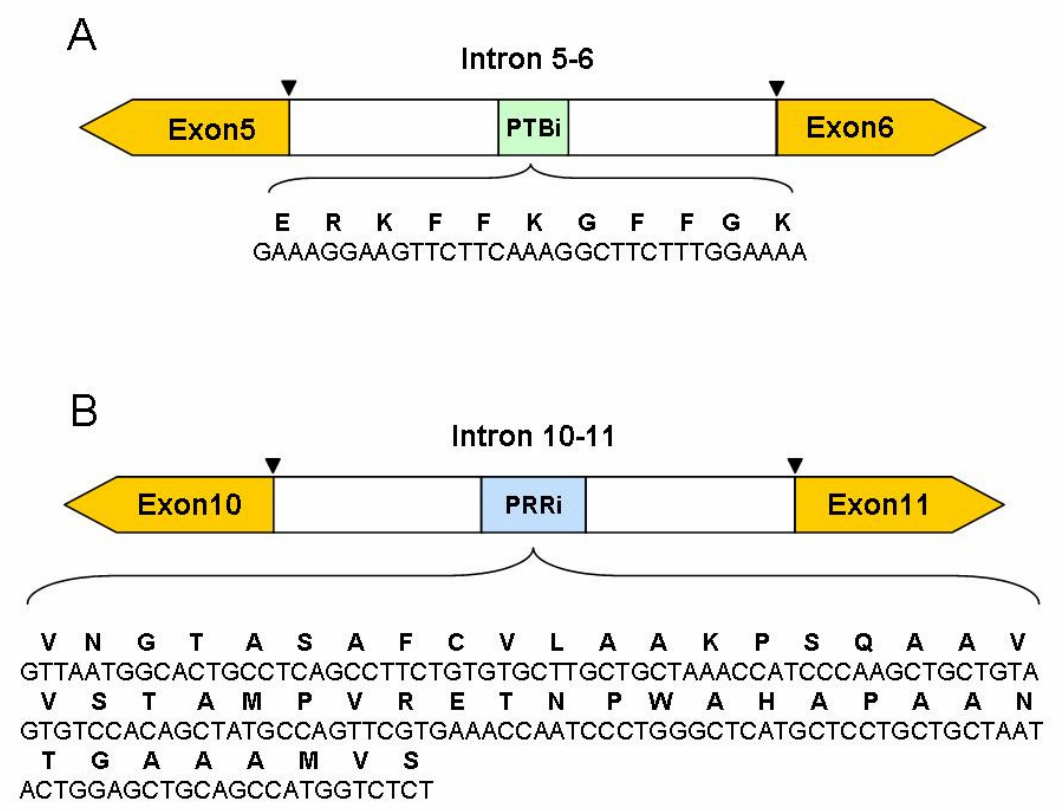

Figure 33. Genomic locations of the PTB and PRR inserts of chicken Numb.

The corresponding flanking exons are shown as yellow arrow bars. Exon-intron boundaries are indicated with black arrow heads. A) The location of the PTBi is shown as a green box. B) The PRRi is depicted as a blue box.

Sequence analysis of the chicken gene locus showed that the hypothetical PTB- and PRR-encoding inserts are located in different introns. The potential chicken Numb PTBi contains 11 aa which are 100% conserved in mammals and the inserted basepairs can be found in the intron 5-6 (between exons 5 and 6), from bp

28,447,302 to 28,460,389, which is 13,088 bp long (Fig. 33, A). The PRRi is 48 aa long and the encoding insert is located in the intron10-11 (between exons 10 and 11), which is 2,242 bp long and stretches from bp 28,468,277 to 28,470,518 (Fig. 33, B). The PRRi shares about 56% sequence identity with the mammalian PRR inserts.

Cloning of the chicken Numb isoform1

Total RNA was isolated from DKO-R cells and RT-PCR was performed using the sequence-specific forward primer, 5'-AAGAATTCCATGAATAAATTACGGCAG-3' (containing an EcoRI site, underlined), and the reverse primer 5'-GTCTCGAGAAGTTCAATCTCAAATGTC-3' (containing an XhoI site, underlined).
DKO-R cells are DT40 cells, which express the human clathrin cDNA under the control of a Tet-Off expression system. The DT40 cell line is a chicken B cell line and a popular tool for gene targeting in vertebrate cells (Buerstedde and Takeda 1991; Winding and Berchtold 2001).
DKO-R cells remain viable in the absence of clathrin (Wettey, Hawkins et al. 2002).
The sequence of ggNumb was verified by DNA sequencing, but it differs from both the Ensembl sequence and the sequence published by Wakamatsu et al (Fig. 34); in the following, this sequence was designated chicken/ggNumb isoform1.

```
ggNumb-isoform1       MNKLRQSFRRKKDVYVPEASRPHQWQTDEEGVRTGKCSFPVKYLGHVEVDESRGMHICED 60
ensembl-ggNumb        MNKLRQSFRRKKDVYVPEASRPHQWQTDEEGVRTGKCSFPVKYLGHVEVDESRGMHICED 60
wakamatsu-ggNumb      MNKLRQSFRRKKDVYVPEASRPHQWQTDEEGVRTGKCSFPVKYLGHVEVDESRGMHICED 60
                      ************************************************************

ggNumb-isoform1       AVKRLKSTGKKAVKAVLWVSADGLRVVDEKTKDLIVDQTIEKVSFCAPDRNFDRAFSYIC 120
ensembl-ggNumb        AVKRLKSTGKKAVKAVLWVSADGLRVVDEKTKDLIVDQTIEKVSFCAPDRNFDRAFSYIC 120
wakamatsu-ggNumb      AVKRLKSTGKKAVKAVLWVSADGLRVVDEKTKDLIVDQTIEKVSFCAPDRNFDRAFSYIC 120
                      ************************************************************

ggNumb-isoform1       RDGTTRRWICHCFMAVKDTGERLSHAVGCAFAACLERKQKREKECGVTATFDASRTTFTR 180
ensembl-ggNumb        RDGTTRRWICHCFMAVKDTGERLSHAVGCAFAACLERKQKREKECGVTATFDASRTTFTR 180
wakamatsu-ggNumb      RDGTTRRWICHCFMAVKDTGERLSHAVGCAFAACLERKQKREKECGVTATFDASRTTFTR 180
                      ************************************************************

ggNumb-isoform1       EGSFRVTTATEQAEREEVMRQMPDAKAETEVKTAAPGAAPTTAPSPGSPASPTAEVAAS 240
ensembl-ggNumb        EGSFRVTTATEQAEREEVMRQMPDAKAETEVKTAAPGAAPTTAPSPGSPASPTAEVAAS 240
wakamatsu-ggNumb      EGSFRVTTATEQAEREEVMRQMPDAKAETEVKTAAPGAAPATTAPSPGSPASPTAEVAAS 240
                      ****************************************:*******************

ggNumb-isoform1       VEKEMSNPHAIPRRHAPIEQLARQGSFRGFPALSQKMSPFKRQLSLRINELPSTVQRKTD 300
ensembl-ggNumb        VEKEMSNPHAIPRRHAPIEQLARQGSFRGFPALSQKMSPFKRQLSLRINELPSTVQRKTD 300
wakamatsu-ggNumb      VEKEMSNPHAIPRRHAPIEQLARQGSFRGFPALSQKMSPFKRQLSLRINELPSTVQRKTD 300
                      ************************************************************

ggNumb-isoform1       FPMKNSVPEVEGEVDSISALCSQITSAFSTPSEDPFSSAPMTKPVTVVAPQSPAFQGTEW 360
ensembl-ggNumb        FPMKNSVPEVEGEVDSISALCSQITSAFSTPSEDPFSSAPMTKPVTVVAPQSPAFQGTEW 360
wakamatsu-ggNumb      FPMKNSVPEVEGEVDSISALCSQITSAFSTPSEDPFSSAPMTKPVTVVAPQSPAFQGTEW 360
                      ************************************************************

ggNumb-isoform1       NSSTPGTASPSLFQGNHRRTPSEADRWLEEVSKTVRAQQQQQPAPAPQPPLQPPPAASQA 420
ensembl-ggNumb        NSSTPGTASPSLFQGNHRRTPSEADRWLEEVSKTVRAQQQQQPAPAPQPPLQPPPAASQA 420
wakamatsu-ggNumb      NSSTPGTASPSLFQGNHRRTPSEADRWLEEVSKTVRAQQQQQPAPAPQPPLQPPPAASQA 420
                      ************************************************************

ggNumb-isoform1       AAAAYPVSTFIAPQPVPVGVVPPMQPPFIPAQPYAVANGMTYAAAPSVPVVGITPSQMVA 480
ensembl-ggNumb        AAAAYPVSTFIAPQPVPVGVVPPMQPPFIPAQPYAVANGMTYAAAPSVPVVGITPSQMVA 480
wakamatsu-ggNumb      AAAAYPVSTFIAPQPVPVGVVPPMQPPFIPAQPYAVANGMTYAAAPSVPVVGITPSQMVA 480
                      ************************************************************

ggNumb-isoform1       NVFGTASHAPAAHPHQSPSLVKQQTFPQYEAGSATASPFFNPPAQHNGSAAFNGVDGGKW 540
ensembl-ggNumb        NVFGTASHAPAAHPHQSPSLVKQQTFPQYEASSATASPFFNPPAQHNGSAAFNG------ 534
wakamatsu-ggNumb      NVFGTASHAPAAHPHQSPSLVKQQTFPQYEAGSATASPFFNPPAQHDGSA---------- 530
                      *****************************.***************:***

ggNumb-isoform1       AAEDKHPQPPAAAPQVDPFEAQWAALESKAKQRTNPSPTNPFSSDLQKTFEIEL 594
ensembl-ggNumb        ---DKHPQPPAAAPQVDPFEAQWAALESKAKQRTNPSPTNPFSSDLQKTFEIEL 585
wakamatsu-ggNumb      --EDKHPQPPAVDQQVDPFDAQWAALESKAKQRTNPSPTNPFSSDLQKTFEIEL 582
                        ********.*****:**********************************
```

Figure 34. Protein sequence alignment of ggNumb-isoform1, ensembl-ggNumb, and wakamatsu-ggNumb.

Differences in the sequences are highlighted in orange.

Bacterial expression of recombinant chicken Numb isoform1

The pET25b+-vector expression system was used to bacterially produce His_6-tagged ggNumb isoform1.

Figure 35. Schematic representation of the recombinant chicken Numb-isoform1•HSV•6xHis fusion protein.

Full-length ggNumb isoform1 (shown as a yellow bar) was cloned into the pET25b+-expression vector, which carries an optional C-terminal HSV•Tag (blue box) and a 6xHis•Tag (red box) sequence.

The full-length ggNumb cDNA fragment was cloned between the EcoRI and XhoI sites into the pET25b+-vector providing a C-terminal HSV-Tag and a 6xHis-Tag (Fig. 35). The construct was verified by DNA sequencing. The recombinant chicken Numb-isoform1•HSV•6xHis fusion protein was bacterially expressed in BL21 cells. The induction of protein expression of the approximately 80 kDa ggNumb-iso1-His fusion protein is shown in Fig. 36 A. and B. The His-tagged ggNumb-iso1 was subsequently used for studies on binding of Numb to cytoplasmic tails of various members of the LDLR family.

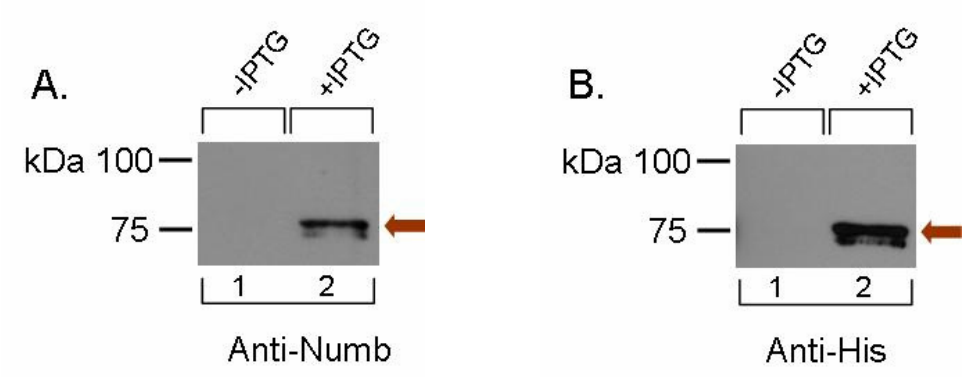

Figure 36. Bacterial expression of ggNumb-isoform1•His fusion protein.

The recombinant ggNumb isoform1 fusion protein was expressed in BL21 cells. Cell extracts, before (lane 1) and after (lane 2) 3 h of induction with 1mM IPTG, were subjected to SDS-PAGE under reducing conditions and analyzed by Western blotting using anti-ggNumb antiserum (A.) and anti-His antibody (B.). The bound primary antibodies were detected with HRP-conjugated goat anti-rabbit IgG (1:50000, A.), HRP-conjugated goat anti-mouse IgG (1:1500, B.), and enhanced chemiluminescence. The positions of migration (kDa) of marker proteins are indicated.

Cloning of the chicken Numb isoform2

Different chicken tissues were screened for the insert in the PTB domain with the PTBi-specific forward primer 5'-ATGAATAAATTACGGCAGAGC-3' and reverse primer 5'-AGCCTTTGAAGAACTTCC-3'. Based on the results, I concentrated on chicken embryo cDNA and performed full-length RT-PCR with sequence-specific primers (mentioned above) containing the EcoRI and XhoI restriction sites. The sequence was verified by DNA sequencing. The alignment of chicken Numb isoform1 and 2 (Fig. 37) shows that the PTB insert is present in the isoform2. Additionally, an

in-frame insert immediately before the canonical PTB inserted sequence was present in the chicken isoform2. The methionine in this insert is an isoleucine in the Ensembl database.

```
ggNumb-isoform1      MNKLRQSFRRKKDVYVPEASRPHQWQTDEEGVRTGKCSFPVKYLGHVEVDESRGMHICED 60
ggNumb-isoform2      MNKLRQSFRRKKDVYVPEASRPHQWQTDEEGVRTGKCSFPVKYLGHVEVDESRGMHICED 60
                     ************************************************************

ggNumb-isoform1      AVKRLKS-------------------------TGKKAVKAVLWVSADGLRVVDEKTKDL 94
ggNumb-isoform2      AVKRLKSLPSVMALDLSPLFLQERKFFKGFFGKTGKKAVKAVLWVSADGLRVVDEKTKDL 120
                     *******                          ***************************

ggNumb-isoform1      IVDQTIEKVSFCAPDRNFDRAFSYICRDGTTRRWICHCFMAVKDTGERLSHAVGCAFAAC 154
ggNumb-isoform2      IVDQTIEKVSFCAPDRNFDRAFSYICRDGTTRRWICHCFMAVKDTGERLSHAVGCAFAAC 180
                     ************************************************************

ggNumb-isoform1      LERKQKREKECGVTATFDASRTTFTREGSFRVTTATEQAEREEVMRQMPDAKAETEVKTA 214
ggNumb-isoform2      LERKQKREKECGVTATFDASRTTFTREGSFRVTTATEQAEREEVMRQMPDAKAETEVKTA 240
                     ************************************************************

ggNumb-isoform1      APGAAPTTTAPSPGSPASPTAEVAASVEKEMSNPHAIPRRHAPIEQLARQGSFRGFPALS 274
ggNumb-isoform2      APGAAPTTTAPSPGSPASPTAEVAASVEKEMSNPHAIPRRHAPIEQLARQGSFRGFPALS 300
                     ************************************************************

ggNumb-isoform1      QKMSPFKRQLSLRINELPSTVQRKTDFPMKNSVPEVEGEVDSISALCSQITSAFSTPSED 334
ggNumb-isoform2      QKMSPFKRQLSLRINELPSTVQRKTDFPMKNSVPEVEGEVDSISALCSQITSAFSTPSED 360
                     ************************************************************

ggNumb-isoform1      PFSSAPMTKPVTVVAPQSPAFQGTEWNSSTPGTASPSLFQGNHRRTPSEADRWLEEVSKT 394
ggNumb-isoform2      PFSSAPMTKPVTVVAPQSPAFQGTEWNSSTPGTASPSLFQGNHRRTPSEADRWLEEVSKT 420
                     ************************************************************

ggNumb-isoform1      VRAQQQQQPAPAPQPPLQPPPAASQAAAAAYPVSTFIAPQPVPVGVVPPMQPPFIPAQPY 454
ggNumb-isoform2      VRAQQQQQPAPAPQPPLQPPPAASQAAAAAYPVSTFIAPQPVPVGVVPPMQPPFIPAQPY 480
                     ************************************************************

ggNumb-isoform1      AVANGMTYAAAPSVPVVGITPSQMVANVFGTASHAPAAHPHQSPSLVKQQTFPQYEAGSA 514
ggNumb-isoform2      AVANGMTYAAAPSVPVVGITPSQMVANVFGTASHAPAAHPHQSPSLVKQQTFPQYEASSA 540
                     ************************************************************.**

ggNumb-isoform1      TASPFFNPPAQHNGSAAFNGVDGGKWAAEDKHPQPPAAAPQVDPFEAQWAALESKAKQRT 574
ggNumb-isoform2      TASPFFNPPAQHNGSAAFNGVDGGKWAAEDKHPQPPAAAPQVDPFEAQWAALESKAKQRT 600
                     ************************************************************

ggNumb-isoform1      NPSPTNPFSSDLQKTFEIEL 594
ggNumb-isoform2      NPSPTNPFSSDLQKTFEIEL 620
                     ********************
```

Figure 37. Protein sequence alignment of chicken Numb-isoform1 and -isoform2.

The PTBi domain also found in mammalian Numb is enboxed in green. The blue frame shows the additional sequence present in the chicken protein.

Bacterial expression of recombinant chicken Numb isoform2

For the bacterial production of His_6-tagged ggNumb isoform2 the pET25b+-vector expression system was used.

Figure 38. Schematic drawing of the recombinant chicken Numb-isoform2•HSV•6xHis fusion protein containing the insert in the PTB domain.

Full-length ggNumb isoform2 (shown as a yellow bar) was cloned into the pET25b+-expression vector, which carries an optional C-terminal HSV•Tag (blue box) and a 6xHis•Tag (red box) sequence. The insert in the PTB domain (PTBi) is represented as a green box.

The full-length ggNumb cDNA fragment was cloned into the pET25b+-vector providing a C-terminal HSV-Tag and a 6xHis-Tag (Fig. 38). The construct was verified by DNA sequencing. The recombinant chicken Numb-isoform2•HSV•6xHis fusion protein was bacterially expressed in BL21 cells. The induction of protein expression of the approximately 90 kDa ggNumb-iso2-His fusion protein is shown in Fig. 39 A., B., and C. The His-tagged ggNumb-iso2 was subsequently used for binding studies.

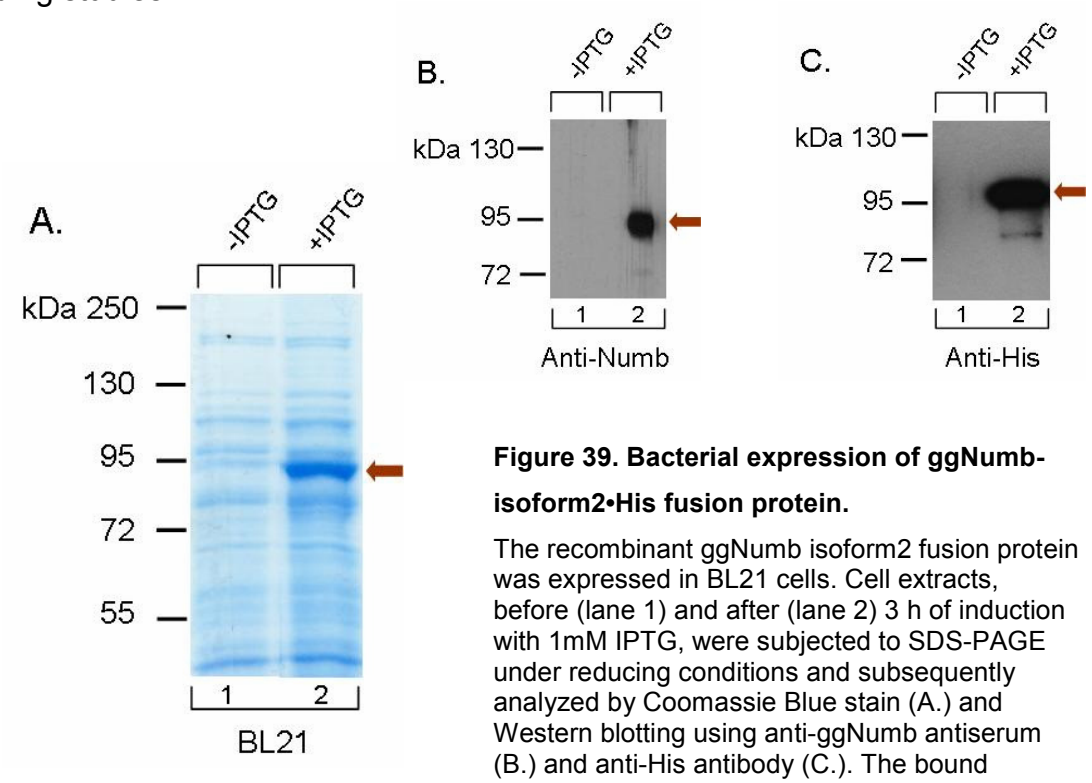

Figure 39. Bacterial expression of ggNumb-isoform2•His fusion protein.

The recombinant ggNumb isoform2 fusion protein was expressed in BL21 cells. Cell extracts, before (lane 1) and after (lane 2) 3 h of induction with 1mM IPTG, were subjected to SDS-PAGE under reducing conditions and subsequently analyzed by Coomassie Blue stain (A.) and Western blotting using anti-ggNumb antiserum (B.) and anti-His antibody (C.). The bound primary antibodies were detected with HRP-conjugated goat anti-rabbit IgG (1:50000, B.), HRP-conjugated goat anti-mouse IgG (1:1500, C.) and enhanced chemiluminescence. The positions of migration (kDa) of marker proteins are indicated.

Cloning of the chicken Numb isoform3

Different chicken tissues were screened for the insert in the PRR domain with PRRi specific primers, forward: 5'-ATCACCAGTGCGTTCAGCACG-3'; reverse: 5'-GCTGGCTGCTGCTGCTGCT-3'. Based on the results, I focused on the chicken kidney, and full-length RT-PCR with sequence-specific primers (see above), was performed. The sequence was verified by DNA sequencing. The protein sequence

alignment of chicken Numb isoforms1 and 3 is shown in Fig. 40. The PRR insert (enboxed in green) is present in the isoform3.

```
ggNumb-isoform1      MNKLRQSFRRKKDVYVPEASRPHQWQTDEEGVRTGKCSFPVKYLGHVEVDESRGMHICED 60
ggNumb-isoform3      MNKLRQSFRRKKDVYVPEASRPHQWQTDEEGVRTGKCSFPVKYLGHVEVDESRGMHICED 60
                     ************************************************************
ggNumb-isoform1      AVKRLKSTGKKAVKAVLWVSADGLRVVDEKTKDLIVDQTIEKVSFCAPDRNFDRAFSYIC 120
ggNumb-isoform3      AVKRLKSTGKKAVKAVLWVSADGLRVVDEKTKDLIVDQTIEKVSFCAPDRNFDRAFSYIC 120
                     ************************************************************
ggNumb-isoform1      RDGTTRRWICHCFMAVKDTGERLSHAVGCAFAACLERKQKREKECGVTATFDASRTTFTR 180
ggNumb-isoform3      RDGTTRRWICHCFMAVKDTGERLSHAVGCAFAACLERKQKREKECGVTATFDASRTTFTR 180
                     ************************************************************
ggNumb-isoform1      EGSFRVTTATEQAEREEVMRQMPDAKAETEVKTAAPGAAPTTTAPSPGSPASPTAEVAAS 240
ggNumb-isoform3      EGSFRVTTATEQAEREEVMRQMPDAKAETEVKTAAPGAAPTTTAPSPGSPASPTAEVAAS 240
                     ************************************************************
ggNumb-isoform1      VEKEMSNPHAIPRRHAPIEQLARQGSFRGFPALSQKMSPFKRQLSLRINELPSTVQRKTD 300
ggNumb-isoform3      VEKEMSNPHAIPRRHAPIEQLARQGSFRGFPALSQKMSPFKRQLSLRINELPSTVQRKTD 300
                     ************************************************************
ggNumb-isoform1      FPMKNSVPEVEGEVDSISALCSQITSAFSTPSEDPFSSAPMTKPVTVVAPQSPAFQ---- 357
ggNumb-isoform3      FPMKNSVPEVEGEVDSISALCSQITSAFSTPSEDPFSSAPMTKPVTVVAPQSPAFQVNGT 360
                     ************************************************
ggNumb-isoform1      ------------------------------------------GTEWNSSTPGTASPSL 372
ggNumb-isoform3      ASAFCVLAAKPSQAAVVSTAMPVRETNPWAHAPAANTGAAAMVSGTEWNSSTPGTASPSL 420
                                                               ***************
ggNumb-isoform1      FQGNHRRTPSEADRWLEEVSKTVRAQQQQQPAPAPQPPLQPPPAASQAAAAAYPVSTFIA 432
ggNumb-isoform3      FQGNHRRTPSEADRWLEEVSKTVRAQQQQQPAPAPQPPLQPPPAASQAAAAAYPVSTFIA 480
                     ************************************************************
ggNumb-isoform1      PQPVPVGVVPPMQPPFIPAQPYAVANGMTYAAAPSVPVVGITPSQMVANVFGTASHAPAA 492
ggNumb-isoform3      PQPVPVGVVPPMQPPFIPAQPYAVANGMTYAAAPSVPVVGITPSQMVANVFGTASHAPAA 540
                     ************************************************************
ggNumb-isoform1      HPHQSPSLVKQQTFPQYEAGSATASPFFNPPAQHNGSAAFNGVDGGKWAAEDKHPQPPAA 552
ggNumb-isoform3      HPHQSPSLVKQQTFPQYEAGSATASPFFNPPAQHNGSAAFNGVDGGKWAAEDKHPQPPAA 600
                     ************************************************************
ggNumb-isoform1      APQVDPFEAQWAALESKAKQRTNPSPTNPFSSDLQKTFEIEL 594
ggNumb-isoform3      APQVDPFEAQWAALESKAKQRTNPSPTNPFSSDLQKTFEIEL 642
                     *******************************************
```

Figure 40. Alignment of the chicken Numb-isoform1 and -isoform3.

Differences in the sequences are shown in orange. The PRRi is enboxed in green.

Bacterial expression of recombinant chicken Numb isoform3

The pET25b+-vector expression system was used to bacterially produce His_6-tagged ggNumb isoform3.

Figure 41. Schematic representation of the recombinant chicken Numb-isoform3•HSV•6xHis fusion protein containing the insert in the PRR domain.

Full-length ggNumb isoform3 (shown as a yellow bar) was cloned into the pET25b+-expression vector, which carries an optional C-terminal HSV•Tag (blue box) and a 6xHis•Tag (red box) sequence. The PRRi is shown as a green box.

The full-length ggNumb cDNA fragment was cloned between the EcoRI and XhoI sites into the pET25b+-vector providing a C-terminal HSV-Tag and a 6xHis-Tag (Fig. 41). The construct was verified by DNA sequencing. The recombinant chicken Numb-isoform3•HSV•6xHis fusion protein was bacterially expressed in BL21 cells. The induction of protein expression of the approximately 95 kDa ggNumb-iso3-His fusion protein is shown in Fig. 42 A. to C. The His-tagged ggNumb-iso3 was also subsequently used for studies on binding of Numb to cytoplasmic tails of various members of the LDLR family and to investigate whether the PRR insert makes a difference in binding ability, in contrast to isoform1 and 2.

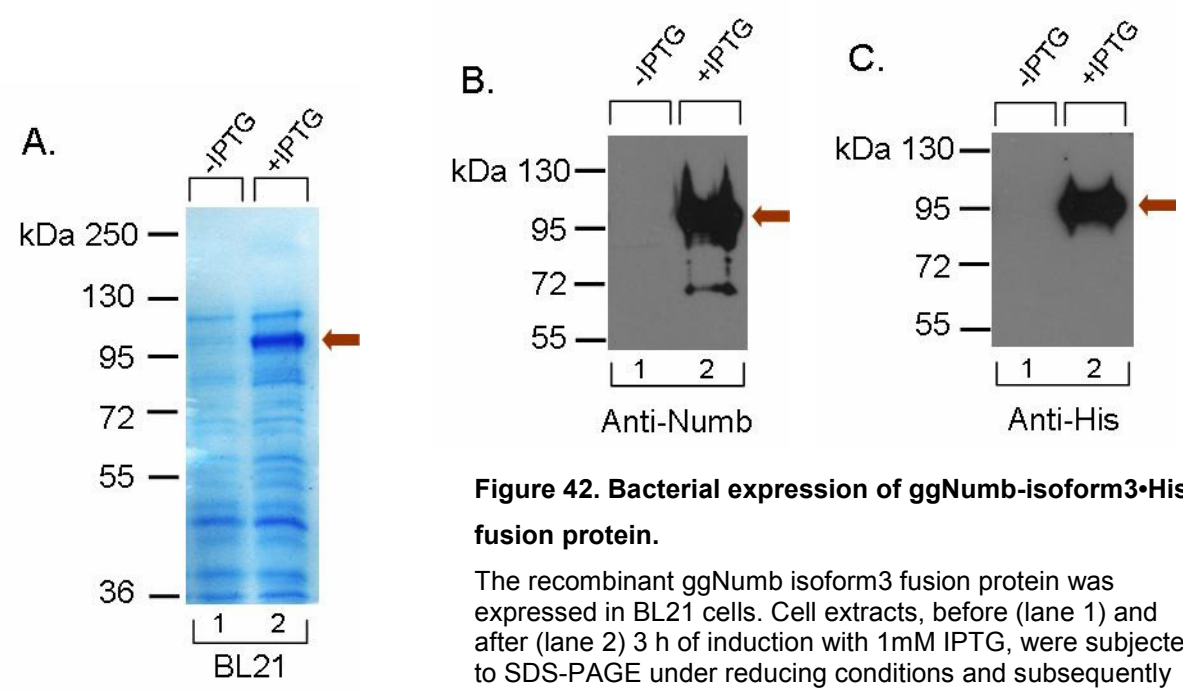

Figure 42. Bacterial expression of ggNumb-isoform3•His fusion protein.

The recombinant ggNumb isoform3 fusion protein was expressed in BL21 cells. Cell extracts, before (lane 1) and after (lane 2) 3 h of induction with 1mM IPTG, were subjected to SDS-PAGE under reducing conditions and subsequently analyzed by Coomassie Blue stain (A.) and Western blotting using anti-ggNumb antiserum (B.) and anti-His antibody (C.). The bound primary antibodies were detected with HRP-conjugated goat anti-rabbit IgG (1:50000, B.), HRP-conjugated goat anti-mouse IgG (1:1500, C.) and enhanced chemiluminescence. The positions of migration (kDa) of marker proteins are indicated.

Binding of chicken Numb isoforms to the cytoplasmic tails of chicken and human LDLR

It has been shown that the PTB domain of ARH binds to the cytoplasmic domain of the human LDLR, and that this binding requires the integrity of the FDNPVY sequence (He, Gupta et al. 2002). Instead of FDNPVY, the chicken LDLR harbors

the supposed internalization signal FGNPLF (Hummel, Lynn et al. 2003).

The aim was to investigate whether the different chicken Numb isoforms are able to interact with the human or chicken intracellular domain of the LDLR, based on the fact that the Numb PTB is related to that of ARH.

For this purpose the ligand blotting method, as described in Materials and Methods, was used.

First, the interaction of chicken Numb isoforms with the human LDLRct was tested (see Fig. 43 A. and B.).

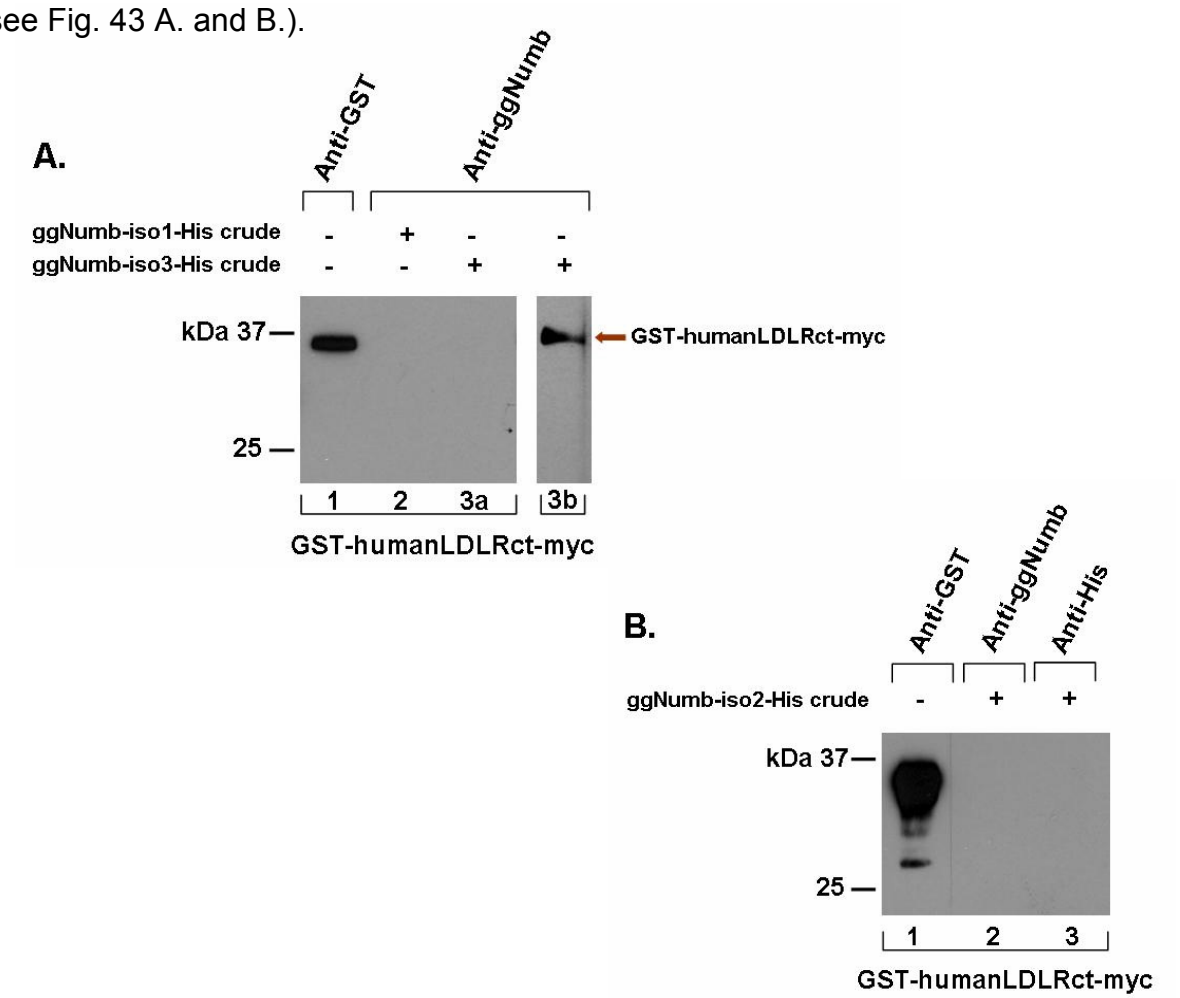

Figure 43. Human LDLRct fusion protein binds to the chicken Numb isoform3.

Nitrocellulose strips containing GST-humanLDLRct-myc (A. and B. lane 1: 0,5µg; lanes 2-3b: 1µg), separated by 12% SDS-PAGE under non-reducing conditions, were incubated with ggNumb-iso1-His crude extract (600µg, A. lane 2), ggNumb-iso3-His crude extract (600µg, A. lanes 3a and 3b), and ggNumb-iso2-His crude extract (600µg, B. lanes 2 and 3). The strips were washed and incubated with anti-ggNumb antiserum (A. lanes 2-3b; B. lane 2) and anti-His antibody (B. lane 3), respectively. GST-humanLDLRct-myc was visualized by Western blotting by using anti-GST antibody (A. and B. lane 1). The primary antibodies were detected with HRP-conjugated goat anti-rabbit IgG (1:50000, A. lanes 2-3b; B. lane 2) or HRP-conjugated goat anti-mouse IgG (1:1500, A. and B. lane 1; B. lane 3) and enhanced chemiluminescence. The difference between A. lane 3a and 3b is a longer exposure time in lane 3b.The positions of migration (kDa) of marker proteins are indicated.

The position of the bound ligands was visualized by immunoblotting with anti-ggNumb antiserum (Fig. 43, A. lanes 2-3b; B. lane 2) and anti-His antibody (Fig. 43, B. lane 3), respectively. Chicken Numb isoform3 clearly bound to the approximately 35kDa human LDLRct (Fig. 43, A. lane 3b). The position of the cytoplasmic tail was immunologically shown by using anti-GST antibody (Fig. 43, A. and B., lane 1). No signals could be obtained, when chicken Numb isoform1 (Fig. 43, A. lane 2) or chicken Numb isoform2 (Fig. 43, B. lanes 2 and 3) were used as a ligand.

In the following experiments the chicken LDLRct was tested for interaction with chicken Numb isoforms.

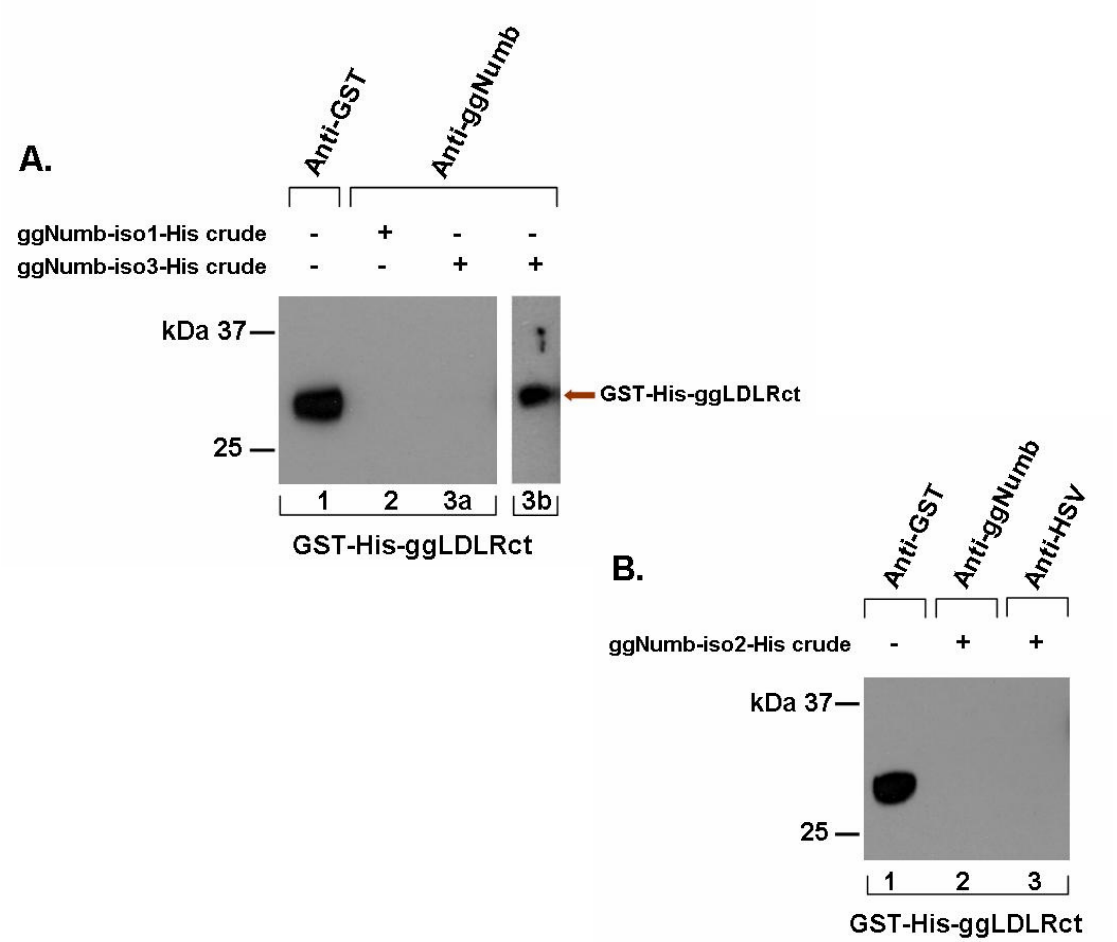

Figure 44. Chicken LDLRct fusion protein binds to the chicken Numb isoform3.

Nitrocellulose strips containing GST-His-ggLDLRct (A. and B. lane 1: 0,5µg; lanes 2-3b: 1µg), separated by 12% SDS-PAGE under non-reducing conditions, were incubated with ggNumb-iso1-His crude extract (600µg, A. lane 2), ggNumb-iso3-His crude extract (600µg, A. lanes 3a and 3b), and ggNumb-iso2-His crude extract (600µg, B. lanes 2 and 3) . The strips were washed and incubated with anti-ggNumb antiserum (A. lanes 2-3b; B. lane 2) and anti-HSV antibody (B. lane 3). GST-His-ggLDLRct was visualized by Western blotting by using anti-GST antibody (A. and B. lane 1). The primary antibodies were detected with HRP-conjugated goat anti-rabbit IgG (1:50000, A. lanes 2-3b; B. lane 2) or HRP-conjugated goat anti-mouse IgG (1:1500, A. lane 1; B. lanes 1 and 3) and enhanced chemiluminescence. The difference between A. lane 3a and 3b is a longer exposure time in lane 3b.The positions of migration (kDa) of marker proteins are indicated.

The approximately 30kDa chicken LDLRct was visualized with anti-GST antibody (Fig. 44, A. and B. lane 1). The bound ligands were detected with anti-ggNumb antiserum (Fig. 44, A. lanes 2-3b; B. lane 2) and anti-HSV antibody (Fig. 44, B. lane 3). Chicken Numb isoform3 clearly bound to the chicken LDLRct (Fig. 44, A. lane 3b). No signals could be obtained with chicken Numb isoform1 or isoform2 as ligands (Fig. 44, A. lane 2; B. lanes 2 and 3).

Cloning of the chicken Numb PRR insert

As shown above the chicken Numb isoform3 containing the PRR insert binds to the cytoplasmic tails of the human and chicken LDLR, but isoforms 1 and 2 do not.
The question arises whether the PRR inserted sequence is responsible for the observed interaction. To address this question, I cloned the 48-residue PRR insert to investigate the binding of this PRRi stretch to the human and chicken LDLR cytoplasmic tails.
The chicken Numb isoform3 was used as a template for the RT-PCR, which was performed using the sequence-specific forward primer, 5'-CAGAATTCCGTTAATGGCACTGCC-3' (containing an EcoRI site, underlined), and the reverse primer 5'-GTCTCGAGGCCAGAGACCATGGC-3' (containing an XhoI site, underlined). The sequence was verified by DNA sequencing.

Bacterial expression of the recombinant chicken Numb PRR insert

For the bacterially production of His_6-tagged ggNumb PRRi the pET25b+-vector expression system was used.

Figure 45. Schematic drawing of the recombinant chicken Numb-PRRi•HSV•6xHis fusion protein.

The PRR insert (shown as a green box) was cloned into the pET25b+-expression vector, which carries an optional C-terminal HSV•Tag (blue box) and a 6xHis•Tag (red box) sequence.

The PRR insert cDNA was cloned between the EcoRI and XhoI sites of the pET25b+-vector, providing a C-terminal HSV-Tag and a 6xHis-Tag (Fig. 45). The construct was verified by DNA sequencing. The recombinant chicken Numb-PRRi•HSV•6xHis fusion protein was bacterially expressed in BL21 cells. The induction of protein expression of the approximately 15 kDa ggNumb-PRRi-His fusion protein is shown in Fig. 46 A. to C.

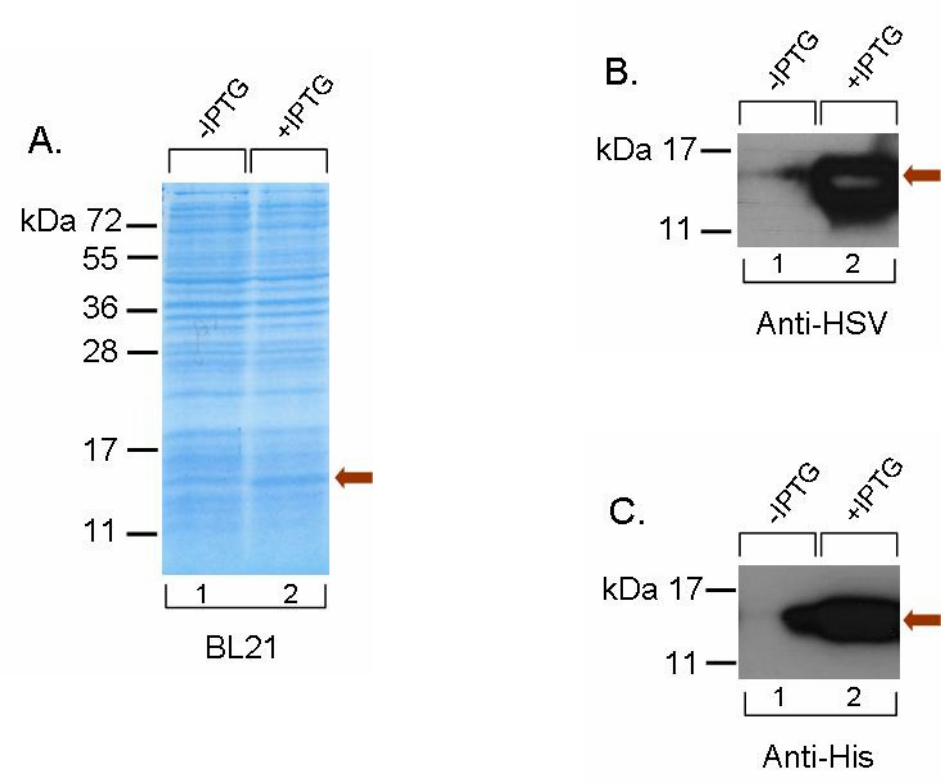

Figure 46. Bacterial expression of chicken Numb-PRRi•His fusion protein.

The recombinant fusion protein was expressed in BL21 cells. Cell extracts, before (lane 1) and after (lane 2) 3 h of induction with 1mM IPTG, were subjected to SDS-PAGE under reducing conditions and subsequently analyzed by Coomassie Blue stain (A.) and Western blotting using anti-HSV (B.) and anti-His (C.) antibodies. The bound primary antibodies were detected with with HRP-conjugated goat anti-mouse IgG (1:1500) (B. and C.) and enhanced chemiluminescence. The positions of migration (kDa) of marker proteins are indicated.

Interaction of the chicken Numb PRR insert with cytoplasmic domains of the chicken and human LDLR

To test whether the PRRi stretch is involved in binding of chicken Numb isoform3 to the chicken and human LDLRct, the expressed PRR insert was used to perform ligand blots (Fig. 47).

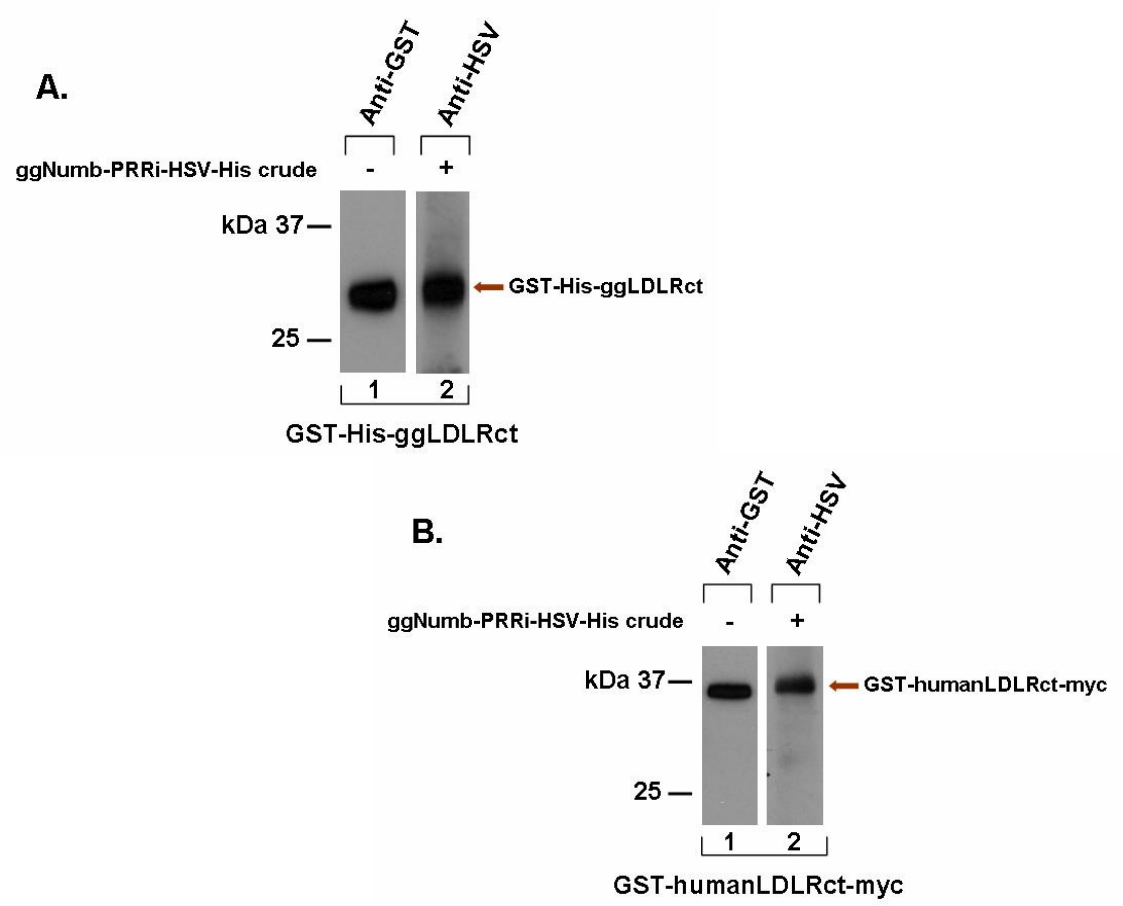

Figure 47. Interaction of the chicken Numb PRR insert with the chicken and human LDLR cytoplasmic tail.

Nitrocellulose strips containing GST-His-ggLDLRct (A. lane 1: 0,5µg; lane 2: 1µg) or GST-humanLDLRct-myc (B. lane 1: 0,5µg; lane 2: 1µg), separated by 12% SDS-PAGE under non-reducing conditions, were incubated with ggNumb-PRRi-HSV-His crude extract (150µg, A. and B. lane 2) . The strips were washed and incubated with anti-HSV antibody (A. and B. lane 2). GST-His-ggLDLRct and GST-humanLDLRct-myc were visualized by Western blotting by using anti-GST antibody (A. and B. lane 1). The primary antibodies were detected with HRP-conjugated goat anti-mouse IgG (1:1500) and enhanced chemiluminescence. The positions of migration (kDa) of marker proteins are indicated.

The bound ligand was depicted by immunoblotting with anti-HSV antibody (Fig. 47, A. and B. lane 2). The chicken Numb PRRi stretch bound to the chicken and human LDLR cytoplasmic tails, which were immunologically identified with anti-GST antibody (Fig. 47, A. and B. lane 1).
These results produced clear evidence that the PRR insert is involved in, if not responsible for, the interaction of chicken Numb isoform3 with the chicken and human LDLR cytoplasmic tails.

Binding of chicken LR8 and LR8B to chicken Numb

LR8, the avian homologue of VLDLR, and LR8B, the chicken homologue of apoER2, are both engaged in receptor-mediated endocytosis. LR8 is responsible for the massive uptake of VLDL and VTG into the growing oocytes (Bujo, Hermann et al. 1994; Schneider 1995).
LR8B, expressed only in the brain, is participating in the clearance of α_2-macroglobulin-proteinase complexes (Novak, Hiesberger et al. 1996; Brandes, Novak et al. 1997; Stockinger, Hengstschlager-Ottnad et al. 1998).
Due to their involvement in receptor-mediated endocytosis, I considered that Numb, as an adaptor protein, binds to the intracellular domains of chicken LR8 and/or LR8B. Therefore, ligand blots were performed with bacterially expressed and purified cytoplasmic tails of chicken LR8 (Fig. 48) and LR8B (Fig. 49) and chicken Numb isoforms.

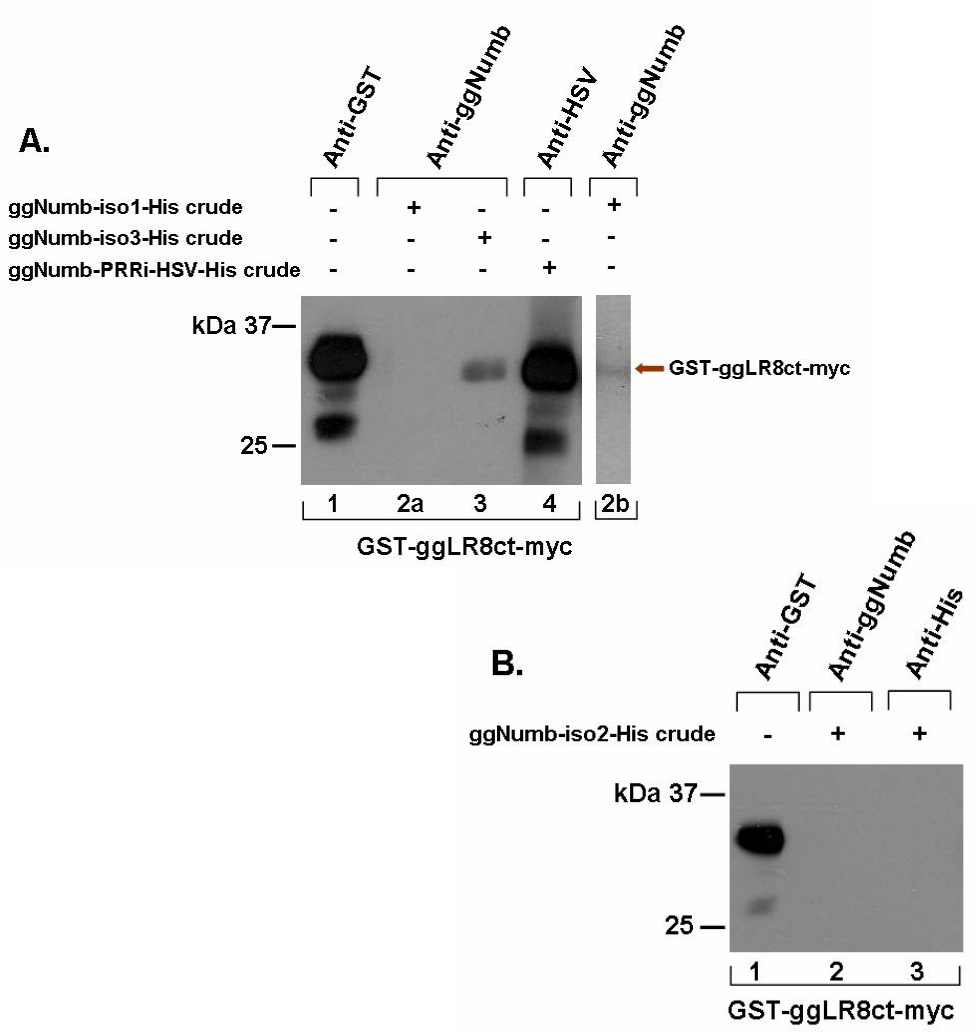

Figure 48. Binding of chicken Numb to the cytoplasmic domain of chicken LR8.

Nitrocellulose strips containing GST-ggLR8ct-myc (A. lane 1: 2µg; lanes 2a-4: 3µg; B. lane 1: 1,5µg; lanes 2-3: 3µg), separated by 12% SDS-PAGE under non-reducing conditions, were incubated with ggNumb-iso1-His crude extract (600µg, A. lanes 2a and 2b), ggNumb-iso3-His crude extract (600µg, A. lane 3), ggNumb-PRRi-HSV-His crude (150µg, A. lane 4), and ggNumb-iso2-His crude extract (600µg, B. lanes 2-3). The strips were washed and incubated with anti-ggNumb antiserum (A. lanes 2a-3; B. lane 2), anti-HSV (A. lane 4), and anti-His (B. lane 3) antibodies. GST-ggLR8ct-myc was visualized by Western blotting by using anti-GST antibody (A. and B. lane 1). The primary antibodies were detected with HRP-conjugated goat anti-rabbit IgG (1:50000, A. lanes 2a-3; B. lane 2) or HRP-conjugated goat anti-mouse IgG (1:1500, A. lanes 1 and 4; B. lanes 1 and 3) and enhanced chemiluminescence. The difference between A. lane 2a and 2b is a different exposure time. The positions of migration (kDa) of marker proteins are indicated.

Anti-ggNumb antiserum (Fig. 48, A. lanes 2a-3; B. lane 2), anti-HSV (Fig. 48, A. lane 4), and anti-His (Fig. 48, B. lane 3) antibodies visualized binding of chicken Numb isoform1, isoform3, and the PRRi stretch. Furthermore the position of GST-ggLR8ct-myc was identified with the anti-GST antibody (Fig. 48, A. and B. lane 1). The signal

for the chicken Numb isoform1 binding was very weak (Fig. 48, A. lane 2b) and only could be demonstrated after a prolonged exposure time. Binding of isoform2 could not be detected (Fig. 48, B. lanes 2 and 3). The analogous experiment was performed with GST-ggLR8Bct-myc (Fig. 49).

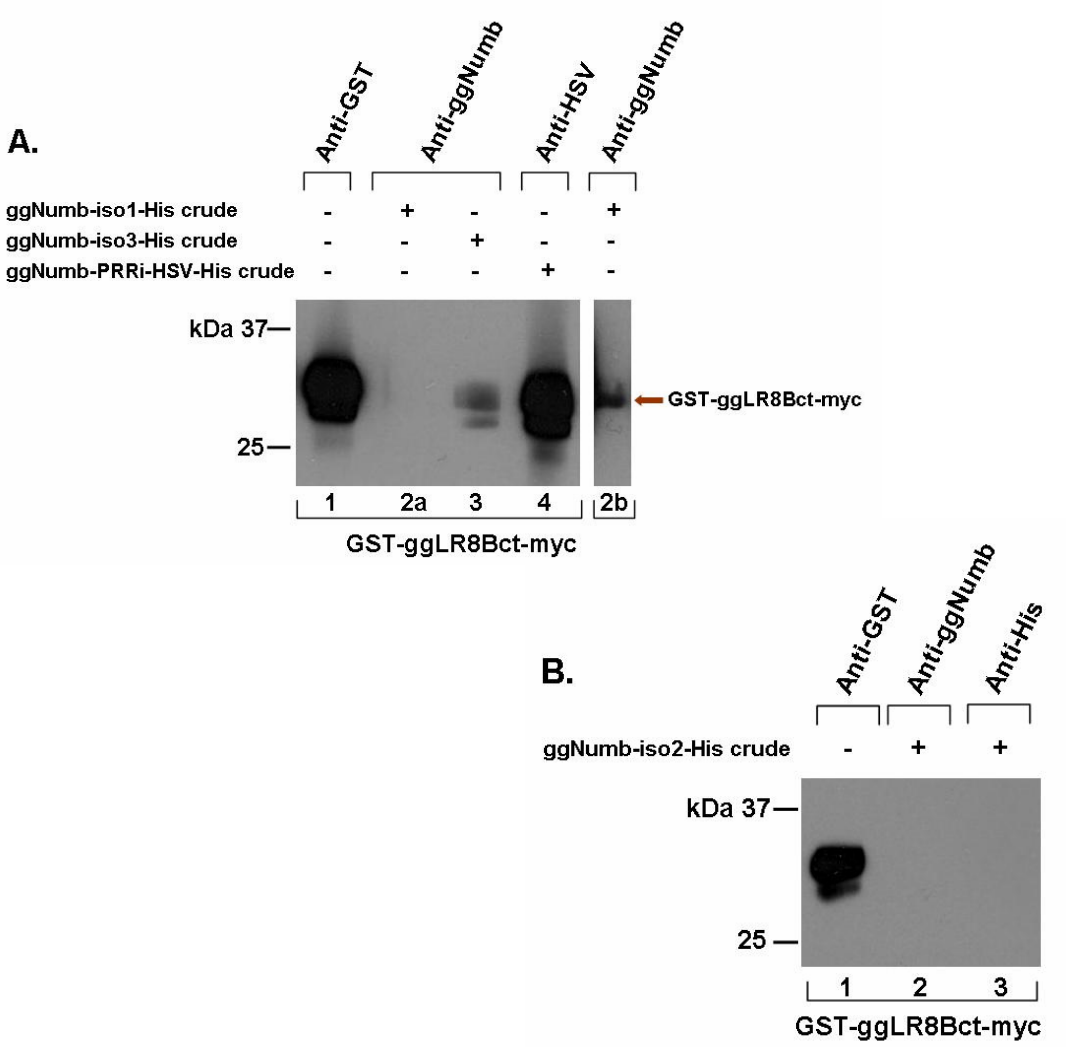

Figure 49. Interaction of the cytoplasmic tail of chicken LR8B with chicken Numb.

Nitrocellulose strips containing GST-ggLR8Bct-myc (A. lane 1: 2µg; lanes 2a-4: 3µg; B. lane 1: 1,5µg; lanes 2 and 3: 3µg), separated by 12% SDS-PAGE under non-reducing conditions, were incubated with ggNumb-iso1-His crude extract (600µg, A. lanes 2a and 2b), ggNumb-iso3-His crude extract (600µg, A. lane 3), ggNumb-PRRi-HSV-His crude (150µg, A. lane 4), and ggNumb-iso2-His crude extract (600µg, B. lanes 2 and 3). The strips were washed and incubated with anti-ggNumb antiserum (A. lanes 2a-3; B. lane 2), anti-HSV (A. lane 4), and anti-His (B. lane 3) antibodies. GST-ggLR8ct-myc was visualized by Western blotting by using anti-GST antibody (A. and B. lane 1). The primary antibodies were detected with HRP-conjugated goat anti-rabbit IgG (1:50000, A. lanes 2a-3; B. lane 2) or HRP-conjugated goat anti-mouse IgG (1:1500, A. lanes 1 and 4; B. lanes 1 and 3) and enhanced chemiluminescence. The difference between lane A. 2a and 2b is a longer exposure time. The positions of migration (kDa) of marker proteins are indicated.

Chicken LR8B cytoplasmic tail fusion protein was subjected to SDS-PAGE under non-reducing conditions, blotted onto nitrocellulose and incubated with the crude extracts of BL21 cells expressing ggNumb-iso1-His (Fig. 49, A. lanes 2a and 2b), ggNumb-iso2-His (Fig. 49, B. lanes 2 and 3), ggNumb-iso3-His (Fig. 49, A. lane 3), and ggNumb-PRRi-HSV-His (Fig. 49, A. lane 4). The GST-tagged LR8B cytoplasmic tail was visualized using anti-GST antibody (Fig. 49, A. and B. lane 1).
As for the LR8 cytoplasmic tail (Fig. 48) chicken Numb isoform1 bound to the chicken LR8B cytoplasmic domain, but to a significantly smaller extent than ggNumb isoform3 and PRR insert did. Again, no binding of isoform2 could be obtained (Fig. 49, B. lanes 2 and 3).
The tails used in Fig. 47 to 49, namely the ggLDLRct, the human LDLRct, the ggLR8ct, and the ggLR8Bct were checked, if they cross-react with anti-HSV antibody, but no signal could be obtained (data not shown).

Interaction of the chicken Amnionless cytoplasmic tail with adaptor proteins

ARH (Autosomal Recessive Hypercholesterolemia) is another endocytic adaptor protein, which binds to the cytoplasmic tails of certain LDLR family members (Mishra, Watkins et al. 2002; Traub 2003). Endocytic adaptors are necessary to connect transmembrane proteins with the clathrin-mediated endocytosis machinery (Mousavi, Malerod et al. 2004). For instance, ARH has been shown to be important for LRP2-mediated endocytosis (Nagai, Meerloo et al. 2003). Amnionless, like LRP2, is a co-receptor for Cubilin and contains internalization sequences for receptor-mediated endocytosis.
It was shown in preliminary experiments that the cytoplasmic tail of chicken Amnionless binds to chicken ARH (Christian 2006). Thus, first I confirmed this finding by performing a co-immunoprecipitation (Co-IP) and a ligand blot as described in Materials and Methods. The antiserum against ARH used (anti-ARH), was described in (Grünstäudl 2005), and originally designated antiserum #65. The anti-ARH antiserum was generated against a peptide corresponding to amino acid 89-117 of human ARH, and it was shown that this antibody cross-reacts with the chicken ARH.

His-tagged chicken Amnionless cytoplasmic tail (ggAmnionless ct-His) was incubated with GST-ggARH and the mixture was precipitated by using anti-ARH antiserum. The precipitate was analyzed for the presence of co-precipitated ggAmnionless ct-His by Western blotting using the anti-His antibody as the primary antibody (Fig. 50).

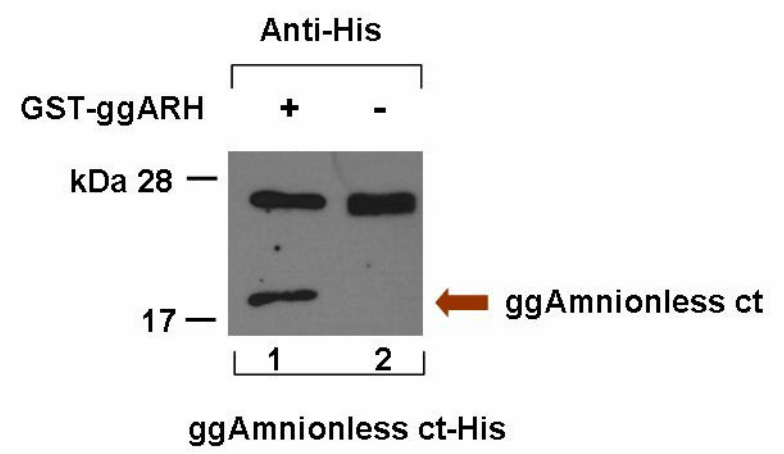

Figure 50. Chicken Amnionless intacellular domain binds to the chicken adaptor protein ARH.

1µg of ggAmnionless ct-His protein was preincubated with (lane 1) or without (lane 2) 7,5µg of purified GST-ggARH and then mixed with anti-ARH antiserum. Subsequently, Protein A Sepharose was added, and the immunoprecipitated material was separated by 15% SDS-PAGE under reducing conditions. The nitrocellulose membrane was then incubated with anti-His antibody. The primary antibody was detected with HRP-conjugated goat anti-mouse IgG (1:1500) and enhanced chemiluminescence. The positions of migration (kDa) of marker proteins are indicated.

It could be shown that the cytoplasmic tail of chicken Amnionless binds to the chicken ARH (Fig. 50, lane 1). When the chicken Amnionless ct was incubated with Protein A Sepharose alone (Fig. 50, lane 2) or only with the anti-ARH antibody and Protein A Sepharose (not shown), no binding was detectable.
The same result could be observed by ligand blotting (Fig. 51).

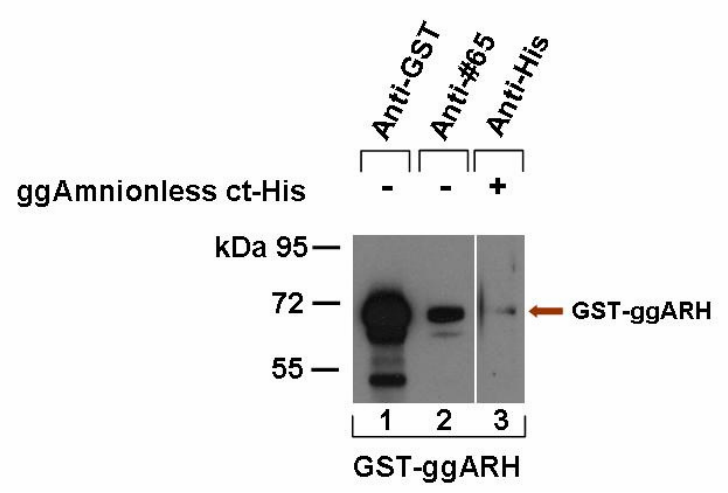

Figure 51. Recombinant His-tagged ggAmnionless cytoplasmic tail binds to the GST-tagged ARH.

Nitrocellulose strips containing purified GST-ggARH protein (lanes 1 and 2: 0,5µg; lane 3: 2µg) separated by 10% SDS-PAGE under non-reducing conditions, were incubated with ggAmnionless ct-His (20µg, lane 3). The strip shown in lane 3 was washed and incubated with anti-His antibody. GST-ggARH was visualized by Western blotting by using either anti-GST antibody (lane 1) or anti-ARH antiserum (lane 2). The primary antibodies were detected with HRP-conjugated goat anti-rabbit IgG (1:50000, lane 2) or HRP-conjugated goat anti-mouse IgG (1:1500, lanes 1 and 3) and enhanced chemiluminescence. In lane 3, a longer exposure time was used.
The positions of migration (kDa) of marker proteins are indicated.

The bound ligand was visualized with anti-His antibody (Fig. 51, lane 3). GgAmnionless ct-His clearly bound to GST-ggARH, which migrate as an approximately 65 kDa protein. The position of migration of GST-ggARH was identified with anti-GST (Fig. 51, lane 1) and anti-ARH (Fig. 51, lane 2) antibodies, respectively.

ARH binds to the FxNPxY motif in the cytoplasmic tails of the LDLR receptor family members via the phosphotyrosine-binding (PTB) domain (Mishra, Watkins et al. 2002; Yan, Kuti et al. 2002). Numb also possesses such a PTB domain, which is evolutionarily and most closely related to that of ARH (Mishra, Watkins et al. 2002). Numb is known to associate with clathrin-coated pits (CCPs), vesicles, and endosomes, and therefore was suggested to function as an endocytic adaptor protein (Santolini, Puri et al. 2000).
Since chicken ARH is able to bind to the chicken Amnionless cytoplasmic tail, the question arose whether the chicken Numb isoforms are also able to bind to it.

Therefore, a ligand blot with the chicken Amnionless cytoplasmic tail and the different chicken Numb isoforms was performed (Fig. 52).

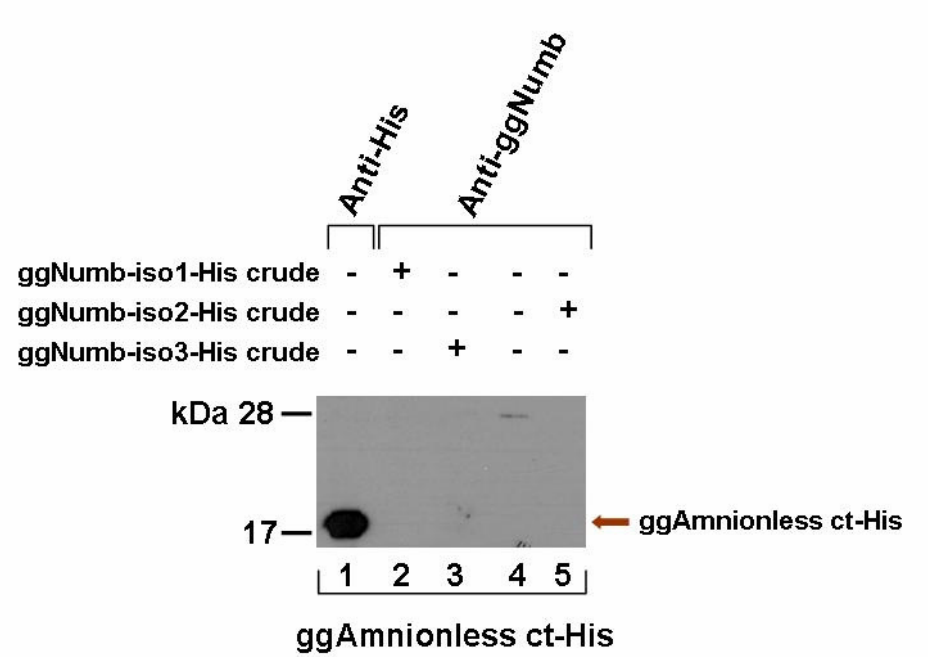

Figure 52. Chicken Numb isoforms do not bind the chicken Amnionless cytoplasmic tail.

Nitrocellulose strips containing ggAmnionless ct-His (1,5µg/lane), separated by 15% SDS-PAGE under non-reducing conditions, were incubated with 300µg crude extract of ggNumb isoform1 (lane 2), ggNumb isoform2 (lane 5), and ggNumb isoform3 (lane 3). The strips were washed and incubated with anti-ggNumb antiserum (lanes 2, 3, and 5). GgAmnionless ct was visualized by Western blotting with anti-His antibody (lane 1). In lane 4 the blot was incubated with anti-ggNumb to test for cross-reactivity with the ggAmnionless ct. The primary antibodies were detected with HRP-conjugated goat anti-mouse IgG (lane 1; 1:1500) or HRP-conjugated goat anti-rabbit IgG (lanes 2-5; 1:50000) and enhanced chemiluminescence. The postions of migration (kDa) of marker proteins are indicated.

The results obtained with the various chicken Numb isoforms are depicted in Fig. 52. As I wanted to determine the ability of Numb to bind to the chicken Amnionless cytoplasmic tail, the proteins were electrophoretically separated under non-reducing conditions (Fig. 52, lanes 1-5). The proteins were blotted onto nitrocellulose membrane and incubated with crude extracts of bacteria expressing ggNumb isoform1 (Fig. 52, lane 2), ggNumb isoform2 (Fig. 52, lane 5), and ggNumb isoform3 (Fig. 52, lane 3). The binding of the Numb isoforms was tested by using anti-ggNumb antiserum (Fig. 52, lanes 2-5). The position of ggAmnionless ct-His was visualized by Western blotting with anti-His antibody (Fig. 52, lane 1).

Interestingly, although chicken Amnionless (Ensembl database, ENSGALT00000018581), contains the presumptive internalization signals FDNPMF and YINPLY (Fig. 53), it interacts with chicken ARH, but does not appear to bind to chicken Numb.

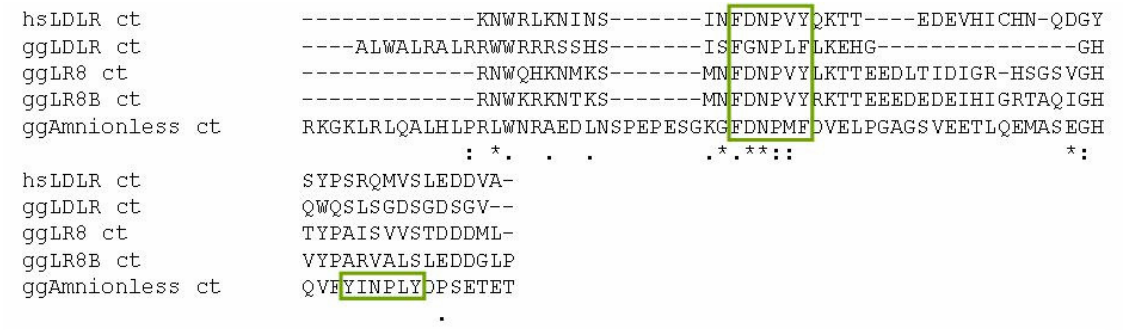

Figure 53. Alignment of cytoplasmic tails of receptors studied.

The human LDLR, the chicken LDLR, the chicken LR8, and the chicken LR8B cytoplasmic tails contain one internalization signal (enboxed in green). While the chicken Amnionless cytoplasmic tail contains two internalization motifs.

All shown alignments in this thesis were made with the alignment program from www.ebi.ac.uk, except for Fig. 53, the alignment program from www.ch.embnet.org was used.

Discussion

Characterization of the chicken LDLR ligand binding domain

The first part of this thesis deals with the elucidation of binding properties of the avian LDLR's extracellular domain based on our knowledge about the human LDLR. This receptor is the first characterized and most prominent member of the LDLR gene family (Brown and Goldstein 1974; Goldstein and Brown 1974). The investigation of the human genetic disease, familial hypercholesterolemia (FH), led to the discovery of the LDLR and to the identification of the LDLR as the key component in the feedback-regulated maintenance of cholesterol homeostasis in the body (Goldstein, Brown et al. 1985). The LDLR binds and internalizes cholesterol-rich lipoproteins containing apolipoprotein B100 (apoB100) or E (apoE), and thereby plays a role in both supplying all cells with cholesterol and reducing the risk of atherosclerosis. The high degree of specificity of the LDLR for apoB100 and apoE is recognized to reside in its domain structure. The LDLR is composed of structurally and functionally defined modules. These modules are: i) the ligand binding domain consisting of seven ligand binding type A (LA) repeats, ii) the so-called EGF precursor homology domain, iii) an O-linked sugar domain, iv) a membrane anchoring domain, and v) a cytoplasmic tail.

While much is known about the features required for recognition of ligands and for receptor internalization, respectively, there are still some open issues. For this study, the ligand binding domain, which mediates the interaction between the receptor and lipoproteins containing apoB100 and apoE (Esser, Limbird et al. 1988), and the cytoplasmic tail containing an internalization signal involved in connecting the LDLR to the clathrin-mediated endocytosis machinery, are of great interest.

In the chicken, which is the model organism in our laboratory, the LDLR has been identified a few years ago (Hummel, Lynn et al. 2003). The structure of the avian LDLR is largely congruent with that of mammalian LDLRs, in that it contains all of the common structural elements of the LDLR family members.

One notable difference in the chicken LDLR is an Alanine/Glutamate-rich stretch (also termed linker) between LA binding repeats 4 and 5, which is not present in the human LDLR (see Fig. 22).

It has been shown that rabbit β–VLDL, an apoE-rich class of lipoprotein particles, binds to the human LDLR via apoE. The major chicken oocyte lipoprotein receptor, LR8, is highly homologous to the mammalian VLDLR, which is known to bind apoE (Bujo, Hermann et al. 1994). LR8 is responsible for the uptake of VLDL and vitellogenin (VTG) into the growing oocyte. Chicken LR8 can interact with human apoE (Fig. 24), but the chicken LDLR does not (Hayashi, Nimpf et al. 1989; Steyrer, Barber et al. 1990). The observation that chicken LR8 binds human apoE is remarkable considering that birds do not synthesize apoE (Steyrer, Barber et al. 1990). In this context, since LR8 transports VTG, this ligand has been suggested to represent a functional analog of apoE (Steyrer, Barber et al. 1990).

It is known that the negatively charged cluster Ser-Asp-Glu (SDE) in the fifth repeat of the LDLR ligand binding domain plays a crucial role in the interaction of β–VLDL/apoE and LDL with the LDLR (Esser, Limbird et al. 1988). Therefore, the fifth repeat is probably the most important LA repeat for the binding of LDL and β–VLDL. However, as described below, other features also appear to be involved.

The approach to shed further light on receptor/ligand interactions was to introduce mutations into the chicken ligand binding domain to render the chicken LDLR's extracellular domain more similar to that of the human receptor, and to possibly enable the binding of human apoE to the altered chicken LDLR. In order to search for sequence motifs necessary for these interactions, SDEE in repeat 1 was replaced by SDES (see Fig. 23, LA7m), because the apoE-binding human LDLR and chicken LR8 contain an SDES motif at this position, suggesting that this sequence maybe required for the interaction.

The LA7m5 mutant (Fig. 23), in which SDED in repeat 5 was replaced by SDEE, was generated because as mentioned above, the SDE cluster in the fifth repeat in the human LDLR likely is crucial. In LA7Δ (Fig. 23) the insert into the linker between repeats 4 and 5 was deleted, and only the number of amino acids present between the two repeats in the human LDLR remained. The assumption was that the long linker may change the conformation of the LA repeats, and/or their positioning within the ligand binding domain, so that human apoE is unable to bind. In the LA7 double mutant, LA7dbl (Fig. 23), the mutations LA7m and LA7m5 were introduced together

in order to cover the possibility that a combination of these mutations is necessary for mediating the interaction of human apoE with the chicken LDLR's ligand binding domain.

The mutations leading to these substitutions and the deletion, respectively (Fig. 23), were achieved using site-directed mutagenesis. The wt and the four different mutated LA7 domains were expressed and refolded. The refolding in the presence of RAP-Sepharose was necessary to gain the full binding activity of the ligand binding domains, as was also shown in a recent publication using the β–propeller domains of the LDLR relative LRP6 (Liu, Pearson et al. 2009). The refolding, which is essentially dependent on disulfide bridges, is abolished when reducing conditions are used. This is also reflected by the fact that the proteins migrate slower in SDS gels under reducing conditions (Fig. 26 and 27). The binding ability of the folded wt and mutant LA7 domains was analyzed by co-immunoprecipitation with His-RAP-myc (Fig. 28), which showed that the mutated LA7s are active and are able to form receptor-ligand complexes.

Subsequently, the different LA7 domains were tested for their ability to bind the 3 different human apoE isoforms by performing ligand blotting, but signals could unfortunately not be obtained (data not shown). Maybe this failure to interact is due to the recovery of correctly folded protein being too low for demonstrating apoE-binding, albeit it is sufficient for showing interaction with RAP. Alternatively, the refolding of the bacterially expressed proteins in the presence of RAP-Sepharose may not be sufficient, and production of the different LA domains by the intrinsic folding machinery of eukaryotic cells for secretion would result in a better yield. Another reason could be that the analysis of the interaction via ligand blotting, although successfully applied in many studies from our laboratory [e.g. (Dichlberger, Cogburn et al. 2007)], is not the most sensitive method. In a recent publication, fluorescence resonance energy transfer (FRET) was used for analysis of such interactions (Yamamoto and Ryan 2009); however, such experiments were beyond the frame of this thesis.

The chicken LDLR has only been detected in somatic cells, does not bind β-VLDL/apoE, and is not able to cross-react with an antibody against bovine LDLR; in contrast, LR8 is present in oocytes, does bind β-VLDL, and cross-reacts with an antibody against the bovine LDLR (Hayashi, Ando et al. 1989; Hayashi, Nimpf et al. 1989). Since VTG may represent the equivalent of apoE in oviparous species, and

the chicken LDLR is not directly involved in oocyte growth, it appears logical that apoE is not a ligand for the chicken LDLR. Based on these assumptions, another approach would be to compare the sequences of ggLR8 and the ggLDLR and introduce mutations into the ggLDLR to render it more similar to ggLR8, as already achieved in the LA7m mutant.

Protein interaction properties of the intracellular domains of LDLR family members

The cytoplasmic tails of the LDLR family members interact with classical adaptor proteins such as AP2, and with alternative adaptors including ARH, Dab2, and Numb (Traub 2003). The adaptor proteins are required to select receptors for clathrin-mediated internalization (Mousavi, Malerod et al. 2004). It is known that ARH binds to the NPxY motif in the cytoplasmic tails of the LDLR family members as well as to components of clathrin-coated pits (He, Gupta et al. 2002; Mishra, Watkins et al. 2002). It has been shown that human and chicken ARH bind to the cytoplasmic tails of LDLRs from chicken as well as man (Grünstäudel 2005). It was of interest to investigate whether Numb, which is closely related to ARH, is also able to interact with the LDLR's cytoplasmic tail (Mishra, Watkins et al. 2002). Numb was originally identified as a cell fate determinant in the nervous sytem of *Drosophila* (Uemura, Shepherd et al. 1989; Rhyu, Jan et al. 1994). Due to the fact that Numb interacts with AP2 and associates with clathrin-coated pits, vesicles, and endosomes, it was suggested that it functions as an endocytic adaptor (Santolini, Puri et al. 2000; Tokumitsu, Hatano et al. 2006). The group of Wakamatsu also identified a chicken Numb protein (Fig. 31) (Wakamatsu, Maynard et al. 1999).

Chicken Numb displays 83% sequence identity with human and murine Numb (Fig. 30) and appears to be evolutionarily well conserved. In mammals, four different isoforms of Numb are known. By BLAST search, different chicken Numb isoforms have been revealed that differ in the presence or absence of inserts in the phosphotyrosine-binding domain (PTB) and in the proline-rich region (PRR) (Fig. 33). It is interesting that the potential chicken Numb phosphotyrosine-binding domain insert (PTBi) contains 11 amino acids (aa), which are 100% conserved in mammals, whereas the proline-rich region insert (PRRi) is 48 aa long and shares about 56% sequence identity with the mammalian insert, which lies adjacent to the PRR domain

(Dho, French et al. 1999). The PRR insert is less conserved, which is compatible with the PRR inserted sequence in the chicken protein having specific functions not required in mammalian systems. The chicken Numb isoforms 1 to 3 were cloned, expressed, and used for interaction studies. The chicken Numb isoform2 contains an additional in-frame insert immediately before the canonical PTB insert (Fig. 37), whose sequence was also found in the chicken Ensembl database. This novel insert preceding the PTB insert is not present in the Numb isoform2 of any organism and thus is a new finding in the chicken. The difference may result from alternative splicing only in the avian species, and may allow to increase or decrease the binding ability of Numb isoform2 to cytoplasmic tails of the chicken LDLR family members.

I could not clearly obtain cDNA for chicken Numb isoform4. One reason could be that the transcripts for isoforms 3 and 4 are nearly the same size, with a difference of only 33 bp, and so it was not feasible to separate them. Other reasons could be that chicken Numb isoform4 is not at all expressed, or simply that the gene sequence reported in the Ensembl database is wrong.

Mammalian Numb, containing an insert in the PTB domain or not, is able to efficiently bind to Ligand of Numb-protein X (LNX) and both domains show binding to acidic phospholipids (Dho, Jacob et al. 1998; Dho, French et al. 1999). In contrast, the PRR domain of the human Numb containing the insert promotes neuronal proliferation during mammalian neurogenesis, whereas the PRR domain without the insert enhances neuronal differentiation. Thus, the Numb-PRRs with and without the insert, respectively, can fulfill different functions (Verdi, Bashirullah et al. 1999). Thus, if chicken Numb is able to bind LDLR's cytoplasmic tails, the question arises whether the inserts make a difference.

The finding that chicken Numb isoform3 binds to the human and to the chicken LDLRct, but Numb isoforms 1 and 2 do not, was surprising. Possibly, this difference is caused by the fact that the insert in the mammalian Numb PTB domain did not change the binding ability of the PTB domain to the NPxY sequence motif (Dho, Jacob et al. 1998). Maybe the newly identified additional insert in chicken Numb isoform2 alters the binding capacity or leads to an conformational change, or both, which leads to an inhibition of the interaction.

The astonishing fact that only chicken Numb isoform3 interacts with the cytoplasmic tails of the human and chicken LDLR raises the question whether the PRR insert is actually responsible for this interaction. Indeed, by testing whether the insert alone is

able to bind to the human and chicken LDLR's cytoplasmic tails or not, I showed that the PRRi stretch binds to both tails (Fig. 47). This result produced clear evidence that the PRR inserted sequence plays a role in the interaction of chicken Numb isoform3 with the chicken and human LDLR's cytoplasmic tails, which is a new finding, because thus far only the PTB domain was shown to bind to the NPxY motif in the cytoplasmic tail (Yan, Kuti et al. 2002).

Based on the fact that Numb is an endocytic adaptor protein (Santolini, Puri et al. 2000) and is able to bind cytoplasmic tails of the human and chicken LDLR (see above), it was of interest to test whether Numb may bind to other cytoplasmic tails of receptors involved in receptor-mediated endocytosis. Candidate receptors in the chicken include LR8 and LR8B. LR8 is highly homologous to the mammalian VLDLR and has a well established function in the avian species (Bujo, Hermann et al. 1994; Schneider 1995). LR8B, the chicken homologue of the mammalian apoE receptor type 2 (apoER2), is apparently only expressed in the brain (Novak, Hiesberger et al. 1996; Brandes, Novak et al. 1997), where it takes part in the clearance of α_2-macroglobulin-proteinase complexes (Stockinger, Hengstschlager-Ottnad et al. 1998).

As observed in the case of the human and chicken LDLRs, an interaction of the cytoplasmic tails of LR8 and LR8B with chicken Numb isoform2 could not be detected; however, the PRRi stretch alone is able to bind (Fig. 48 and 49), which is indistinguishable from the situation with the cytoplasmic tails of the chicken and human LDLR (see above). Reasons for the apparently weaker interaction of the intracellular domains of the LR8 and LR8B with chicken Numb isoform1 than with isoform3 (Fig. 48 and 49) or with the PRR insert could be that isoform1 is a poorer binding partner for LR8 and LR8B than isoform3, and that the PRRi stretch is necessary to gain the full binding activity of chicken Numb to intracellular domains. The insert in the PTB domain in isoform2 may abolish the interaction between Numb and the cytoplasmic tails. Thus, the PTB insert may disturb the binding activity of isoform2 compared to isoform1. In a recent publication it was shown that Numb proteins that differ in the PTB domains have opposite effects on the transport and processing of amyloid precursor protein (APP) (Kyriazis, Wei et al. 2008). It may be that in the chicken, the insert in the PTB domain abolishes the binding ability of Numb, while the insert in the PRR domain promotes this interaction. The PRR

inserted sequence may employ other motifs for binding than the PTB domain is known to use (He, Gupta et al. 2002).

I also investigated the properties of a receptor whose extracellular domain is very different from those of the LDLR family and thus appears unrelated to the LDLR family, but due to its containing two internalization motifs in its cytoplasmic domain was of obvious interest. This membrane protein is Amnionless, initially identified as a yolk sac protein for formation of the amnion and primitive streak in the mouse (Kalantry, Manning et al. 2001). Amnionless is a type I transmembrane protein and contains two receptor internalization NPxY motifs reminiscent of those in LDLR family members (Kalantry, Manning et al. 2001). Recently, it was shown that mutations in the *amnionless* gene can cause the autosomal recessive disorder, Imerslund-Gräsbeck syndrome (IGS) (Aminoff, Carter et al. 1999; Tanner, Aminoff et al. 2003). IGS is characterized by selective malabsorption of cobalamin (vitamin B_{12}) in the intestine, leading to megaloblastic anemia and degeneration of the nervous system (Grasbeck, Gordin et al. 1960; Imerslund 1960). The malabsorption is caused by the inability of the Cubilin/Amnionless (cubam) complex to bind to intrinsic factor, a glycoprotein tightly binding cobalamin and ensuring its absorption from the intestine (Fyfe, Madsen et al. 2004). The interaction of Amnionless and Cubilin is the key to the co-internalization of ligands bound to Cubilin. Surprisingly, Amnionless was previously demonstrated also in the chicken (Christian 2006) as a 51kDa protein with a high degree of sequence similarity with the murine and canine homologues. It is intriguing to hypothesize that the two internalization sequences in Amnionless, FDNPMF and YINPLY, may be important for a direct role in receptor-mediated endocytosis, especially for ligand transport into the chicken embryo's yolk sac.
Thus, the binding of chicken ARH to the chicken Amnionless intracellular domain demonstrated by co-immunoprecipitation (Fig. 50) and ligand blotting (Fig. 51) may indicate an involvement in mediating endocytosis of Amnionless.
Furthermore, since Numb is an adaptor protein, and its PTB domain is closely related to that in ARH, the question arose whether chicken Amnionless and chicken Numb are able to interact with each other as well. However, ligand blot analysis revealed that chicken Amnionless likely does not bind chicken Numb (Fig. 52), despite the fact that Amnionless contains internalization motifs and interacts with ARH. One explanation for the lack of interaction between the cytoplasmic tail of Amnionless with

chicken Numb could be that the anti-ggNumb antiserum does not have sufficient avidity to detect interaction. Alternatively, the binding may not take place because chicken Numb fails to interact with the internalization motifs, which are similar to, but nevertheless different from those in the tails of the LDLR family members, I investigated.
The failure to bind may also indicate that the different physiology of avian species does not require specific adaptor interaction for internalization, or that uptake pathways involving Amnionless, a protein required for the formation of the amnion, are dispensable in oviparous species.

In conclusion, mutating the LDLR's extracellular domain produced different LA domains that were active and were able to form certain receptor-ligand complexes. However, the binding of human apoE may require highly specific conformations that were not met by the mutant forms, and the nature of which remains to be elucidated.
Four different chicken Numb isoforms were identified at the genome level, and isoform3 was determined as binding partner of the cytoplasmic tails of the human and the avian LDLR, of chicken LR8, and of LR8B, likely via the extra-long insert in the PRR domain of this isoform. Additionally, the insert-lacking chicken Numb isoform1 binds to the intracellular domains of LR8 and LR8B, possibly enhancing endocytosis of these receptors.
Finally, the results of studies on the interaction between the cytoplasmic tail of chicken Amnionless and chicken Numb isoforms indicate that such interaction may not be as crucial to the physiological roles of this receptor in avian species as in mammals.

References

Aggerbeck, L. P., J. R. Wetterau, et al. (1988). "Human apolipoprotein E3 in aqueous solution. II. Properties of the amino- and carboxyl-terminal domains." J Biol Chem **263**(13): 6249-58.

Aminoff, M., J. E. Carter, et al. (1999). "Mutations in CUBN, encoding the intrinsic factor-vitamin B12 receptor, cubilin, cause hereditary megaloblastic anaemia 1." Nat Genet **21**(3): 309-13.

Andersen, O. M., J. Reiche, et al. (2005). "Neuronal sorting protein-related receptor sorLA/LR11 regulates processing of the amyloid precursor protein." Proc Natl Acad Sci U S A **102**(38): 13461-6.

Andersen, O. M. and T. E. Willnow (2006). "Lipoprotein receptors in Alzheimer's disease." Trends Neurosci **29**(12): 687-94.

Andersen, O. M., C. H. Yeung, et al. (2003). "Essential role of the apolipoprotein E receptor-2 in sperm development." J Biol Chem **278**(26): 23989-95.

Arias-Moreno, X., A. Velazquez-Campoy, et al. (2008). "Mechanism of low density lipoprotein (LDL) release in the endosome: implications of the stability and Ca2+ affinity of the fifth binding module of the LDL receptor." J Biol Chem **283**(33): 22670-9.

Bajari, T. M., V. Strasser, et al. (2005). "LDL receptor family: isolation, production, and ligand binding analysis." Methods **36**(2): 109-16.

Beglova, N. and S. C. Blacklow (2005). "The LDL receptor: how acid pulls the trigger." Trends Biochem Sci **30**(6): 309-17.

Beglova, N., H. Jeon, et al. (2004). "Cooperation between fixed and low pH-inducible interfaces controls lipoprotein release by the LDL receptor." Mol Cell **16**(2): 281-92.

Berdnik, D., T. Torok, et al. (2002). "The endocytic protein alpha-Adaptin is required for numb-mediated asymmetric cell division in Drosophila." Dev Cell **3**(2): 221-31.

Blacklow, S. C. and P. S. Kim (1996). "Protein folding and calcium binding defects arising from familial hypercholesterolemia mutations of the LDL receptor." Nat Struct Biol **3**(9): 758-62.

Brandes, C., S. Novak, et al. (1997). "Avian and murine LR8B and human apolipoprotein E receptor 2: differentially spliced products from corresponding genes." Genomics **42**(2): 185-91.

Brown, M. S. and J. L. Goldstein (1974). "Familial hypercholesterolemia: defective binding of lipoproteins to cultured fibroblasts associated with impaired regulation of 3-hydroxy-3-methylglutaryl coenzyme A reductase activity." Proc Natl Acad Sci U S A **71**(3): 788-92.

Brown, M. S. and J. L. Goldstein (1979). "Receptor-mediated endocytosis: insights from the lipoprotein receptor system." Proc Natl Acad Sci U S A **76**(7): 3330-7.

Brown, M. S. and J. L. Goldstein (1986). "A receptor-mediated pathway for cholesterol homeostasis." Science **232**(4746): 34-47.

Buerstedde, J. M. and S. Takeda (1991). "Increased ratio of targeted to random integration after transfection of chicken B cell lines." Cell **67**(1): 179-88.

Bujo, H., R. G. Elkin, et al. (1996). "A rapid, polymerase chain reaction-based procedure for identifying mutant restricted ovulator chickens." Poult Sci **75**(9): 1113-7.

Bujo, H., M. Hermann, et al. (1994). "Chicken oocyte growth is mediated by an eight ligand binding repeat member of the LDL receptor family." Embo J **13**(21): 5165-75.

Bujo, H., K. A. Lindstedt, et al. (1995). "Chicken oocytes and somatic cells express different splice variants of a multifunctional receptor." J Biol Chem **270**(40): 23546-51.

Bujo, H., T. Yamamoto, et al. (1995). "Mutant oocytic low density lipoprotein receptor gene family member causes atherosclerosis and female sterility." Proc Natl Acad Sci U S A **92**(21): 9905-9.

Christensen, E. I. and H. Birn (2002). "Megalin and cubilin: multifunctional endocytic receptors." Nat Rev Mol Cell Biol **3**(4): 256-66.

Christensen, E. I., J. Gliemann, et al. (1992). "Renal tubule gp330 is a calcium binding receptor for endocytic uptake of protein." J Histochem Cytochem **40**(10): 1481-90.

Christian, S. (2006). "Molecular characterization of chicken Boca and Amnionless, two distinct key molecules in lipoprotein metabolism." PhD Thesis.

Corder, E. H., A. M. Saunders, et al. (1993). "Gene dose of apolipoprotein E type 4 allele and the risk of Alzheimer's disease in late onset families." Science **261**(5123): 921-3.

Coudroy, G., J. Gburek, et al. (2005). "Contribution of cubilin and amnionless to processing and membrane targeting of cubilin-amnionless complex." J Am Soc Nephrol **16**(8): 2330-7.

Davidson, N. O. and G. S. Shelness (2000). "APOLIPOPROTEIN B: mRNA editing, lipoprotein assembly, and presecretory degradation." Annu Rev Nutr **20**: 169-93.

Davis, C. G., A. Elhammer, et al. (1986). "Deletion of clustered O-linked carbohydrates does not impair function of low density lipoprotein receptor in transfected fibroblasts." J Biol Chem **261**(6): 2828-38.

Debose-Boyd, R. A. (2004). "Knowing when to let go: endosomal release of LDL from the LDL-Receptor." Mol Cell **16**(2): 160-2.

Dho, S. E., M. B. French, et al. (1999). "Characterization of four mammalian numb protein isoforms. Identification of cytoplasmic and membrane-associated variants of the phosphotyrosine binding domain." J Biol Chem **274**(46): 33097-104.

Dho, S. E., S. Jacob, et al. (1998). "The mammalian numb phosphotyrosine-binding domain. Characterization of binding specificity and identification of a novel PDZ domain-containing numb binding protein, LNX." J Biol Chem **273**(15): 9179-87.

Dichlberger, A. (2004). "Modulators of lipoprotein metabolism." Diploma Thesis.

Dichlberger, A., L. A. Cogburn, et al. (2007). "Avian apolipoprotein A-V binds to LDL receptor gene family members." J Lipid Res **48**(7): 1451-6.

Dodson, S. E., O. M. Andersen, et al. (2008). "Loss of LR11/SORLA enhances early pathology in a mouse model of amyloidosis: evidence for a proximal role in Alzheimer's disease." J Neurosci **28**(48): 12877-86.

Dong, L. M., S. Parkin, et al. (1996). "Novel mechanism for defective receptor binding of apolipoprotein E2 in type III hyperlipoproteinemia." Nat Struct Biol **3**(8): 718-22.

Eden, E. R., D. D. Patel, et al. (2002). "Restoration of LDL receptor function in cells from patients with autosomal recessive hypercholesterolemia by retroviral expression of ARH1." J Clin Invest **110**(11): 1695-702.

Esser, V., L. E. Limbird, et al. (1988). "Mutational analysis of the ligand binding domain of the low density lipoprotein receptor." J Biol Chem **263**(26): 13282-90.

Evans, P. R. and D. J. Owen (2002). "Endocytosis and vesicle trafficking." Curr Opin Struct Biol **12**(6): 814-21.

Fisher, C., D. Abdul-Aziz, et al. (2004). "A two-module region of the low-density lipoprotein receptor sufficient for formation of complexes with apolipoprotein E ligands." Biochemistry **43**(4): 1037-44.

Fyfe, J. C., M. Madsen, et al. (2004). "The functional cobalamin (vitamin B12)-intrinsic factor receptor is a novel complex of cubilin and amnionless." Blood **103**(5): 1573-9.

Garcia, C. K., K. Wilund, et al. (2001). "Autosomal recessive hypercholesterolemia caused by mutations in a putative LDL receptor adaptor protein." Science **292**(5520): 1394-8.

Gaultier, A., S. Arandjelovic, et al. (2008). "Regulation of tumor necrosis factor receptor-1 and the IKK-NF-kappaB pathway by LDL receptor-related protein explains the antiinflammatory activity of this receptor." Blood **111**(11): 5316-25.

Glass, C. K. and J. L. Witztum (2001). "Atherosclerosis. the road ahead." Cell **104**(4): 503-16.

Goldstein, J. L. and M. S. Brown (1974). "Binding and degradation of low density lipoproteins by cultured human fibroblasts. Comparison of cells from a normal subject and from a patient with homozygous familial hypercholesterolemia." J Biol Chem **249**(16): 5153-62.

Goldstein, J. L., M. S. Brown, et al. (1985). "Receptor-mediated endocytosis: concepts emerging from the LDL receptor system." Annu Rev Cell Biol **1**: 1-39.

Grasbeck, R. (2006). "Imerslund-Grasbeck syndrome (selective vitamin B12 malabsorption with proteinuria)." Orphanet J Rare Dis **1**: 17.

Grasbeck, R., R. Gordin, et al. (1960). "Selective vitamin B12 malabsorption and proteinuria in young people. A syndrome." Acta Med Scand **167**: 289-96.

Grünstäudl, K. (2005). "Molecular characterization of modulators of receptor-mediated endocytosis." PhD Thesis.

Gschmeidler, B. (2004). "Molecular studies on the Autosomal Recessive Hypercholesterolemia protein." Diploma Thesis.

Guo, M., L. Y. Jan, et al. (1996). "Control of daughter cell fates during asymmetric division: interaction of Numb and Notch." Neuron **17**(1): 27-41.

Hatters, D. M., C. A. Peters-Libeu, et al. (2006). "Apolipoprotein E structure: insights into function." Trends Biochem Sci **31**(8): 445-54.

Hayashi, K., S. Ando, et al. (1989). "A novel sterol-regulated surface protein on chicken fibroblasts." J Lipid Res **30**(9): 1421-8.

Hayashi, K., J. Nimpf, et al. (1989). "Chicken oocytes and fibroblasts express different apolipoproteins-B-specific receptors." J Biol Chem **264**(6): 3131-9.

He, G., S. Gupta, et al. (2002). "ARH is a modular adaptor protein that interacts with the LDL receptor, clathrin, and AP-2." J Biol Chem **277**(46): 44044-9.

He, Q., J. C. Fyfe, et al. (2003). "Canine Imerslund-Grasbeck syndrome maps to a region orthologous to HSA14q." Mamm Genome **14**(11): 758-64.

He, Q., M. Madsen, et al. (2005). "Amnionless function is required for cubilin brush-border expression and intrinsic factor-cobalamin (vitamin B12) absorption in vivo." Blood **106**(4): 1447-53.

Herz, J. and H. H. Bock (2002). "Lipoprotein receptors in the nervous system." Annu Rev Biochem **71**: 405-34.

Herz, J., J. L. Goldstein, et al. (1991). "39-kDa protein modulates binding of ligands to low density lipoprotein receptor-related protein/alpha 2-macroglobulin receptor." J Biol Chem **266**(31): 21232-8.

Herz, J., U. Hamann, et al. (1988). "Surface location and high affinity for calcium of a 500-kd liver membrane protein closely related to the LDL-receptor suggest a physiological role as lipoprotein receptor." Embo J **7**(13): 4119-27.

Hiesberger, T., M. Trommsdorff, et al. (1999). "Direct binding of Reelin to VLDL receptor and ApoE receptor 2 induces tyrosine phosphorylation of disabled-1 and modulates tau phosphorylation." Neuron **24**(2): 481-9.

Hummel, S., E. G. Lynn, et al. (2003). "Molecular characterization of the first avian LDL receptor: role in sterol metabolism of ovarian follicular cells." J Lipid Res **44**(9): 1633-42.

Hutterer, A. and J. A. Knoblich (2005). "Numb and alpha-Adaptin regulate Sanpodo endocytosis to specify cell fate in Drosophila external sensory organs." EMBO Rep **6**(9): 836-42.

Imerslund, O. (1960). "Idiopathic chronic megaloblastic anemia in children." Acta Paediatr Suppl **49(Suppl 119)**: 1-115.

Jeon, H., W. Meng, et al. (2001). "Implications for familial hypercholesterolemia from the structure of the LDL receptor YWTD-EGF domain pair." Nat Struct Biol **8**(6): 499-504.

Kalantry, S., S. Manning, et al. (2001). "The amnionless gene, essential for mouse gastrulation, encodes a visceral-endoderm-specific protein with an extracellular cysteine-rich domain." Nat Genet **27**(4): 412-6.

Kerjaschki, D. and M. G. Farquhar (1982). "The pathogenic antigen of Heymann nephritis is a membrane glycoprotein of the renal proximal tubule brush border." Proc Natl Acad Sci U S A **79**(18): 5557-61.

Kim, D. H., H. Iijima, et al. (1996). "Human apolipoprotein E receptor 2. A novel lipoprotein receptor of the low density lipoprotein receptor family predominantly expressed in brain." J Biol Chem **271**(14): 8373-80.

Knisely, J. M., Y. Li, et al. (2007). "Slow endocytosis of the LDL receptor-related protein 1B: implications for a novel cytoplasmic tail conformation." Exp Cell Res **313**(15): 3298-307.

Koch, S., V. Strasser, et al. (2002). "A secreted soluble form of ApoE receptor 2 acts as a dominant-negative receptor and inhibits Reelin signaling." Embo J **21**(22): 5996-6004.

Kozyraki, R. and F. Gofflot (2007). "Multiligand endocytosis and congenital defects: roles of cubilin, megalin and amnionless." Curr Pharm Des **13**(29): 3038-46.

Kyriazis, G. A., Z. Wei, et al. (2008). "Numb endocytic adapter proteins regulate the transport and processing of the amyloid precursor protein in an isoform-dependent manner: implications for Alzheimer disease pathogenesis." J Biol Chem **283**(37): 25492-502.

Li, L., P. A. Thompson, et al. (2008). "Infection induces a positive acute phase apolipoprotein E response from a negative acute phase gene: role of hepatic LDL receptors." J Lipid Res **49**(8): 1782-93.

Li, Y., J. Cam, et al. (2001). "Low-density lipoprotein receptor family: endocytosis and signal transduction." Mol Neurobiol **23**(1): 53-67.

Li, Y., M. P. Marzolo, et al. (2000). "The YXXL motif, but not the two NPXY motifs, serves as the dominant endocytosis signal for low density lipoprotein receptor-related protein." J Biol Chem **275**(22): 17187-94.

Lin, C. T., Y. F. Xu, et al. (1986). "Immunoreactive apolipoprotein E is a widely distributed cellular protein. Immunohistochemical localization of apolipoprotein E in baboon tissues." J Clin Invest **78**(4): 947-58.

Liu, C. C., C. Pearson, et al. (2009). "Cooperative folding and ligand-binding properties of LRP6 beta-propeller domains." J Biol Chem **284**(22): 15299-307.

Liu, C. X., Y. Li, et al. (2001). "The putative tumor suppressor LRP1B, a novel member of the low density lipoprotein (LDL) receptor family, exhibits both overlapping and distinct properties with the LDL receptor-related protein." J Biol Chem **276**(31): 28889-96.

Liu, C. X., S. Musco, et al. (2000). "LRP-DIT, a putative endocytic receptor gene, is frequently inactivated in non-small cell lung cancer cell lines." Cancer Res **60**(7): 1961-7.

Magrane, J., M. Reina, et al. (1998). "Bovine aortic endothelial cells express a variant of the very low density lipoprotein receptor that lacks the O-linked sugar domain." J Lipid Res **39**(11): 2172-81.

Mahley, R. W. (1988). "Apolipoprotein E: cholesterol transport protein with expanding role in cell biology." Science **240**(4852): 622-30.

Mahley, R. W. and Y. Huang (1999). "Apolipoprotein E: from atherosclerosis to Alzheimer's disease and beyond." Curr Opin Lipidol **10**(3): 207-17.

Mahley, R. W. and S. C. Rall, Jr. (2000). "Apolipoprotein E: far more than a lipid transport protein." Annu Rev Genomics Hum Genet **1**: 507-37.

Maxfield, F. R. and T. E. McGraw (2004). "Endocytic recycling." Nat Rev Mol Cell Biol **5**(2): 121-32.

McGill, M. A. and C. J. McGlade (2003). "Mammalian numb proteins promote Notch1 receptor ubiquitination and degradation of the Notch1 intracellular domain." J Biol Chem **278**(25): 23196-203.

Mikhailenko, I., W. Considine, et al. (1999). "Functional domains of the very low density lipoprotein receptor: molecular analysis of ligand binding and acid-dependent ligand dissociation mechanisms." J Cell Sci **112 (Pt 19)**: 3269-81.

Mishra, S. K., S. C. Watkins, et al. (2002). "The autosomal recessive hypercholesterolemia (ARH) protein interfaces directly with the clathrin-coat machinery." Proc Natl Acad Sci U S A **99**(25): 16099-104.

Moestrup, S. K., R. Kozyraki, et al. (1998). "The intrinsic factor-vitamin B12 receptor and target of teratogenic antibodies is a megalin-binding peripheral membrane protein with homology to developmental proteins." J Biol Chem **273**(9): 5235-42.

Moestrup, S. K. and P. J. Verroust (2001). "Megalin- and cubilin-mediated endocytosis of protein-bound vitamins, lipids, and hormones in polarized epithelia." Annu Rev Nutr **21**: 407-28.

Morrow, J. A., K. S. Arnold, et al. (2000). "Effect of arginine 172 on the binding of apolipoprotein E to the low density lipoprotein receptor." J Biol Chem **275**(4): 2576-80.

Morrow, J. A., M. L. Segall, et al. (2000). "Differences in stability among the human apolipoprotein E isoforms determined by the amino-terminal domain." Biochemistry **39**(38): 11657-66.

Morwald, S., H. Yamazaki, et al. (1997). "A novel mosaic protein containing LDL receptor elements is highly conserved in humans and chickens." Arterioscler Thromb Vasc Biol **17**(5): 996-1002.

Mousavi, S. A., L. Malerod, et al. (2004). "Clathrin-dependent endocytosis." Biochem J **377**(Pt 1): 1-16.

Nagai, M., T. Meerloo, et al. (2003). "The adaptor protein ARH escorts megalin to and through endosomes." Mol Biol Cell **14**(12): 4984-96.

Nathan, B. P., S. Bellosta, et al. (1994). "Differential effects of apolipoproteins E3 and E4 on neuronal growth in vitro." Science **264**(5160): 850-2.

Nimpf, J., R. George, et al. (1988). "Apolipoprotein specificity of the chicken oocyte receptor for low and very low density lipoproteins: lack of recognition of apolipoprotein VLDL-II." J Lipid Res **29**(5): 657-67.

Nimpf, J., M. J. Radosavljevic, et al. (1989). "Oocytes from the mutant restricted ovulator hen lack receptor for very low density lipoprotein." J Biol Chem **264**(3): 1393-8.

Nimpf, J. and W. J. Schneider (2000). "From cholesterol transport to signal transduction: low density lipoprotein receptor, very low density lipoprotein receptor, and apolipoprotein E receptor-2." Biochim Biophys Acta **1529**(1-3): 287-98.

Nimpf, J., S. Stifani, et al. (1994). "The somatic cell-specific low density lipoprotein receptor-related protein of the chicken. Close kinship to mammalian low density lipoprotein receptor gene family members." J Biol Chem **269**(1): 212-9.

Novak, S., T. Hiesberger, et al. (1996). "A new low density lipoprotein receptor homologue with 8 ligand binding repeats in brain of chicken and mouse." J Biol Chem **271**(20): 11732-6.

Olofsson, S. O. and J. Boren (2005). "Apolipoprotein B: a clinically important apolipoprotein which assembles atherogenic lipoproteins and promotes the development of atherosclerosis." J Intern Med **258**(5): 395-410.

Pitas, R. E., J. K. Boyles, et al. (1987). "Lipoproteins and their receptors in the central nervous system. Characterization of the lipoproteins in cerebrospinal fluid and identification of apolipoprotein B,E(LDL) receptors in the brain." J Biol Chem **262**(29): 14352-60.

Plieschnig, J. (2008). "Characterization of chicken LRP-2 and its role in embryonic development." Diploma Thesis

Puertollano, R. (2004). "Clathrin-mediated transport: assembly required. Workshop on Molecular Mechanisms of Vesicle Selectivity." EMBO Rep **5**(10): 942-6.

Rall, S. C., Jr., K. H. Weisgraber, et al. (1982). "Human apolipoprotein E. The complete amino acid sequence." J Biol Chem **257**(8): 4171-8.

Rhyu, M. S., L. Y. Jan, et al. (1994). "Asymmetric distribution of numb protein during division of the sensory organ precursor cell confers distinct fates to daughter cells." Cell **76**(3): 477-91.

Rosenblatt DS, Fenton WA. (1999) "Inborn errors of cobalamin metabolism." In: Banerjee R, ed. Chemistry and Biochemistry of Vitamin B_{12}. New York, NY: John Wiley and Sons;367-384.

Rudenko, G., L. Henry, et al. (2002). "Structure of the LDL receptor extracellular domain at endosomal pH." Science **298**(5602): 2353-8.

Sacre, S. M., A. K. Stannard, et al. (2003). "Apolipoprotein E (apoE) isoforms differentially induce nitric oxide production in endothelial cells." FEBS Lett **540**(1-3): 181-7.

Salcini, A. E., S. Confalonieri, et al. (1997). "Binding specificity and in vivo targets of the EH domain, a novel protein-protein interaction module." Genes Dev **11**(17): 2239-49.

Santolini, E., C. Puri, et al. (2000). "Numb is an endocytic protein." J Cell Biol **151**(6): 1345-52.

Saunders, A. M., W. J. Strittmatter, et al. (1993). "Association of apolipoprotein E allele epsilon 4 with late-onset familial and sporadic Alzheimer's disease." Neurology **43**(8): 1467-72.

Schneider, W. J. (1995). "Yolk precursor transport in the laying hen." Curr Opin Lipidol **6**(2): 92-6.

Schneider, W. J. and J. Nimpf (2003). "LDL receptor relatives at the crossroad of endocytosis and signaling." Cell Mol Life Sci **60**(5): 892-903.

Schneider, W.J. (2008). " Lipoprotein receptors." Biochemistry of Lipids, Lipoproteins, and Membranes 5th edition, chapt. 20.

Skalen, K., M. Gustafsson, et al. (2002). "Subendothelial retention of atherogenic lipoproteins in early atherosclerosis." Nature **417**(6890): 750-4.

Smith, B. T., J. C. Mussell, et al. (2006). "Targeted disruption of cubilin reveals essential developmental roles in the structure and function of endoderm and in somite formation." BMC Dev Biol **6**: 30.

Sorensen, E. B. and S. D. Conner (2008). "AAK1 regulates Numb function at an early step in clathrin-mediated endocytosis." Traffic **9**(10): 1791-800.

Sorkin, A. (2004). "Cargo recognition during clathrin-mediated endocytosis: a team effort." Curr Opin Cell Biol **16**(4): 392-9.

Stannard, A. K., D. R. Riddell, et al. (2001). "Cell-derived apolipoprotein E (ApoE) particles inhibit vascular cell adhesion molecule-1 (VCAM-1) expression in human endothelial cells." J Biol Chem **276**(49): 46011-6.

Steyrer, E., D. L. Barber, et al. (1990). "Evolution of lipoprotein receptors. The chicken oocyte receptor for very low density lipoprotein and vitellogenin binds the mammalian ligand apolipoprotein E." J Biol Chem **265**(32): 19575-81.

Stifani, S., D. L. Barber, et al. (1991). "The laying hen expresses two different low density lipoprotein receptor-related proteins." J Biol Chem **266**(28): 19079-87.

Stockinger, W., E. Hengstschlager-Ottnad, et al. (1998). "The low density lipoprotein receptor gene family. Differential expression of two alpha2-macroglobulin receptors in the brain." J Biol Chem **273**(48): 32213-21.

Strickland, D. K., S. L. Gonias, et al. (2002). "Diverse roles for the LDL receptor family." Trends Endocrinol Metab **13**(2): 66-74.

Strickland, D. K., M. Z. Kounnas, et al. (1995). "LDL receptor-related protein: a multiligand receptor for lipoprotein and proteinase catabolism." Faseb J **9**(10): 890-8.

Strope, S., R. Rivi, et al. (2004). "Mouse amnionless, which is required for primitive streak assembly, mediates cell-surface localization and endocytic function of cubilin on visceral endoderm and kidney proximal tubules." Development **131**(19): 4787-95.

Szymkiewicz, I., O. Shupliakov, et al. (2004). "Cargo- and compartment-selective endocytic scaffold proteins." Biochem J **383**(Pt 1): 1-11.

Takahashi, S., Y. Kawarabayasi, et al. (1992). "Rabbit very low density lipoprotein receptor: a low density lipoprotein receptor-like protein with distinct ligand specificity." Proc Natl Acad Sci U S A **89**(19): 9252-6.

Tanner, S. M., M. Aminoff, et al. (2003). "Amnionless, essential for mouse gastrulation, is mutated in recessive hereditary megaloblastic anemia." Nat Genet **33**(3): 426-9.

Tokumitsu, H., N. Hatano, et al. (2006). "Phosphorylation of Numb regulates its interaction with the clathrin-associated adaptor AP-2." FEBS Lett **580**(24): 5797-801.

Tomita, Y., D. H. Kim, et al. (1998). "A novel low-density lipoprotein receptor-related protein with type II membrane protein-like structure is abundant in heart." J Biochem **124**(4): 784-9.

Traub, L. M. (2003). "Sorting it out: AP-2 and alternate clathrin adaptors in endocytic cargo selection." J Cell Biol **163**(2): 203-8.

Trommsdorff, M., M. Gotthardt, et al. (1999). "Reeler/Disabled-like disruption of neuronal migration in knockout mice lacking the VLDL receptor and ApoE receptor 2." Cell **97**(6): 689-701.

Uemura, T., S. Shepherd, et al. (1989). "numb, a gene required in determination of cell fate during sensory organ formation in Drosophila embryos." Cell **58**(2): 349-60.

Verdi, J. M., A. Bashirullah, et al. (1999). "Distinct human NUMB isoforms regulate differentiation vs. proliferation in the neuronal lineage." Proc Natl Acad Sci U S A **96**(18): 10472-6.

Verdi, J. M., R. Schmandt, et al. (1996). "Mammalian NUMB is an evolutionarily conserved signaling adapter protein that specifies cell fate." Curr Biol **6**(9): 1134-45.

Wakamatsu, Y., T. M. Maynard, et al. (1999). "NUMB localizes in the basal cortex of mitotic avian neuroepithelial cells and modulates neuronal differentiation by binding to NOTCH-1." Neuron **23**(1): 71-81.

Wang, X., E. A. Bornslaeger, et al. (1996). "A candidate gene for the amnionless gastrulation stage mouse mutation encodes a TRAF-related protein." Dev Biol **177**(1): 274-90.

Weisgraber, K. H. (1994). "Apolipoprotein E: structure-function relationships." Adv Protein Chem **45**: 249-302.

Wetterau, J. R., L. P. Aggerbeck, et al. (1988). "Human apolipoprotein E3 in aqueous solution. I. Evidence for two structural domains." J Biol Chem **263**(13): 6240-8.

Wettey, F. R., S. F. Hawkins, et al. (2002). "Controlled elimination of clathrin heavy-chain expression in DT40 lymphocytes." Science **297**(5586): 1521-5.

Willnow, T. E., A. Nykjaer, et al. (1999). "Lipoprotein receptors: new roles for ancient proteins." Nat Cell Biol **1**(6): E157-62.

Willnow, T. E., A. Rohlmann, et al. (1996). "RAP, a specialized chaperone, prevents ligand-induced ER retention and degradation of LDL receptor-related endocytic receptors." Embo J **15**(11): 2632-9.

Winding, P. and M. W. Berchtold (2001). "The chicken B cell line DT40: a novel tool for gene disruption experiments." J Immunol Methods **249**(1-2): 1-16.

Yamamoto, T. and R. O. Ryan (2009). "Domain swapping reveals LDL type A repeat order affects ligand binding to the low-density lipoprotein receptor." J Biol Chem.

Yamamoto, T. and R. O. Ryan (2009). "Domain swapping reveals that low density lipoprotein (LDL) type A repeat order affects ligand binding to the LDL receptor." J Biol Chem **284**(20): 13396-400.

Yamazaki, H., H. Bujo, et al. (1996). "Elements of neural adhesion molecules and a yeast vacuolar protein sorting receptor are present in a novel mammalian low density lipoprotein receptor family member." J Biol Chem **271**(40): 24761-8.

Yan, K. S., M. Kuti, et al. (2002). "PTB or not PTB -- that is the question." FEBS Lett **513**(1): 67-70.

Young, S. G. (1990). "Recent progress in understanding apolipoprotein B." Circulation **82**(5): 1574-94.

Acknowledgements

I want to thank my lab colleagues for the nice working atmosphere, the scientific chicken discussions, their absolute support during my work, the numerous, funny “At Hellin’s” coffee breaks and the time we spent together outside the laboratory!
Ahead of all, Andrea und Desiree for listening to and answering many of my questions!

I want to thank my supervisor Prof. Dr. Wolfgang J. Schneider for giving me the opportunity to perform my thesis in his laboratory. I thank him for his constant support, his scientific input, his motivation and the fruitful discussions!

I thank my parents, Erni and Peter, for their great support, for giving me the feeling to do the right thing and for being proud of me!!

I thank my dear, little niece, Louise! She gives me the capability to look at things from a different perspective and makes “big” problems very small!!

Finally, I thank Stefan, who was by my side all the time! I thank him for listening to me, for his patience, his encouragement under all circumstances, and his love!!!

Addendum

Curriculum vitae

Personal data

Name	Mag. Melanie Schiff
Address	1090 Vienna, Liechtensteinstrasse 91/4
Telephone	0650/4789348
Email	melanie.schiff@meduniwien.ac.at; melanieschiff@gmx.at
Date of birth	26.09.1978
Place of birth	Vienna, Austria

Education

02/2006-08/2009	PhD thesis at the Department of Medical Biochemistry, Institute of Molecular Genetics, Medical University of Vienna Title: “Comparative studies of the avian and the mammalian LDLR.” Supervisor: Univ.Prof.Dr. Wolfgang J. Schneider
09/2005-12/2005	Scientific collaboration in the research group of Univ.Prof.Dr. Gert Lubec
02/2004-07/2005	Diploma thesis entitled “Mechanisms of STAT1 activation by Serine 727 phosphorylation” at the Institute of Microbiology and Genetics, University of Vienna Supervisor: Univ.Prof.Dr. Pavel Kovarik
09/1998-2005	Studies of Microbiology and Genetics at the University of Vienna
06/1997	High school diploma
1989-1997	Erich Fried Bundesrealgymnasium, 1090 Vienna
1985-1989	Volksschule Schubert-Schule, 1090 Vienna

Employment

07/2002	RSC Raiffeisen Daten Service Center GmbH
07/2000	Wiener Städtische Versicherung AG Vienna Insurance Group
08/1999	Ankerbrot AG
03/1998-09/1998	Andritz AG

Further training and achievement

2006-dato	Teaching and supervision of students in Microbiology, Genetics and Molecular Biology of the University of Vienna within practical courses in the lab of Prof. Dr. W.J. Schneider
2005	Tutor in a practical course for Biology students

Additional Information

Computer Skills

Windows XP
MS-Office
Adobe Photoshop
Online databases (e.g. Pubmed, Ensembl)
Endnote

Languages

German: native language
English: fluently in writing and speaking

Publication

I Sadzak, **M Schiff**, I Gattermeier, R Glinitzer, I Sauer, A Saarmüller, E Yang, B Schaljo, and P Kovarik; PNAS; Volume 105, 2008; Recruitment of Stat1 to chromatin is required for interferon-induced serine phosphorylation of Stat1 transactivation domain